ÉCOLE DE TECHNOLOGIE SUPÉRIEURE

UNIVERSITÉ DU QUÉBEC

THESIS SUBMITTED TO

ÉCOLE DE TECHNOLOGIE SUPÉRIEURE

IN PARTIAL FULFILMENT OF THE REQUIREMENTS FOR THE DEGREE OF

MASTER OF SCIENCE IN ENGINEERING

M. Ing.

BY

ANDREI VLADIMIR POPOV

PROOF-OF-MATCH TECHNIQUE

FOR BELL 427 HELICOPTER LEVEL D SIMULATOR

MONTRÉAL, 15th of DECEMBER, 2005

THIS THESIS IS EVALUATED

BY A JURY COMPOSED OF:

Mrs. Ruxandra Botez, director of thesis
Department of Automated Production Engineering at École de technologie supérieure

Mr. Adrian Hiliuta, co-director
Department of Automated Production Engineering at École de technologie supérieure

Mr. Éric Granger, president of jury
Department of Automated Production Engineering at École de technologie supérieure

Mr. Joey Seto, external jury member
Aerodynamics and Handling Qualities Group, Bell Helicopter Textron Canada

THIS THESIS WAS PRESENTED IN FRONT OF JURY AND PUBLIC

ON 9th of DECEMBER, 2005

AT ÉCOLE DE TECHNOLOGIE SUPÉRIEURE

TECHNIQUE DE VALIDATION
POUR UN SIMULATEUR DU NIVEAU D POUR
L'HÉLICOPTÈRE BELL 427

Andrei Vladimir Popov

RÉSUMÉ

Dans ce mémoire, on présente les étapes de réalisation et de certification d'un modèle mathématique complet pour un simulateur d'hélicoptère Bell 427 certifié au niveau D de la circulaire FAA AC 120 – 63. Le modèle doit être validé avec les données des essais en vol ainsi que pour plusieurs conditions de vol et plusieurs poids. Les données ont été obtenues par Bell Helicopter Textron, et les dérivés de stabilité et contrôle ont été estimées par la méthode MLE et assemblées dans un modèle couplé de 6 DoF au Conseil National de Recherche du Canada. La procédure de validation a été implémentée dans un logiciel intitulé POM (Proof of Match). Les conditions de vol spéciales qui ont été analysées dans ce mémoire en utilisant le POM sont le mouvement latéral, le vol au point fixe sans l'effet de sol, le vol au point fixe dans l'effet de sol et l'autorotation.

TECHNIQUE DE VALIDATION
POUR UN SIMULATEUR DU NIVEAU D POUR
L'HÉLICOPTÈRE BELL 427

Andrei Vladimir Popov

SOMMAIRE

Les simulateurs de vol sont parmi les principales applications de l'identification des systèmes dans l'industrie aéronautique. Ce mémoire présente les étapes de réalisation et de certification d'un modèle mathématique complet pour un simulateur d'hélicoptère Bell 427.

Ce projet de recherche de l'organisme gouvernemental le Consortium de Recherche et d'innovation en aérospatiale au Québec, le CRIAQ, a été réalisé à l'École de Technologie Supérieure en collaboration avec le Conseil National de Recherche Canadien et Bell Helicopter Textron. Le modèle mathématique complet doit passer les conditions pour certification requises par la circulaire FAA AC 120 – 63, et il doit être validé avec les données des essais en vol. Les données des essais en vol ainsi que plusieurs conditions de vol et plusieurs pesées ont été obtenues de Bell Helicopter Textron, et les dérivés de stabilité et contrôle ont été estimées par la Méthode de Maximum Ressemblance Estimation et assemblées dans un modèle couplé de 6 degrés de liberté au Conseil National de Recherche Canadien (CNRC). La procédure de validation a été implémentée dans un logiciel dénommé POM (Proof of Match) par le CNRC. Les conditions de vol spéciales qui ont été analysées dans ce mémoire sont le mouvement latéral, le vol au point fixe sans l'effet de sol, le vol au point fixe dans l'effet de sol et l'autorotation.

Le modèle complet est encore dans une étape de développement et n'inclut pas le modèle de transition, le modèle du moteur et le modèle de la dynamique du sol à l'atterrissage, mais il est capable de simuler les conditions de vol en hauteur pour des périodes de temps courtes référées comme « snapshots » et l'hélicoptère dans un état d'équilibre initial. Le procès de validation démontre que le simulateur peut être certifié au niveau D de la circulaire FAA AC 120 – 63.

PROOF-OF-MATCH TECHNIQUE
FOR BELL 427 HELICOPTER LEVEL D SIMULATOR

Andrei Vladimir Popov

ABSTRACT

The helicopter flight simulators domain is one of major interest among multiple applications of system identification in the aeronautical industry. This document presents the steps of building and certification of a complete mathematical model of a Bell 427 helicopter flight simulator.

This research was performed in the context of a CRIAQ project and done by École de Technologie Supérieure in collaboration with the Canadian National Research Council (NRC) and Bell Helicopter Textron. The complete mathematical model has to pass the certification requirements in according with the FAA AC 120 – 63, and had to be validated with flight test data. From flight test data at different gross weight and different flight conditions obtained from Bell Helicopter Textron, the stability and control derivatives were estimated by the Maximum Likelihood Estimation Method and assembled in a fully coupled, 6 degree of freedom (6 DoF) modified state space model at National Research Council (NRC). The validation procedure is incorporated in NRC software referred to as POM (Proof of Match). The flight condition cases analysed in this document, are lateral motion, hover out of ground effect, hover in ground effect, and autorotation.

The complete model is still in a development phase and does not include the transition model, engine model and landing ground dynamics model, yet it is capable of simulating the up and away flight cases for short periods of time which are referred to as "snapshots" and trimmed helicopter states. The validation process demonstrates that in this stage the model can be certified as a level D simulator.

ACKNOWLEDGEMENTS

TABLE OF CONTENTS

LIST OF TABLES

LIST OF FIGURES

Page

ABBREVIATIONS

α	Angle of attack
β	Angle of sideslip
θ	Pitch attitude angle
φ	Roll attitude angle
ψ	Yaw attitude angle
Ω	Rotor speed
a_x	F/A load factor
a_y	Lateral load factor
a_z	Normal load factor
deg	Degree
deg/s	Degree per second
ft	Feet
ft/s	Feet per second
g	Gravitational acceleration
lbs	Pounds
p	Roll attitude rate
q	Pitch attitude rate
r	Yaw attitude rate
u	Longitudinal speed component in body axes system
u	Control vector
v	Lateral speed component in body axes system
w	Vertical speed component in body axes system
x	State vector
A/C	Aircraft
AC	Advisory Circular
C	Celsius
CG	Center of Gravity

DoF	Degrees of Freedom
F/A	Forward – Aft
FAA	US Federal Aviation Administration
FFGE	Forward Flight in Ground Effect
GDF	Graphic Definition File
GW	Gross Weight
Hd	Density altitude
IAS	Indicated Air Speed
IC	Instrumentation Center
IGE	In Ground Effect
L	Longitudinal moment component
M	Lateral moment component
MLE	Maximum Likelihood Estimation
N	Directional moment component
NB	Nose Boom
NRC	National Research Council
OAT	Outside Air Temperature
OEI	One Engine Inoperative
OGE	Out of Ground Effect
QTG	Quality Test Guide
RPM	Revolutions Per Minute
ROC	Rate Of Climb
T	oscillation period
TAS	True Air Speed
TDF	Test Definition File
T/O	Take Off
UAA	Up And Away
Vh	Maximum cruise speed
X	Longitudinal force component

Y Lateral force component

Z Vertical force component

INTRODUCTION

The Bell 427, 8 seat helicopter, executive, commuter or cargo transport is a proof of excellence in the modern aviation. The Bell 427 is assembled at Bell Helicopter Canada, a division of Textron Canada Ltd. It received the basic certification by Transport Canada in December 1999. It presents new challenges due to its advanced technology of the four-blade composite main rotor system. To overcome the increased number of failure analyses required by certification agencies worldwide, Bell Helicopter Textron chose to utilize a model-centered design methodology. Simulation models would thereby be utilized in all phases of the design process and would be deployed from desktop analysis to hardware in the loop test rigs. Furthermore, a single model would be used in as many different applications as possible, minimizing model maintenance and maximizing efficiency.

To use a single model for many different applications, such as flight dynamics analysis, training, control law design, functional hazard analysis and hardware in the loop test rigs, the model had to be matched beyond standard requirements and the complexity extended beyond the norm.

In the present aviation era, most flight dynamics simulation models are built with the focus on the need for training simulators. The level D requirement (simulator certification level) is the target of model matching. The flight-control team needs fairly sophisticated controls and aerodynamics models to design the control law. The handling qualities team needs the same kind of models to guarantee design objectives. The engine team needs a complete engine model to evaluate integration issues. The systems team needs to analyze all possible combinations of failure cases, and so on. The demands on the simulation model have grown substantially.

Another great challenge in the development of such simulation models has become the accuracy of their prediction, especially given the extremes (flight envelope and configuration) to which these models would be run.

The problem raised in this project is the building of a mathematical model for a Bell 427 helicopter simulator, which in the final step has to satisfy the certification requirements accordingly with the advisory circular FAA AC 120-63. The previous experience accumulated in this research field showed that a semi-empirical approach based on flight test data is the best approach. To describe the helicopter flight dynamics is necessary to generate an 6 degrees of freedom model formulation based on flight test records. A system identification method has to be used in order to generate the stability and control derivatives. These derivatives are assembled into a software program which enables to simulate the flight parameters and compare the results with the recorded parameters.

A huge data base of flight tests at different gross weight and different flight conditions was built by Bell Helicopter Textron. This data base contains two sets of flight tests: a first set of 2311 control input maneuvers flight tests which was used to create the model and a second set of flight tests recorded in the same conditions as the first set, which was used for the validation process of the model but for different control inputs.

The stability and control derivatives were estimated by the Maximum Likelihood Estimation (MLE) method and assembled in a fully coupled, 6 degrees of freedom modified state space model at National Research Council (CNRC). This part of the project was studied by Crisan in his master thesis [7].

However, the focus of this thesis will be mainly limited to a description of the methodology and tools of the model validation process. The tool used to validate the model is the NRC copyrighted software referred to as POM$^©$ (Proof of Match). The validation process is the most work and time consuming part of the project. During this

process a number of almost 600 flight tests had to be analyzed in according with the advisory circular FAA AC 120-63 requirements. The Quality Test Guide list which is based on the AC requirements contains at least 73 points of flight tests to be fitted. If the requirements were not fulfilled, the model had to be adjusted and the flight tests analysis reloaded. In the Table I are shown the analyzed flight test cases and the number of well fitted flight tests versus the total of flight tests (expressed in percentage form) here called pass %.

Table I

Flight tests validation

AC chapter	Number of flight tests	Pass %
Longitudinal Handling Qualities	172	59
Lateral and Directional Handling Qualities	115	95
Level Flight	59	95
Descent Performance	11	95
Climb Performance	14	86
Hover	74	77
Low Speed Handling Qualities	50	89
Autorotation Entry	7	79
Turns on One Control	24	97
Vertical Climb	3	93
Take-Off Flight	18	89
Landing	6	97

The project had a length of approximately two years and six months. During the first year, the data formatting and corrections were done and the POM software was completed. During the rest of time, the validation process was performed. ÉTS team contributed mainly in the data corrections and validation process.

In Chapter 1 the mathematical equations and models are presented. In Chapter 2 the flight test data collection and formatting are described. The integrated simulation model was entirely built with Simulink/MATLAB® (MathWorks, Natick, Massachusetts) and is presented in Chapter 3. Requirements for the level D simulator certification in Chapter 4 are succinctly presented. Chapters 5, 6 and 7 present the model validation results.

CHAPTER 1

LITERATURE OVERVIEW

1.1   Equations of motions for a rotorcraft

In order to develop a mathematical model for a rotorcraft simulator we need to recall the basic laws of physics. The purpose of this mathematical model is the validation of a real flight simulator which is done by the implementation of a programming code to calculate real time motion of the helicopter. Several assumptions are made to simplify the model and should give close results to the reality in order not to compromise the real motion described by the model.

Although a rotorcraft is a vehicle which flies in the air and obeys the laws of aerodynamics, its motion is different from an airplane due to its different design. Its particularities are given by the rotor which is the main sustentation device. A vehicle flying in the air, such as a helicopter or an airplane, develops forces to counterbalance the gravitational attraction force. Airplanes develop aerodynamic forces by the relative motion of the air around stationary wings, while helicopters create aerodynamic forces by the rotational motions of a device named rotor-wing, or shortly rotor. Figure 1 shows the aerodynamic forces diagram on a helicopter and on an aircraft.
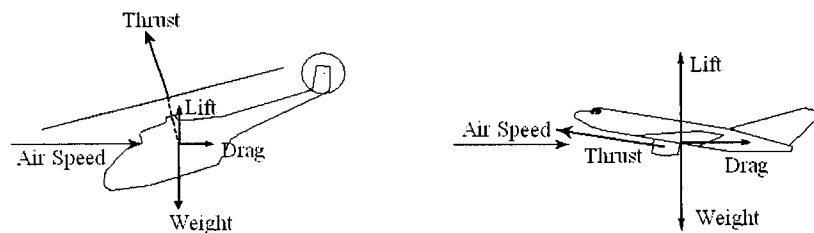
Figure 1 Forces acting on a helicopter and on an aircraft

1.1.1 Newton's laws of motion

The first assumption is that the helicopter is a rigid body, in which the relative motions of the rotor with respect to the helicopter's structure, and the vibrations dues to engine, gearbox, pumps, or shafts are not considered. In this section, Newton's laws of motion which are known from various references are described [1], [2].

According to Newton's laws of motion for a rigid body, the sum of all forces acting on the body has to be calculated. A set of rectangular axes (O, x, y, z) called body fixed axes is attached to the helicopter in the manner shown graphically in Figure 2. The centre of body axes is located in the centre of gravity ($CG \equiv O$), the Ox axis is oriented in the longitudinal direction of the fuselage pointing to the helicopter's front, the Oy axis is oriented to the right direction of the pilot, perpendicular on the xOz plane formed by the longitudinal and vertical axes, and the Oz axis is oriented downwards perpendicular to the xOy plane formed by the longitudinal and lateral axes.
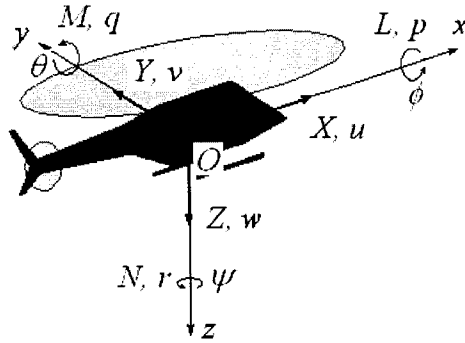
Figure 2 Body axes system viewed from a frontal-down-lateral right direction

The total force $\vec{F}$ and total torque $\vec{M}$ acting upon the body are projected along the three axes of the body system (O, x, y, z). The components of total force $\vec{F}$ are X, Y and Z, and the components of total torque $\vec{M}$ are L, M and N. The velocity of the body $\vec{V}_b$ is

projected along the three axes in components u, v and w. The rotational momentum $\vec{\omega}_b$ has its components along the three axes the rotational angles rates p, q and r.

The Newton's law in the Earth coordinates is given by the following equation:

$$\vec{F} = \frac{d}{dt}\left(m\vec{V}\right)_e \tag{1.1}$$

By changing the coordinates of velocity derivatives from the Earth axes system e to body axes system b, the following equation is obtained:

$$\left(\frac{d\vec{V}}{dt}\right)_e = \left(\frac{d\vec{V}}{dt}\right)_b + \left(\vec{\omega} \times \vec{V}\right)_b \tag{1.2}$$

Then, by replacing equation (1.2) into equation (1.1), we obtain:

$$\vec{F} = m\left(u\vec{i} + v\vec{j} + w\vec{k} + \begin{vmatrix} \vec{i} & \vec{j} & \vec{k} \\ p & q & r \\ u & v & w \end{vmatrix}\right) \tag{1.3}$$

where m is the mass of the body which is constant.

The forces along the three axes X, Y and Z may be further calculated. The Newton's equations in the body axes system are decomposed along their three axes and written under the following matrix form:

$$\begin{bmatrix} X \\ Y \\ Z \end{bmatrix} = m\left(\begin{bmatrix} \dot{u} \\ \dot{v} \\ \dot{w} \end{bmatrix} + \begin{bmatrix} p \\ q \\ r \end{bmatrix} \times \begin{bmatrix} u \\ v \\ w \end{bmatrix}\right) = m\left(\begin{bmatrix} \dot{u} \\ \dot{v} \\ \dot{w} \end{bmatrix} + \begin{bmatrix} 0 & -r & q \\ r & 0 & -p \\ -q & p & 0 \end{bmatrix}\begin{bmatrix} u \\ v \\ w \end{bmatrix}\right) \qquad (1.4)$$

In the same manner, the total torque $\vec{M}$ that acts upon the body is given by the equation:

$$\vec{M} = \left(\frac{d\vec{H}}{dt}\right)_e = \left(\frac{d\vec{H}}{dt}\right)_b + \left(\vec{\omega} \times \vec{H}\right)_b \qquad (1.5)$$

where $\vec{H}$ is the angular momentum given by the following equation:

$$\vec{H} = \begin{bmatrix} H_x \\ H_y \\ H_z \end{bmatrix} = [I]\vec{\omega} = \begin{bmatrix} I_{xx} & -I_{xy} & -I_{xz} \\ -I_{xy} & I_{yy} & -I_{yz} \\ -I_{xz} & -I_{yz} & I_{zz} \end{bmatrix}\begin{bmatrix} p \\ q \\ r \end{bmatrix} \qquad (1.6)$$

The total torque equation in a matrix form is derived from the equation (1.5) and (1.6):

$$\begin{bmatrix} L \\ M \\ N \end{bmatrix} = [I]\begin{bmatrix} \dot{p} \\ \dot{q} \\ \dot{r} \end{bmatrix} + \begin{bmatrix} p \\ q \\ r \end{bmatrix} \times [I]\begin{bmatrix} p \\ q \\ r \end{bmatrix} = [I]\begin{bmatrix} \dot{p} \\ \dot{q} \\ \dot{r} \end{bmatrix} + \begin{bmatrix} 0 & -r & q \\ r & 0 & -p \\ -q & p & 0 \end{bmatrix}[I]\begin{bmatrix} p \\ q \\ r \end{bmatrix} \qquad (1.7)$$

where I is the inertia matrix expressed by the following matrix,

$$[I] = \begin{bmatrix} I_{xx} & -I_{xy} & -I_{xz} \\ -I_{xy} & I_{yy} & -I_{yz} \\ -I_{xz} & -I_{yz} & I_{zz} \end{bmatrix} \qquad (1.8)$$

where I_{xx}, I_{yy} and I_{zz} are inertia sums and I_{xy}, I_{xz} and I_{yz} are inertia products.

1.1.2 The attitude and the position of the helicopter

The helicopter's translational and rotational motions during the flight described by the Newton's equations, the moments, velocities and attitudes coordinates are expressed in the body axes system b. To simulate the flight of the helicopter between two fixed points on the earth it is needed to express the velocities and attitudes in Earth coordinates system e. The Earth reference system has the z_e axis perpendicular on the Earth and its positive direction is oriented to the center of the Earth and the altitude of the aircraft H is oriented in the opposite (negative) direction of the z_e axis. The x_e axis is oriented arbitrarily to the East and the y_e axis is oriented to the South, perpendicular to the x_e axis. The transformation from body reference to Earth reference is calculated by use of three successive rotations of the Euler angles. The Euler angles are the roll angle ϕ, the pitch angle θ and the yaw angle ψ as shown graphically in Figure 3.
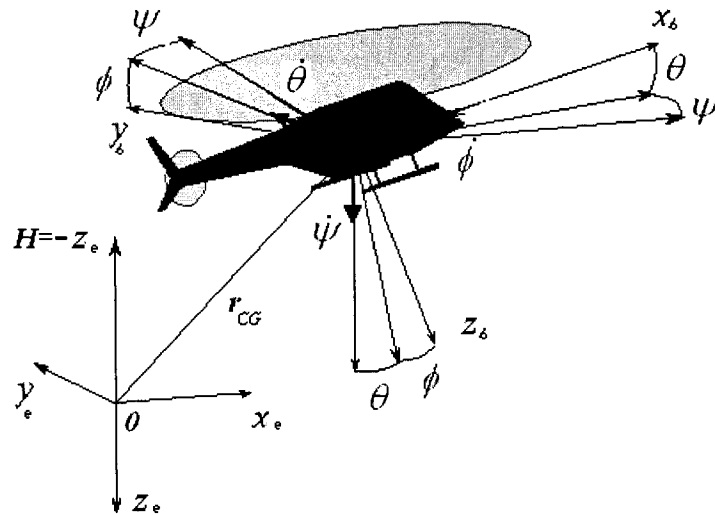
Figure 3 The helicopter's attitudes in the Earth coordinate system e

The components of aircraft velocity in the body coordinates are (u, v, w) and by applying three rotations are written in the Earth coordinates (V_x, V_y, V_z):

$$\begin{bmatrix} V_x \\ V_y \\ V_z \end{bmatrix} = \begin{bmatrix} \cos\psi & -\sin\psi & 0 \\ \sin\psi & \cos\psi & 0 \\ 0 & 0 & 1 \end{bmatrix} \begin{bmatrix} \cos\theta & 0 & \sin\theta \\ 0 & 1 & 0 \\ -\sin\theta & 0 & \cos\theta \end{bmatrix} \begin{bmatrix} 1 & 0 & 0 \\ 0 & \cos\phi & -\sin\phi \\ 0 & \sin\phi & \cos\phi \end{bmatrix} \begin{bmatrix} u \\ v \\ w \end{bmatrix} \qquad (1.9)$$

$$\begin{bmatrix} V_x \\ V_y \\ V_z \end{bmatrix} = \begin{bmatrix} \cos\psi\cos\theta & \cos\psi\sin\theta\sin\phi - \sin\psi\cos\phi & \cos\psi\sin\theta\cos\phi + \sin\psi\sin\phi \\ \sin\psi\cos\theta & \sin\psi\sin\theta\sin\phi + \cos\psi\cos\phi & \sin\psi\sin\theta\cos\phi - \cos\psi\sin\phi \\ -\sin\theta & \cos\theta\sin\phi & \cos\theta\cos\phi \end{bmatrix} \begin{bmatrix} u \\ v \\ w \end{bmatrix} \qquad (1.10)$$

Equation (1.10) allows us to calculate the velocities in Earth system coordinates V_x, V_y, V_z, when the velocities in body system coordinates u, v, w and the Euler angles ϕ, θ, ψ are known. The transformation from Earth system coordinates to body system coordinates is $[T]$ called Direction Cosine Matrix, given by equation (1.12):

$$\begin{bmatrix} u \\ v \\ w \end{bmatrix} = [T] \begin{bmatrix} \dot{x}_{earth} \\ \dot{y}_{earth} \\ \dot{z}_{earth} \end{bmatrix} \qquad (1.11)$$

$$[T] = \begin{bmatrix} \cos\psi\cos\theta & \sin\psi\cos\theta & -\sin\theta \\ \cos\psi\sin\theta\sin\phi - \sin\psi\cos\phi & \sin\psi\sin\theta\sin\phi + \cos\psi\cos\phi & \cos\theta\sin\phi \\ \cos\psi\sin\theta\cos\phi + \sin\psi\sin\phi & \sin\psi\sin\theta\cos\phi - \cos\psi\sin\phi & \cos\theta\cos\phi \end{bmatrix} \qquad (1.12)$$

In order to obtain the helicopter angular velocities p, q, r from the Earth coordinates system into the body coordinates system, same three rotations as the ones shown in equation (1.10) are applied and following equation is obtained:

$$
\begin{bmatrix} p \\ q \\ r \end{bmatrix} = \begin{bmatrix} \dot{\phi} \\ 0 \\ 0 \end{bmatrix} + \left(\begin{bmatrix} \cos\theta & 0 & -\sin\theta \\ 0 & 1 & 0 \\ \sin\theta & 0 & \cos\theta \end{bmatrix} \begin{bmatrix} 0 \\ 0 \\ \dot{\psi} \end{bmatrix} + \begin{bmatrix} 0 \\ \dot{\theta} \\ 0 \end{bmatrix} \right) \begin{bmatrix} 1 & 0 & 0 \\ 0 & \cos\phi & \sin\phi \\ 0 & -\sin\phi & \cos\phi \end{bmatrix} \tag{1.13}
$$

$$
\begin{bmatrix} p \\ q \\ r \end{bmatrix} = \begin{bmatrix} 1 & 0 & -\sin\theta \\ 0 & \cos\phi & \sin\phi\cos\theta \\ 0 & -\sin\phi & \cos\phi\cos\theta \end{bmatrix} \begin{bmatrix} \dot{\phi} \\ \dot{\theta} \\ \dot{\psi} \end{bmatrix} \tag{1.14}
$$

from where:

$$
\begin{bmatrix} \dot{\phi} \\ \dot{\theta} \\ \dot{\psi} \end{bmatrix} = \begin{bmatrix} 1 & \sin\phi\tan\theta & \cos\phi\tan\theta \\ 0 & \cos\phi & -\sin\phi \\ 0 & \sin\phi\sec\theta & \cos\phi\sec\theta \end{bmatrix} \begin{bmatrix} p \\ q \\ r \end{bmatrix} \tag{1.15}
$$

One method of calculating the attitudes of the helicopter is by measuring the angular velocities (p,q,r) on the helicopter and calculating the Euler angles (ϕ,θ,ψ) by the integration of equation (1.15).

Another method of calculating the attitudes rates of the helicopter is by measuring the Euler angles (ϕ,θ,ψ) and calculating the angular velocities (p,q,r) by the derivation of equation (1.14).

By use of equations (1.14) and (1.15), the motion of a helicopter is described with respect to the inertial fixed system. The whole set of equations of forces and moments are nonlinear due to the rotational effect of the body in the Earth reference system.

1.2 Stability and control theory

To build and certificate a flight simulator, a mathematical relationship between flight controls and thrust forces is needed. This relationship gives the control of the helicopter's motion. There are two types of relationships. The first linear relationship describes the mechanical link between controls and rotor blades. The second relationship describes the aerodynamic phenomenon which is very complex. The aerodynamic forces are dependent of the helicopter's state parameters such as the airspeeds. The stability and control theories use the small perturbations assumptions. In a very narrow area around the equilibrium or trim state of the helicopter at a certain moment in time, the forces change linearly with respect to the state parameters, so that the higher order terms of Taylor series describing the non-linearity of the helicopter's motion are assumed to be negligible [2], [3], [4] and [5]. Firstly, the helicopter's state parameters are defined. The helicopter's vector state is given by its velocities and rotational rates or Euler angles in the Earth fixed system. The parameters u, v, w, p, q and r are arranged under a state vector $x = \begin{bmatrix} u & v & w & p & q & r \end{bmatrix}^T$ form. Thus, aerodynamic forces X are expressed as function of state parameters and derivatives under a linear Taylor series form as follows:

$$
\begin{aligned}
X = X_0 &+ \frac{\partial X}{\partial u}\Delta u + \frac{\partial X}{\partial v}\Delta v + \frac{\partial X}{\partial w}\Delta w + \frac{\partial X}{\partial p}\Delta p + \frac{\partial X}{\partial q}\Delta q + \frac{\partial X}{\partial r}\Delta r \\
&+ \frac{\partial X}{\partial \dot{u}}\Delta \dot{u} + \frac{\partial X}{\partial \dot{v}}\Delta \dot{v} + \frac{\partial X}{\partial \dot{w}}\Delta \dot{w} + \frac{\partial X}{\partial \dot{p}}\Delta \dot{p} + \frac{\partial X}{\partial \dot{q}}\Delta \dot{q} + \frac{\partial X}{\partial \dot{r}}\Delta \dot{r}
\end{aligned}
\tag{1.16}
$$

where

X = aerodynamic forces

X_0 = aerodynamic forces in trim state

$\Delta u, \Delta v, \Delta w$ = changes in translational speeds from trim state

$\Delta \dot{u}, \Delta \dot{v}, \Delta \dot{w}$ = changes in translational accelerations from trim state

$\Delta p, \Delta q, \Delta r$ = changes in rotational speeds from trim state

$\Delta \dot{p}, \Delta \dot{q}, \Delta \dot{r}$ = changes in rotational accelerations from trim state

and

$$X_u = \frac{\partial X}{\partial u} \qquad X_v = \frac{\partial X}{\partial v} \qquad X_w = \frac{\partial X}{\partial w} \qquad X_p = \frac{\partial X}{\partial p} \qquad X_q = \frac{\partial X}{\partial q} \qquad X_r = \frac{\partial X}{\partial r}$$

$$X_{\dot{u}} = \frac{\partial X}{\partial \dot{u}} \qquad X_{\dot{v}} = \frac{\partial X}{\partial \dot{v}} \qquad X_{\dot{w}} = \frac{\partial X}{\partial \dot{w}} \qquad X_{\dot{p}} = \frac{\partial X}{\partial \dot{p}} \qquad X_{\dot{q}} = \frac{\partial X}{\partial \dot{q}} \qquad X_{\dot{r}} = \frac{\partial X}{\partial \dot{r}}$$

are the stability derivatives of X with respect to the translational and rotational speeds u, v, w, p, q, r and accelerations $\dot{u}, \dot{v}, \dot{w}, \dot{p}, \dot{q}, \dot{r}$.

Same expression as the one given by equation (1.16) can be derived for all forces, moments, speeds and accelerations given by a specific trimmed flight condition identified by the index 0:

$$\begin{aligned}
X &= X_0 + \Delta X & L &= L_0 + \Delta L & u &= u_0 + \Delta u & p &= p_0 + \Delta p \\
Y &= Y_0 + \Delta Y & M &= M_0 + \Delta M & v &= v_0 + \Delta v & q &= q_0 + \Delta q \qquad (1.17) \\
Z &= Z_0 + \Delta Z & N &= N_0 + \Delta N & w &= w_0 + \Delta w & r &= r_0 + \Delta r
\end{aligned}$$

All the above expressions are presented in the body axes system b.

The same approach is used for the definition of the changes in aerodynamic forces dues to pilot controls.

The pilot uses the following controls with a direct influence on the aerodynamic forces developed by main and tail rotors:

collective stick controls the collective pitch of the main rotor blades which in turn increases or decreases the thrust vector, which creates a translation motion along z body axis. Due to the anti-coupling effect of the main rotor, the collective controls increase or decrease the yaw moment which creates a yaw motion along z body axis,

lateral cyclic stick controls the lateral cyclic pitch of the main rotor blades which in turn creates a lateral tilt of the main rotor, thus the thrust vector creates a roll and a lateral translational motion;

longitudinal cyclic stick controls the longitudinal cyclic pitch of the main rotor blades which creates a longitudinal tilt of the thrust vector, and creates a pitching and aft-forward translational motion, and

pedals control the collective pitch of the tail rotor blades which creates a yaw moment and a yaw motion along the z helicopter's axis.

In the literature ([3], [4], [5]), the following notations are used:

A_l=lateral cyclic pitch, B_l=longitudinal cyclic pitch, θ_c=collective pitch and θ_T=tail rotor collective.

The changes of aerodynamic forces X due to changes in the control positions are given by the following equation:

$$\Delta X = \frac{\partial X}{\partial A_1} \Delta A_1 + \frac{\partial X}{\partial B_1} \Delta B_1 + \frac{\partial X}{\partial \theta_c} \Delta \theta_c + \frac{\partial X}{\partial \theta_T} \Delta \theta_T \qquad (1.18)$$

where

$$X_{A_1} = \frac{\partial X}{\partial A_1} \qquad X_{B_1} = \frac{\partial X}{\partial B_1} \qquad X_{\theta_c} = \frac{\partial X}{\partial \theta_c} \qquad X_{\theta_T} = \frac{\partial X}{\partial \theta_T}$$

are the control derivatives.

The stability and control theory uses the following state space formulation [1], [2], [3]:

$$\dot{x} = [A]x + [B]u$$
$$y = [C]x + [D]u$$

(1.19)

where $x = \begin{bmatrix} \Delta u & \Delta v & \Delta w & \Delta p & \Delta q & \Delta r \end{bmatrix}^T$ is the state vector of changes in translational and rotational speeds from trim state, the input vector $u = \begin{bmatrix} \Delta A_1 & \Delta B_1 & \Delta \theta_c & \Delta \theta_T \end{bmatrix}^T$ is the control vector of changes in controls from trim state, and y is the output vector, which is a set of different parameters determined from any linear combination of state parameters. In equation (1.19), [A] is the matrix which incorporates the *stability derivatives,* [B] is the matrix which incorporates the *control derivatives,* [C] and [D] are the matrices which incorporate the linear relationships between the output vector y and the state vector x. The output vector y represents the aerodynamic forces and moments of the helicopter. The simplified Simulink schematic of a state space system which represents the helicopter and a matrix gain which represent the motion change of the helicopter due to aerodynamic forces and moments is shown in Figure 4. The helicopter mathematical model and the equations of motion make a closed loop as follows: the change of the state vector or the control vector makes a change in the aerodynamic forces and moments, which in turn due to Newton's equations of motion make a change in the helicopter states vector.
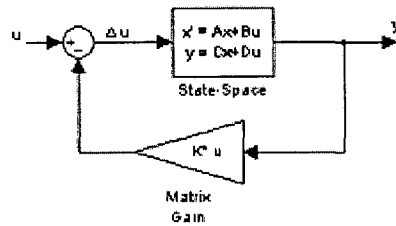
Figure 4 Sample of a state space and matrix gain schematics in Simulink

The calculation of the helicopter state is an iterative algorithm, and when the differences between the input state vector u and the state vector u^- corresponding to the output forces

and moments vector y is zero, the helicopter is in 'trim state' which is an equilibrium state.

The aircraft flight dynamics by use of the stability and control theories is theoretically and experimentally well known. The equations of motion of an aircraft are divided in two main sets: longitudinal and lateral. In the literature, these equations are named *uncoupled* between longitudinal and lateral motion. But the rotorcraft has a more complex motion than an aircraft and the longitudinal and lateral motions are very strongly coupled. For this reason, the uncoupled equations in the aircraft theory cannot be used in the rotorcraft theory. Some aspects of the helicopter flight dynamics research are still not well known and are still in development. The aerodynamics theories used in aircraft dynamics cannot be used in rotorcraft flight dynamics due to its complex nature, and for this reason, very much research in the rotor experimental area, and therefore in flight testing area should be realized. In the following chapter, the experimental methods used in the conception of a flight simulator for a rotorcraft are presented.

CHAPTER 2

FLIGHT TESTS

2.1 Methodology

The methodology used in the development of a mathematical model describing the flight dynamics of a rotorcraft has an experimental approach and three steps are used for its presentation. The first step consists in building of a huge data base of recorded parameters during the flight testing of a helicopter in different flight conditions, loading and CG positions, rotor speeds, flight missions, and manoeuvres etc., so that entire flight envelope is covered by recorded data [5], [6]. This data base contain two sets of flight tests: a set of 2311 control input maneuvers flight tests which was used to create the model and a set of flight tests recorded in the same conditions as the first set, which was used for the validation process of the model and for different initial control inputs.

The second step of this methodology is the preliminary preparation of the gathered data, which consists in the data formatting and organizing in a standardized manner to be "ready to use" by all partners involved in the project.

The third step is the building of the mathematical model by use of the MLE method [7]. This mathematical model is implemented in the software referred to as POM$^©$ (Proof of Match).

The fourth step is the validation of the model by use of the POM software. This validation process is a "trial and error" based tuning of the model. The model has to fulfill all the requirements of a level D simulator certification.

2.1.1 Flight conditions

The flight tests are performed for the following flight conditions:

- Density altitude: Ground, 3000 ft, 6000 ft, 9000 ft;

- Indicated Air Speed: 30 knots, 50 knots, 70 knots, 90 knots, 0.9 Vh;

- Loading and CG position: Heavy/Light, Fwd/Mid/Aft;

- Rotor Speed: 96%, 100%, 104% from the nominal rotor speed;

- Flight mission: Take Off, Hover, Level Flight, Climbing Flight (+500 ft/sec, +1000 ft/sec), Descent Flight (-500 ft/sec, -1000 ft/sec), Autorotation, and Landing.

2.1.2 Flight parameters

The parameters recorded during the flight should be enough to develop all the flight conditions and manoeuvres required in a certain mission. The recorded parameters significant during flight testing are given in Table II.

Table II

Recorded parameters during flight testing

Parameter	Units	Notes
Altitude - pressure	ft	Recorded
Radar altimeter	ft	Recorded
Outside air temperature (OAT)	deg C	Recorded
Main rotor torque	in-lb	Recorded
Main rotor speed	%	Recorded
A/C gross weight (GW)	lb	Real time calculation from fuel quantity
A/C longitudinal CG	in	Real time calculation from fuel quantity
A/C lateral CG	in	Real time calculation from fuel quantity

Table II

(continued)

Parameter	Units	Notes
Lateral cyclic stick position	%	Recorded
Longitudinal cyclic stick position	%	Recorded
Collective position	%	Recorded
Pedal position	%	Recorded
Angle of attack (α)	deg	Recorded, nose boom
Angle of sideslip (β)	deg	Recorded, nose boom
Indicated air speed (IAS)	knots	Recorded
True airspeed (TAS)	knots	Derived from IAS
Aircraft heading	deg	Recorded
Yaw change (ψ)	deg	Derived from A/C Heading
Yaw rate (r)	deg/s	Derived from A/C Heading
Roll attitude (ϕ)	deg	Recorded
Roll rate (p)	deg/s	Recorded
Pitch attitude (θ)	deg	Recorded
Pitch rate (q)	deg/s	Recorded
F/A load factor (a_x)	g	Recorded by longitudinal accelerometer
Normal load factor (a_z)	g	Recorded by vertical accelerometer
Lateral load factor (a_y)	g	Recorded by lateral accelerometer

There are more recorded parameters which are used in the engine model, but we present here only an informative list and not an exhaustive list.

The positive direction of recorded parameters from Table II are defined in the following manner:

Euler angles

Pitch (θ): A/C nose moves up about the pitch axis

Roll (ϕ): A/C has a clockwise motion about the roll axis, as viewed from behind.

Yaw (ψ): A/C nose moves right about the yaw axis

Controls

Longitudinal cyclic: Cyclic stick moves forward

Lateral cyclic: Cyclic stick moves to the right

Pedals: Right pedal moves forward

Nose Boom

Angle of attack (α): A/C nose moves up.

Sideslip angle (β): A/C nose moves left (left yaw = positive sideslip).

2.2   Corrections of the raw data

In the formatting of the raw data gathered from flight tests, the raw data corrections are the following:

- Time delay between parameters due to the instrumentation delay, and instruments calibration,
- Weights, inertias and CG position of A/C calculation,
- Shifting the recorded parameters from the Instrumentation Center (IC) to Center of Gravity (CG), such as calculations of TAS derived from IAS, angle of attack α and angle of sideslip β,
- Correction of the accelerometers due to the gravitational acceleration.

Time delay issue was treated by Crisan [7]. It consisted in a delay between the recorded control input and its effect upon the helicopter movement response.

The instruments calibration was performed on the ground where the parameters readings indicated an offset from their theoretical values. This calibration was performed for pitch attitude, roll attitude, angle of attack, sideslip angle and accelerations.

The inertias were calculated by use of the methodology here described. Since the A/C initial weight and its final weight for a certain flight condition differ only by the amount of fuel burned, the A/C inertias, the fuel weight and CG location (X_{CG}, Y_{CG}, and Z_{CG}) was calculated by use of the following linear mathematical relationships:

$$I_{xx} = a_1 GW + b_1 X_{CG} + c_1 Y_{CG} + d_1 \tag{2.1}$$

$$Z_{CG} = a_2 GW + b_2 \tag{2.2}$$

where a1, b1, c1, d1, a2 and b2 are calculated by linear interpolations.

Results obtained with this method were found to be very good. The four inertias (I_{xx}, I_{yy}, I_{zz} and I_{xz}) were 1000 times bigger than the remaining two inertias (I_{xy} and I_{yz}) and therefore the inertias I_{xy} and I_{yz} were omitted.

2.2.1 Airspeed, angle of attack and angle of sideslip

Due to the rotor's air wake, all the airspeed measurements of the instruments installed on the helicopter are not sufficiently accurate. The airspeed in the vicinity of the helicopter is influenced by the induced airspeed of the rotor wake, so that more precise measurements are done by use of a nose boom as far as possible from the wake of the

measurements are done by use of a nose boom as far as possible from the wake of the rotor, in the front of aircraft. The nose boom contains a static and a Pitot probe, an alpha vane which is installed in the horizontal direction to measure the vertical incidence of the air with respect to the A/C longitudinal axis i.e. angle of attack α, and a beta vane which is installed vertically with respect to the A/C longitudinal axis to measure the sideslip angle of the helicopter, β. The location of the alpha and beta vanes on the nose boom is presented in Figure 5.
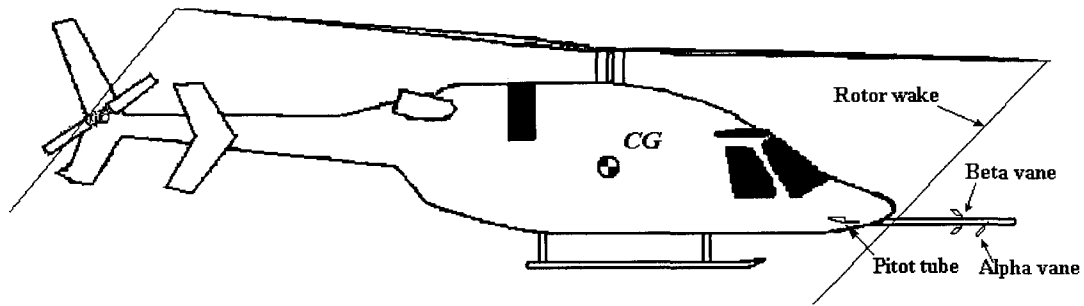
Figure 5 Alpha and Beta vanes installations on the nose boom of the helicopter

Nose boom's alpha and beta vanes are used to record the True Air Speed orientation in the body axes system. The location where TAS measurements are taken (positions of alpha and beta vanes) is different than the Pitot tube location where TAS value is recorded; therefore we need to effectuate corrections to calculate the α and β values recorded in the nose boom location (NB) with respect to the Pitot tube location which is defined as the Instrumentation Center (IC).

To correct the α and β values from NB to IC, the following correction equations applied in both centers NB and IC was used [8]:

$$\alpha_{IC} = \alpha_{CG} - \frac{\Delta x_{\alpha IC}}{TAS_{CG}^2}\left(a_{zCG} - g\cos\theta\cos\phi\right) - \frac{\Delta x_{\alpha IC}}{TAS_{CG}}q \qquad (2.3)$$

$$\alpha_{NB} = \alpha_{CG} - \frac{\Delta x_{\alpha NB}}{TAS_{CG}^2}\left(a_{zCG} - g\cos\theta\cos\phi\right) - \frac{\Delta x_{\alpha NB}}{TAS_{CG}}q \tag{2.4}$$

From equations (2.3) and (2.4) we obtain α_{IC} as function of α_{NB} :

$$\alpha_{IC} = \alpha_{NB} - \frac{\left(\Delta x_{\alpha IC} - \Delta x_{\alpha NB}\right)}{TAS_{CG}^2}\left(a_{zCG} - g\cos\theta\cos\phi\right) - \frac{\left(\Delta x_{\alpha IC} - \Delta x_{\alpha NB}\right)}{TAS_{CG}}q \tag{2.5}$$

The same methodology was next applied to obtain β_{IC} as function of β_{NB} :

$$\beta_{IC} = \beta_{NB} + \frac{\left(\Delta x_{\beta IC} - \Delta x_{\beta NB}\right)}{TAS_{CG}}r - \frac{\left(\Delta z_{\beta IC} - \Delta z_{\beta NB}\right)}{TAS_{CG}}p \tag{2.6}$$

The sideslip angle β_{IC} theoretical is different than the sideslip angle calculated from equation (2.6). As shown in figure 6, therefore, the angle β_{IC} needs the following correction:

$$\beta_{IC} = \arctan\left(\tan\beta_{IC\,measured}\cos\alpha_{IC}\right) \tag{2.7}$$

The speeds components in the Instrumentation Center (IC) are:

$$\begin{aligned}
u_{IC} &= TAS_{IC}\cos\alpha_{IC}\cos\beta_{IC} \\
v_{IC} &= TAS_{IC}\sin\beta_{IC} \\
w_{IC} &= TAS_{IC}\sin\alpha_{IC}\cos\beta_{IC}
\end{aligned} \tag{2.8}$$
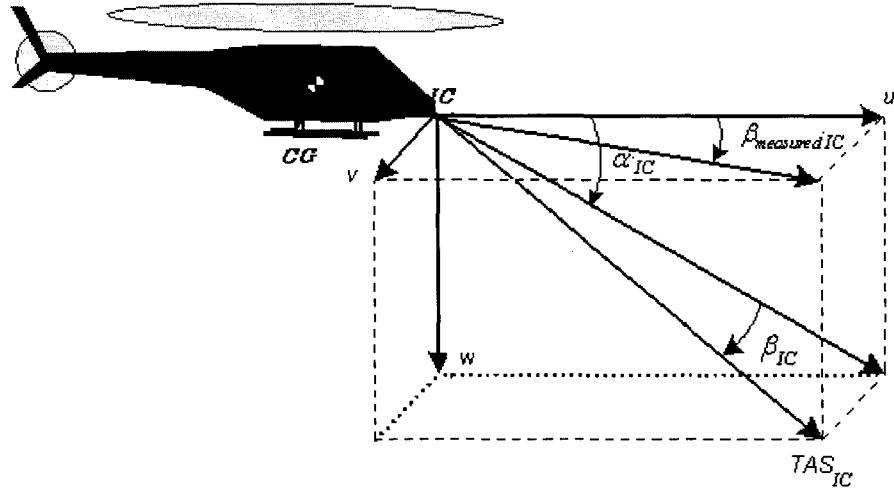
Figure 6 TAS measured at the Instrumentation Center *IC*

The speeds components at *IC* are written as function of the center of gravity (*CG*) components as shown in Figure 7:

$$\vec{V}_{IC} = \vec{V}_{CG} + \vec{\omega} \times \vec{r}$$ (2.9)

from where the velocity at the *CG*, $\vec{V}_{CG}$ is:

$$\vec{V}_{CG} = \vec{V}_{IC} - \vec{\omega} \times \vec{r} = \vec{i}u_{IC} + \vec{j}v_{IC} + \vec{k}w_{IC} - \begin{vmatrix} \vec{i} & \vec{j} & \vec{k} \\ p & q & r \\ x_{IC-CG} & y_{IC-CG} & z_{IC-CG} \end{vmatrix}$$ (2.10)

where

$$\vec{\omega} = \vec{i}p + \vec{j}q + \vec{k}r$$

$$\vec{r} = \vec{i}x_{IC-CG} + \vec{j}y_{IC-CG} + \vec{k}z_{IC-CG}$$

The components of rotational speeds $\vec{\omega}$ on the x_b, y_b, z_b axes are p, q, r and the position of *IC* with respect to *CG* is the r vector with its components on x_b, y_b, z_b axes are $x_{IC-CG}, y_{IC-CG}, z_{IC-CG}$.
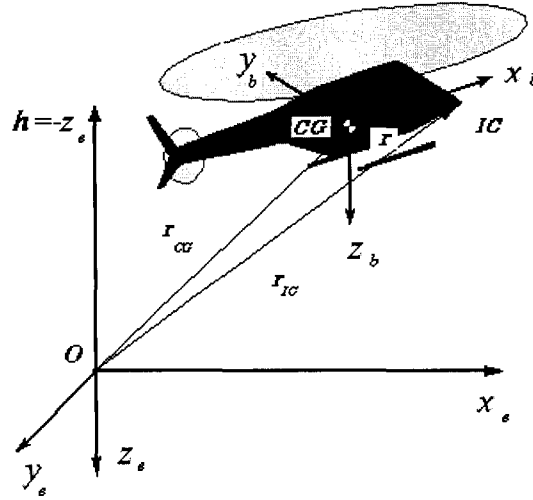
Figure 7 Helicopter's *IC* and *CG* in body and Earth reference systems

The speeds components at the *CG* are:

$$u_{CG} = u_{IC} - qz_{IC-CG} + ry_{IC-CG}$$

$$v_{CG} = v_{IC} - rx_{IC-CG} + pz_{IC-CG} \qquad (2.11)$$

$$w_{CG} = w_{IC} - py_{IC-CG} + qx_{IC-CG}$$

The *TAS* calculated at the *CG* (in the body reference system) is written as follows:

$$TAS_{CG} = \sqrt{u_{CG}^2 + v_{CG}^2 + w_{CG}^2} \qquad (2.12)$$

The *TAS* is calculated by the use of an iterative algorithm from the value measured in the *IC*, then translated in the *CG* and calculated by use of equations 2.11 and 2.12. When the difference between the value measured and the value calculated is zero the iteration stops.

2.2.2 Correction of accelerations

The accelerations are recorded by accelerometers located inside the helicopter at a different position than the CG. This point is considered the instrument center (IC) of the accelerations. The values of the accelerations recorded at the IC need to be corrected and translated to CG position.

The accelerometers located in the IC record the accelerations of the helicopter and the gravitational acceleration dependent on the attitude of the helicopter. The components of the accelerations measured by the accelerometers at the IC point are $a_{x_{IC}}, a_{y_{IC}}, a_{z_{IC}}$ and a_x, a_y, a_z are the calculated accelerations of the helicopter. Equation (2.13) calculates the helicopter accelerations from the recorded acceleration $a_{x_{IC}}, a_{y_{IC}}, a_{z_{IC}}$, corrected with the gravitational acceleration and the helicopter attitude angles.

$$
\begin{aligned}
a_x &= a_{x_{IC}} + g \sin \theta \\
a_y &= a_{y_{IC}} - g \cos \theta \sin \phi \\
a_z &= a_{z_{IC}} - g \cos \theta \cos \phi
\end{aligned}
$$

(2.13)

Next, the accelerations at CG are calculated from the accelerations at IC [1]:

$$
\vec{a}_{IC} = \frac{d\vec{V}_{IC}}{dt} = \dot{\vec{V}}_{IC} + \omega \times \vec{V}_{IC}
$$

(2.14)

By replacing equation (2.9) in equation (2.14) we obtain:

$$
\vec{a}_{IC} = \vec{a}_{CG} + \ddot{\vec{r}} + 2\omega \times \dot{\vec{r}} + \dot{\vec{\omega}} \times \vec{r} + \vec{\omega} \times (\vec{\omega} \times \vec{r})
$$

(2.15)

where $\vec{r} = \vec{i}x_{IC-CG} + \vec{j}y_{IC-CG} + \vec{k}z_{IC-CG}$ is the position of IC with respect to CG. The helicopter is considered a rigid body, thus $\dot{\vec{r}} = 0$ and $\ddot{\vec{r}} = 0$, therefore equation (2.15) becomes:

$$\vec{a}_{CG} = \vec{a}_{IC} - \dot{\vec{\omega}} \times \vec{r} - \vec{\omega} \times (\vec{\omega} \times \vec{r}) \qquad (2.16)$$

The components of linear accelerations in the body reference system corrected with the rotation rates p, q, r and rotation accelerations $\dot{p}, \dot{q}, \dot{r}$ of the helicopter at the CG position are given by the following equations decomposed on the three axes:

$$
\begin{aligned}
a_{x_{CG}} &= a_{x_{IC}} + x_{IC-CG}\left(q^2 + r^2\right) - y_{IC-CG}\left(pq - \dot{r}\right) - z_{IC-CG}\left(pr + \dot{q}\right) \\
a_{y_{CG}} &= a_{y_{IC}} + y_{IC-CG}\left(r^2 + p^2\right) - z_{IC-CG}\left(qr - \dot{p}\right) - x_{IC-CG}\left(qp + \dot{r}\right) \\
a_{z_{CG}} &= a_{z_{IC}} + z_{IC-CG}\left(p^2 + q^2\right) - x_{IC-CG}\left(rp - \dot{q}\right) - y_{IC-CG}\left(rq + \dot{p}\right)
\end{aligned}
\qquad (2.17)
$$

CHAPTER 3

SIMULATION MODEL

3.1 Modified mathematical model

As seen in the Chapter 1, a state space system is constructed to define the helicopter's motion as follows:

$$\dot{x} = [A]x + [B]u$$
$$y = [C]x + [D]u$$

(3.1)

where

$$x = \begin{bmatrix} \Delta u & \Delta v & \Delta w & \Delta p & \Delta q & \Delta r \end{bmatrix}^T \quad \text{and} \quad u = \begin{bmatrix} \Delta A_1 & \Delta B_1 & \Delta \theta_c & \Delta \theta_T \end{bmatrix}^T.$$

The aerodynamic and gravitational forces effects are included in the elements of the *A, B, C, D* matrices. The speeds recorded during particular flight missions such as hover are influenced by the wake of the rotor, and their values cannot be used for validation purposes. For this reason it is preferred to express the rotorcraft motions in terms of forces, i.e. accelerations which can be validated with respect to the recorded accelerations. In order to express the forces and moments acting on the helicopter, a modified mathematical model is needed and expressed as follows:

$$
\begin{bmatrix} \Delta X \\ \Delta Y \\ \Delta Z \\ \Delta L \\ \Delta M \\ \Delta N \end{bmatrix} = \begin{bmatrix} X_u & X_v & X_w & X_p & X_q & X_r \\ Y_u & Y_v & Y_w & Y_p & Y_q & Y_r \\ Z_u & Z_v & Z_w & Z_p & Z_q & Z_r \\ L_u & L_v & L_w & L_p & L_q & L_r \\ M_u & M_v & M_w & M_p & M_q & M_r \\ N_u & N_v & N_w & N_p & N_q & N_r \end{bmatrix} \begin{bmatrix} \Delta u \\ \Delta v \\ \Delta w \\ \Delta p \\ \Delta q \\ \Delta r \end{bmatrix} + \begin{bmatrix} X_{\delta_{long}} & X_{\delta_{coll}} & X_{\delta_{lat}} & X_{\delta_{ped}} \\ Y_{\delta_{long}} & Y_{\delta_{coll}} & Y_{\delta_{lat}} & Y_{\delta_{ped}} \\ Z_{\delta_{long}} & Z_{\delta_{coll}} & Z_{\delta_{lat}} & Z_{\delta_{ped}} \\ L_{\delta_{long}} & L_{\delta_{coll}} & L_{\delta_{lat}} & L_{\delta_{ped}} \\ M_{\delta_{long}} & M_{\delta_{coll}} & M_{\delta_{lat}} & M_{\delta_{ped}} \\ N_{\delta_{long}} & N_{\delta_{coll}} & N_{\delta_{lat}} & N_{\delta_{ped}} \end{bmatrix} \begin{bmatrix} \delta_{long} \\ \delta_{coll} \\ \delta_{lat} \\ \delta_{ped} \end{bmatrix} \quad (3.2)
$$

which is written under the following condensed form:

$$
\begin{bmatrix} \Delta X \\ \Delta Y \\ \Delta Z \\ \Delta L \\ \Delta M \\ \Delta N \end{bmatrix} = \begin{bmatrix} \tilde{C} \end{bmatrix} x + \begin{bmatrix} \tilde{D} \end{bmatrix} u \quad (3.3)
$$

This system of equations expresses the variations of forces and moments dues to the variations of states or controls, $\begin{bmatrix} \tilde{C} \end{bmatrix}$ is the stability derivatives matrix, $\begin{bmatrix} \tilde{D} \end{bmatrix}$ is the control derivatives matrix, $u = \begin{bmatrix} \delta_{long} & \delta_{coll} & \delta_{lat} & \delta_{ped} \end{bmatrix}^T$ is the control vector expressed directly in percentage (%) variations of the controls and $x = \begin{bmatrix} \Delta u & \Delta v & \Delta w & \Delta p & \Delta q & \Delta r \end{bmatrix}^T$ is the state vector of changes in translational and rotational speeds. This system of equations may be written even simpler by combining the two vectors x and u in one single vector of variations x^* and a single unified matrix A^*, as shown in the following equation:

$$
\begin{bmatrix} \Delta X \\ \Delta Y \\ \Delta Z \\ \Delta L \\ \Delta M \\ \Delta N \end{bmatrix} = \begin{bmatrix} X_u & X_v & X_w & X_p & X_q & X_r & X_{\delta_{long}} & X_{\delta_{coll}} & X_{\delta_{lat}} & X_{\delta_{ped}} \\ Y_u & Y_v & Y_w & Y_p & Y_q & Y_r & Y_{\delta_{long}} & Y_{\delta_{coll}} & Y_{\delta_{lat}} & Y_{\delta_{ped}} \\ Z_u & Z_v & Z_w & Z_p & Z_q & Z_r & Z_{\delta_{long}} & Z_{\delta_{coll}} & Z_{\delta_{lat}} & Z_{\delta_{ped}} \\ L_u & L_v & L_w & L_p & L_q & L_r & L_{\delta_{long}} & L_{\delta_{coll}} & L_{\delta_{lat}} & L_{\delta_{ped}} \\ M_u & M_v & M_w & M_p & M_q & M_r & M_{\delta_{long}} & M_{\delta_{coll}} & M_{\delta_{lat}} & M_{\delta_{ped}} \\ N_u & N_v & N_w & N_p & N_q & N_r & N_{\delta_{long}} & N_{\delta_{coll}} & N_{\delta_{lat}} & N_{\delta_{ped}} \end{bmatrix} \begin{bmatrix} \Delta u \\ \Delta v \\ \Delta w \\ \Delta p \\ \Delta q \\ \Delta r \\ \delta_{long} \\ \delta_{coll} \\ \delta_{lat} \\ \delta_{ped} \end{bmatrix} \quad (3.4)
$$

which is written under the following concise form:

$$
\begin{bmatrix} \Delta X \\ \Delta Y \\ \Delta Z \\ \Delta L \\ \Delta M \\ \Delta N \end{bmatrix} = \begin{bmatrix} A^* \end{bmatrix} x^* \qquad \text{where} \quad x^* = \begin{bmatrix} \Delta u & \Delta v & \Delta w & \Delta p & \Delta q & \Delta r & \delta_{long} & \delta_{coll} & \delta_{lat} & \delta_{ped} \end{bmatrix}^T \quad (3.5)
$$

The variations in forces and moments with respect to a trim state are known, and therefore we calculate all helicopter states by Newton's equations integration. The trim states of the helicopter are used as initial conditions.

3.2 Simulink model

The programming environment is Matlab® version 6.5 release 13 with Simulink®, due to its facilities in solving real time simulations. One of its facilities is also the Aerospace Blockset with the 6DoF block which integrates Newton's equations of motion and the conversion from body axes system to Earth axes system.

The $A*$ matrix is obtained by use of the MLE (Maximum Likelihood Estimation) from the recorded parameters during flight tests. This MLE method was extensively described in the ref [7]. The $A*$ matrix is generated by MLE in terms of linear and angular accelerations instead of forces and moments as shown in the paragraph 3.1. For this reason the accelerations are calculated by dividing the equations (1.4) representing forces X, Y, Z, by the mass m:

$$\begin{bmatrix} a_x \\ a_y \\ a_z \end{bmatrix} = \frac{1}{m} \begin{bmatrix} X \\ Y \\ Z \end{bmatrix} = \begin{bmatrix} \dot{u} \\ \dot{v} \\ \dot{w} \end{bmatrix} + \begin{bmatrix} p \\ q \\ r \end{bmatrix} \times \begin{bmatrix} u \\ v \\ w \end{bmatrix} \tag{3.6}$$

The same procedure is applied to the moments in equation (1.7), multiplied by the inertia matrix inverse and the total angular accelerations e_x, e_y, e_z are obtained:

$$\begin{bmatrix} e_x \\ e_y \\ e_z \end{bmatrix} = [I]^{-1} \begin{bmatrix} L \\ M \\ N \end{bmatrix} = \begin{bmatrix} \dot{p} \\ \dot{q} \\ \dot{r} \end{bmatrix} + [I]^{-1} \begin{bmatrix} p \\ q \\ r \end{bmatrix} \times [I] \begin{bmatrix} p \\ q \\ r \end{bmatrix} \tag{3.7}$$

where

$$[I] = \begin{bmatrix} I_{xx} & -I_{xy} & -I_{xz} \\ -I_{xy} & I_{yy} & -I_{yz} \\ -I_{xz} & -I_{yz} & I_{zz} \end{bmatrix}$$

Equations (3.6) represent the Newton's equation of forces expressed in terms of linear accelerations and equations (3.7) represent the momentum equation expressed in terms of angular accelerations.

The A^* matrix shown in equations (3.4) and (3.5), is calculated for a particular flight condition (mission, atmospheric conditions, A/C loading, etc.). The A^* matrix is calculated at a certain neighbourhood around a trim state given by the initial helicopter configuration. The problem arising for a complex simulator is the departure of the helicopter state from the initial conditions, and thus, their estimated values from equilibrium point.

For example, the helicopter accelerates from 30 knots to 90 knots, or climbs from the ground (0 ft) to the altitude of 3000 ft, which in these cases gives the values of A^* matrix elements containing the stability and control derivatives, significantly different from the A^* matrix elements estimated initially.

For the global model with all flight conditions, the building of several modules which contains the mathematical models (the A^* matrices) for all flight conditions is required.

For a better understanding of the mathematical model, Figure 8 shows the Simulink schema of a helicopter simulator for one flight condition corresponding to a unique A^* matrix. Figure 9 shows the 6DoF (Euler angles) Blockset modified as described by equations (3.6) and (3.7).
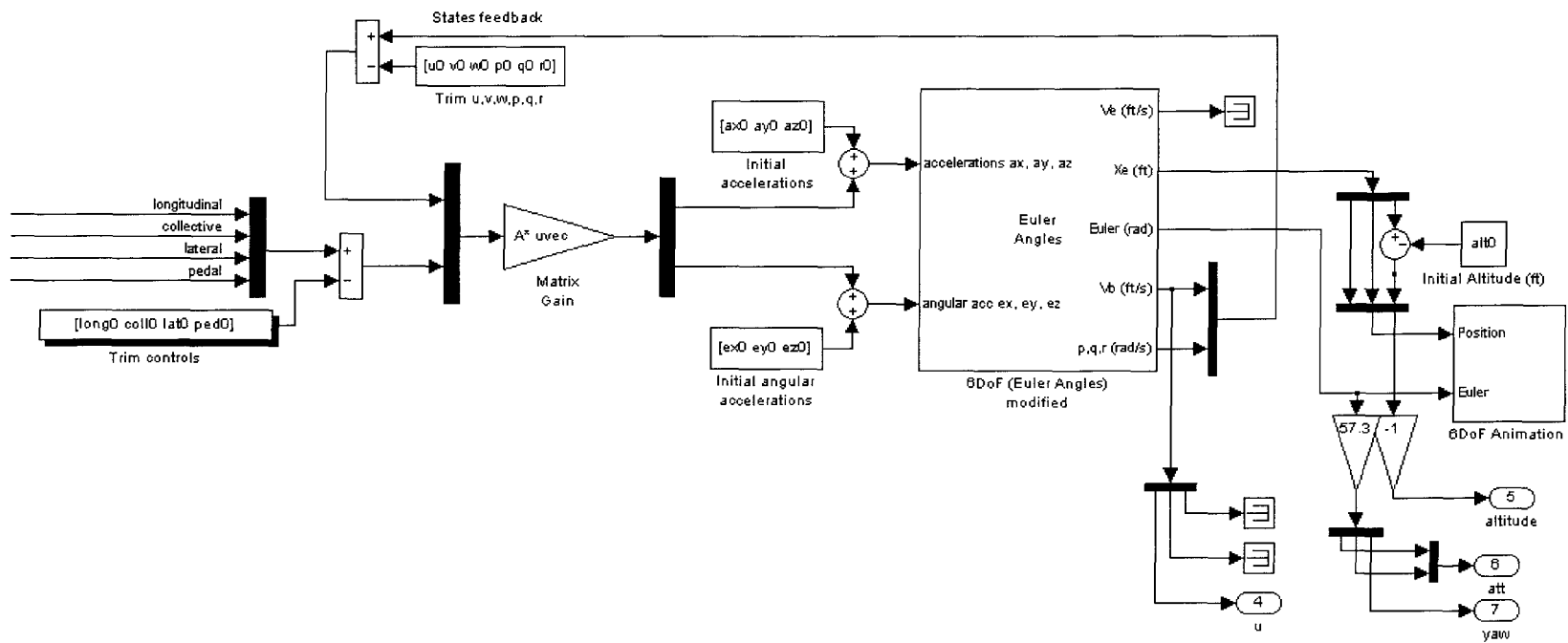
Figure 8   Simulink schematics of a simplified helicopter simulator by use of the Aerospace Blockset
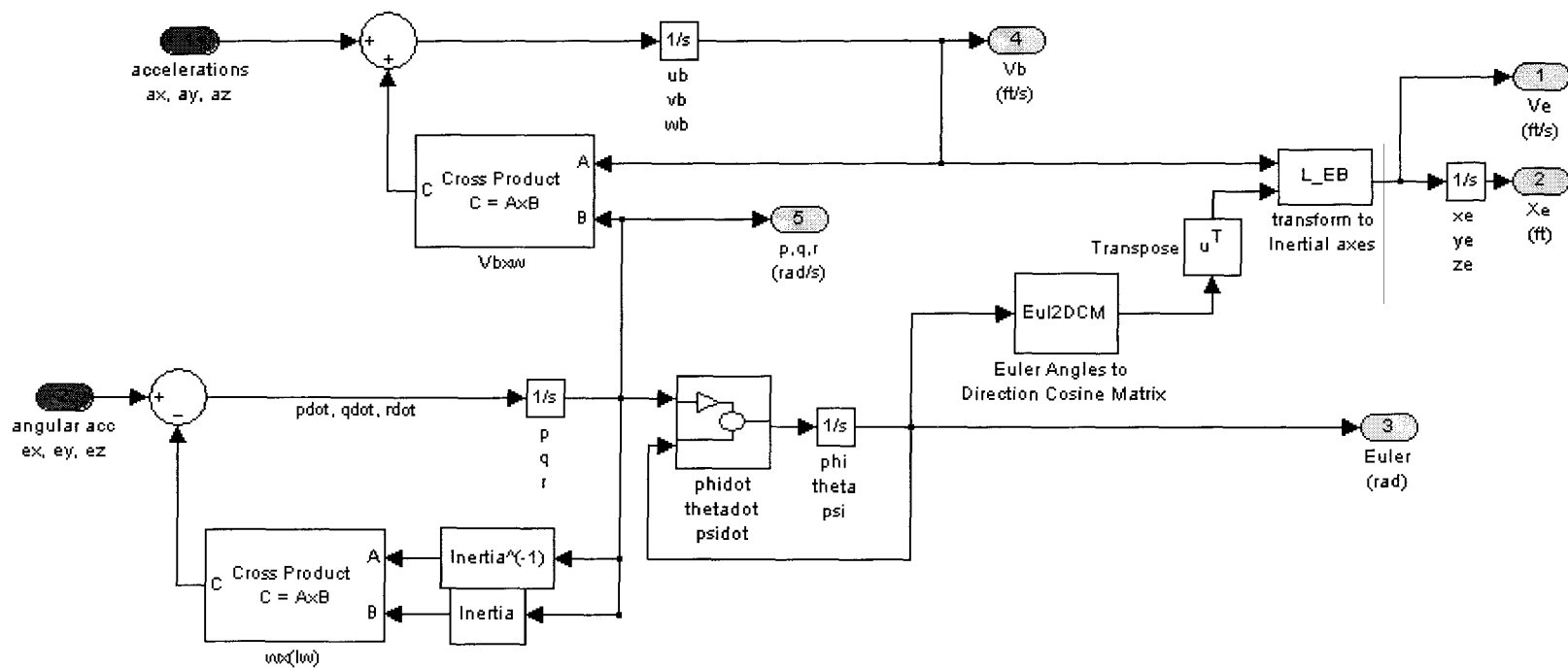
Figure 9   Simulink schematics of modified 6 Dof (Euler Angles) Blockset showing the equations (3.6) and (3.7) integration
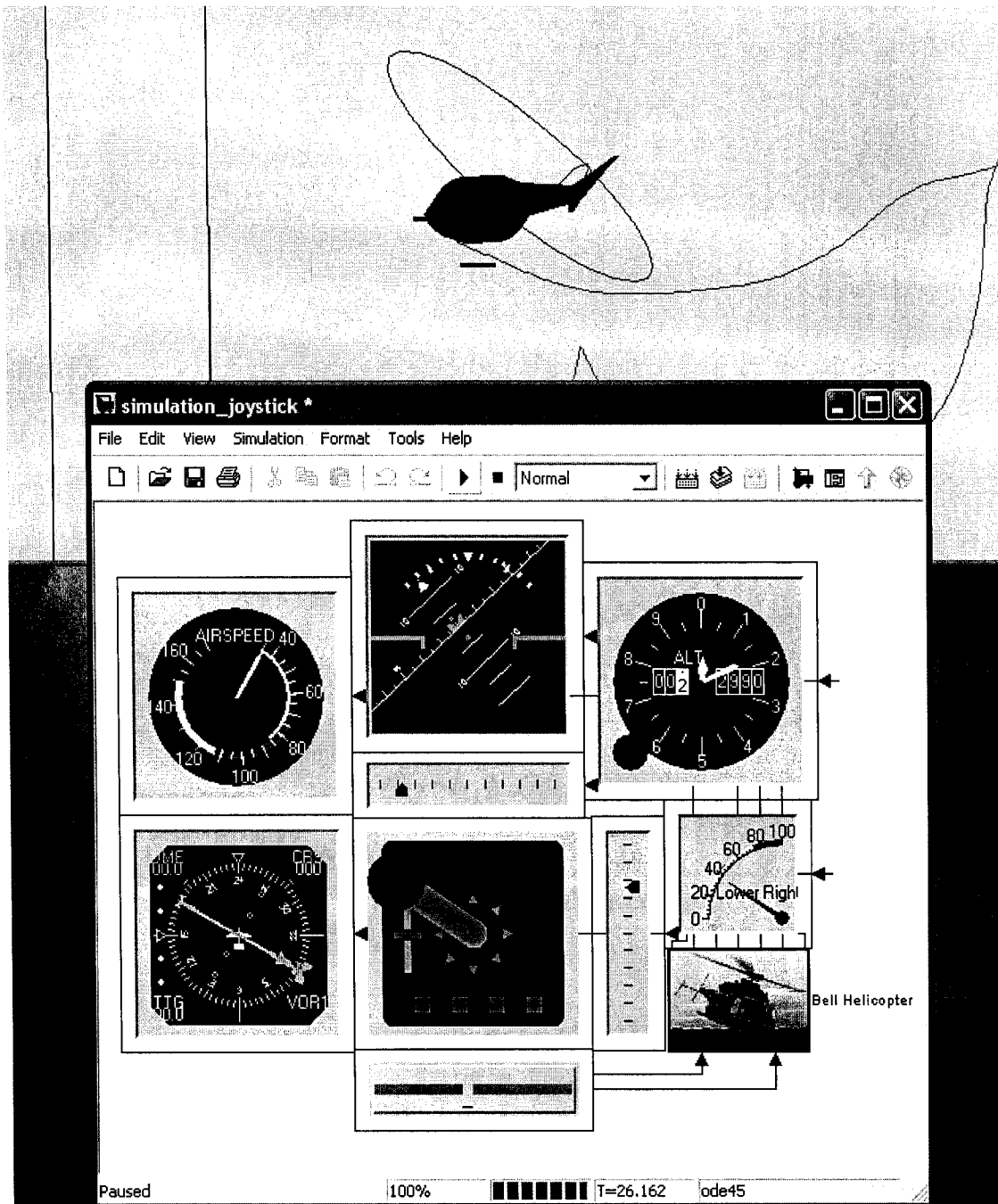
Figure 10 Simulation by use of the Simulink 6 degrees of freedom Animation Blockset, GMS Joystick & Aircraft Instrument ActiveX Control Blockset

3.3 Global model

The global model is a composition of several distinct simulation models for various helicopter loadings and flight conditions. The flight conditions such as Hover, Vertical Climb, Level Flight, Climb or Descent are some particular zones in the flight envelope. From aerodynamical point of view, the Hover and Vertical Climb flight conditions are different from the Level Flight, Climb or Descent flight conditions; therefore there exist two distinct aerodynamic models defining these two sets of flight conditions: the Hover model and the Up And Away (UAA) model. There exist also other distinct models for One Engine Inoperative (OEI) flight condition and Autorotation flight condition. Hover model has two distinct models for defining the In Ground Effect (IGE) and Out of Ground Effect (OGE) aerodynamical interferences. Each model is divided in several sub-models for each point in the flight envelope (each combination airspeed and altitude) where the first set of flight tests were performed.

The same helicopter in different configurations of loading and center of gravity positions acts differently from point of view of aerodynamics laws. Therefore there are three combinations of loading-position of center of gravity defined as: Light-Aft (LA) model which simulates the motion of the helicopter with no loading and the aft CG position due to the weight of the engines; Heavy-Aft (HA) model which simulates the motion of the helicopter with maximum loading allowed for the maximum aft CG position; and Heavy-Forward (HF) model which simulates the motion of the helicopter with the maximum loading allowed for the maximum CG forward position.

For each flight conditions combination of loading, airspeed, altitude (such as: Level Flight, IAS 70 knots, Heavy/Fwd, altitude 6000 ft), there is a unique A^* matrix which defines entirely the helicopter's motion at that specific flight condition.

For a helicopter, the number of A^* matrices is the same as the number of flight conditions to define the entire flight envelope. The A^* matrices are calculated at the helicopter's trim position and for small variations around the trim condition for that specific flight condition.

The simulator software has as input the state of the helicopter and the condition of flight, and by the use of a look-up table function picks the appropriate matrices and by the use of an interpolation function calculates the stability and control derivatives (i.e. matrix A^*) for that flight condition.

Example: Two tables of derivatives X_u calculated for two different loadings (3900 lbs – Light/Aft and 6300 lbs – Heavy/Fwd), two different speeds (70 knots IAS and 90 knots IAS) and two different altitudes (3000 ft and 6000 ft) are known:

Table III

Derivatives of the X_u force in Heavy/Fwd configuration

X_u (Heavy/Fwd,6300 lbs)	3000 ft	6000 ft
70 knots	$X_u^{HF,70,3000}$	$X_u^{HF,70,6000}$
90 knots	$X_u^{HF,90,3000}$	$X_u^{HF,90,3000}$

Table IV

Derivatives of the X_u force in Light/Aft configuration

X_u (Light/Aft, 3900 lbs)	3000 ft	6000 ft
70 knots	$X_u^{LA,70,3000}$	$X_u^{LA,70,6000}$
90 knots	$X_u^{LA,90,3000}$	$X_u^{LA,90,3000}$

The problem is to calculate the derivative X_u at an altitude of 4000 ft, *IAS* 85 knots, and a loading *GW* of 5000 lbs. We calculate the derivatives X_u^{5000} for the loading of 5000 lbs by an interpolation in the two tables for the *GW* by use of a linear variation in the interval 3900 − 6300 lbs as follows:

$$X_u^{5000} = \frac{5000 - 3900}{6300 - 3900}\left(X_u^{HF} - X_u^{LA}\right) + X_u^{LA}$$

We obtain a table of derivatives at the *GW* of 5000 lbs, and by interpolation in the *IAS* interval of 70 − 90 knots, we obtain X_u^{5000} at 85 knots:

Table V

Derivatives of the X_u force at 5000 lbs configuration

X_u (5000 lbs)	3000 ft	6000 ft
70 knots	$X_u^{5000, 70, 3000}$	$X_u^{5000, 70, 6000}$
90 knots	$X_u^{5000, 90, 3000}$	$X_u^{5000, 90, 3000}$

$$X_u^{5000,85} = \frac{85 - 70}{90 - 70}\left(X_u^{5000,90} - X_u^{5000,70}\right) + X_u^{5000,70}$$

We obtained two derivatives both at *GW* of 5000 lbs and *IAS* of 85 knots, one derivative at 3000 ft and the other derivative at 6000 ft, and by the interpolations in altitude in the interval 3000 − 6000 ft, we obtain:

$$X_u^{5000,85,4000} = \frac{4000 - 3000}{6000 - 3000}\left(X_u^{5000,85,6000} - X_u^{5000,85,3000}\right) + X_u^{5000,85,3000}$$

This operation is called "Look-up table" in a 3 dimensional format, with the dimensions of loading, speed and altitude. Actually there are 4 dimensions, the fourth being the *CG*

position. For interpolating in *CG* position, the same linear interpolation principle is applied. Here, an interpolation only by *GW* was shown for simplicity reasons.

The *X* force acting on the helicopter in a specified flight condition is given by the following equation:

$$
\begin{aligned}
\Delta X = \; & X_u \Delta u + X_v \Delta v + X_w \Delta w + X_p \Delta p + X_q \Delta q + X_r \Delta r + \\
& X_{\delta_{long}} \delta_{long} + X_{\delta_{lat}} \delta_{lat} + X_{\delta_{ped}} \delta_{ped} + X_{\delta_{coll}} \delta_{coll}
\end{aligned}
\tag{3.8}
$$

where all stability and control derivatives were calculated in the same manner as the one described above. This operation should be done for each of the six forces and moments and for each of the ten entries, the elements correspondent to the state and control vector x^*, which means 60 individual interpolations for each term of the A^* matrix.

Matlab has the facility in which all operations can be done directly with matrices by vectorization, and thus the entire matrix A^* can be found very fast. For example interpolation in *GW* of 5000 lbs between the intervals of 3900 lbs and 6300 lbs, we find the A^* matrices table for the helicopter loaded at 5000 lbs:

$$
A^{*5000} = \frac{5000-3900}{6300-3900} \left(A^{*HF} - A^{*LA} \right) + A^{*LA}
\tag{3.9}
$$

Equation (3.9) is an example of interpolation in tables in one dimension *GW*. In the two dimensional case, in which the first dimension is *GW* and the second dimension is *IAS*, the general formula is obtained as follows:

$$
A^{*5000,85} = \frac{S_1}{S} A^{*GW_1, IAS_1} + \frac{S_2}{S} A^{*GW_2, IAS_1} + \frac{S_3}{S} A^{*GW_2, IAS_2} + \frac{S_4}{S} A^{*GW_1, IAS_2}
\tag{3.10}
$$

where

$$S = (GW_2 - GW_1)(IAS_2 - IAS_1)$$

$$S_1 = (GW_2 - 5000)(IAS_2 - 85)$$

$$S_2 = (5000 - GW_1)(IAS_2 - 85)$$

$$S_3 = (5000 - GW_1)(85 - IAS_1)$$

$$S_4 = (GW_2 - 5000)(85 - IAS_1)$$

and S_1/S, S_2/S, S_3/S, S_4/S are the weights of interpolation of unknown matrix $A*$ at the GW of 5000 lbs and IAS of 85 knots by the use of four known matrices $A*$ at the loading GW_1, GW_2 and speeds IAS_1 and IAS_2.

In the same manner, in the third dimension, the altitude ALT could be added. For the interpolation in altitude there are required eight known matrices $A*$ at the loading GW_1, GW_2, speeds IAS_1 and IAS_2 and altitudes ALT_1 and ALT_2 as follows:

$$
\begin{aligned}
A^{*5000,85,4000} = &\frac{S_1}{S} A^{*GW_1,IAS_1,ALT_1} + \frac{S_2}{S} A^{*GW_2,IAS_1,ALT_1} + \frac{S_3}{S} A^{*GW_2,IAS_2,ALT_1} + \frac{S_4}{S} A^{*GW_1,IAS_2,ALT_1} \\
&+ \frac{S_5}{S} A^{*GW_1,IAS_1,ALT_2} + \frac{S_6}{S} A^{*GW_2,IAS_1,ALT_2} + \frac{S_7}{S} A^{*GW_2,IAS_2,ALT_2} + \frac{S_8}{S} A^{*GW_1,IAS_2,ALT_2}
\end{aligned}
\tag{3.11}
$$

where

$$S = (GW_2 - GW_1)(IAS_2 - IAS_1)(ALT_2 - ALT_1)$$

$$S_1 = (GW_2 - 5000)(IAS_2 - 85)(ALT_2 - 4000)$$

$$S_2 = (5000 - GW_1)(IAS_2 - 85)(ALT_2 - 4000)$$

$$S_3 = (5000 - GW_1)(85 - IAS_1)(ALT_2 - 4000)$$

$$S_4 = (GW_2 - 5000)(85 - IAS_1)(ALT_2 - 4000)$$

$$S_5 = (GW_2 - 5000)(IAS_2 - 85)(4000 - ALT_1)$$

$$S_6 = (5000 - GW_1)(IAS_2 - 85)(4000 - ALT_1)$$

$$S_7 = (5000 - GW_1)(85 - IAS_1)(4000 - ALT_1)$$

$$S_8 = \left(GW_2 - 5000 \right)\left(85 - IAS_1 \right)\left(4000 - ALT_1 \right)$$

In this way as many dimensions as required can be added.

The global model will contain several modules which define the following flight conditions: Hover IGE, Hover OGE, Horizontal flight IGE, Horizontal flight – climb - descent OGE, Autorotation, Take Off, Landing, etc. Each module contains the $A*$ matrices at different loadings, speeds, altitudes and any other parameters which may bring a difference in the stability and controllability of the helicopter.

The helicopter makes several transitions between flight conditions during a flight. For example, a take off procedure will be performed in the following manner: Hover IGE, Vertical Flight, transition between Vertical Flight and Horizontal Flight, Horizontal Flight IGE, Climb, Horizontal Flight OGE. To simulate such a type of flight condition is required to make the transition between the different models of the helicopter. The transition model will make the links between all flight conditions models.

At this stage, is necessary for the helicopter model to be validated according to the FAA Advisory Circular AC 120-63 [9]. This step is necessary for the model certification and for its implementation in a flight simulator to be used in training programs. The model validation is presented in the following chapter.

CHAPTER 4

MODEL VALIDATION

4.1 Helicopter simulator qualification

For the certification of a helicopter simulator for training programs and airman checking under various parts of the Federal Aviation Regulations it is necessary to be evaluated and approved in according with Advisory Circular AC 120-63 [9]. This AC provides the criteria and the guidelines for the helicopter simulator evaluation and qualification.

There are currently three levels of complexity of helicopter simulators: levels B, C and D. The AC states that the effects of aerodynamic changes for various combinations of drag and thrust normally encountered in flight corresponding to actual flight conditions, including the effect of change in helicopter attitude, aerodynamic and propulsive forces and moments, altitude, temperature, gross weight, center of gravity location should be present in all simulator levels. Also all levels of simulators should include the ground effect and as well as ground reaction for the simulation of a landing procedure. The model simulator of the helicopter Bell 427 has to satisfy the highest level D requirements.

In addition is required a means for quickly and effectively testing simulator programming which may be used for conducting the tests in the Quality Test Guide (QTG). This requirement is fulfilled by a program written in Matlab language, Proof-of-Match (POM) which is proprietary software developed by the National Research Council Canada's (NRC-CNRC) Flight Research Laboratory (FRL). The use of this software will be presented in the paragraph 4.3.

4.2 Quality test guide (QTG)

The QTG is a compulsory requirements list for the validation of a helicopter simulator. This list contains all manoeuvres and several configurations of the helicopter during these manoeuvres which covers the helicopter flight envelope:

Table VI

Quality Test Guide

Code	Manoeuvre	GW	CG	Hd (ft)	IAS (knots)
1a	**Engine Assessment**				
1a1a	**Start to Steady State Idle**				
	Rotor Brake Used - Eng #1	-	-	0	-
	Rotor Brake Used - Eng #2	-	-	0	-
	Rotor Brake NOT Used - Eng #1	-	-	0	
	Rotor Brake NOT Used - Eng #2	-	-	0	-
1a1b	**Steady State Idle to Operation RPM**				
	Rotor Brake Used - Eng #1	-	-	0	-
	Rotor Brake Used - Eng #2	-	-	0	-
	Rotor Brake NOT Used - Eng #1	-	-	0	
	Rotor Brake NOT Used - Eng #2	-	-	0	-
1a2	**Power Turbine Speed Trim (Can use data from other climb/descent tests)**				
	Power Up Collective Step Inputs.	-	-	0	-
	Power Down Collective Step Inputs.	-	-	0	-
1a3	**Engine & Rotor Speed (Climb/Descent)**				
	Engine & Rotor Speed - Climb	-	-	3000	
	Engine & Rotor Speed - Descent	-	-	3000	
1d	**Hover Performance**				
	IGE	Light	-	IGE	0
	IGE	Heavy	-	IGE	0
	OGE	Light	-	OGE	0
	OGE	Heavy	-	OGE	0
1e	**Vertical Climb**				
	Heavy Weight	Heavy	-	OGE	-
	Light Weight	Light	-	OGE	-
1f	**Level Flight (Two gross weigh/CG combination)**				
	Weight/CG Combination #1 - Cruise	Light	Aft	3000	60
	Weight/CG Combination #2 - Cruise	Heavy	Fwd	3000	80

Table VI (continued)

Quality Test Guide

Code	Manoeuvre	GW	CG	Hd (ft)	IAS (knots)
1g	**Climb Performance (Two gross weight/CG combination)**				
	All Engines Operative #1	Light	Aft	1500	60
	All Engines Operative #2	Heavy	Aft	3350	115
	One Engine Inoperative #1	-	-	6000	
	One Engine Inoperative #2	-	-	6000	
1h1	**Descent Performance (Two gross weight/CG combination)**				
	Weight/CG combination #1	Light	Aft	3000	70
	Weight/CG combination #2	Heavy	Fwd	3000	50
1h2	**Autorotation Performance (Two gross weights)**				
	Heavy				
	Light				
1i	**Autorotational Entry (From cruise or climb)**				
	Weight	-	-	3000	
1j	**Landing**				
1j1	All Engines Operative	-	-		
1j2	OEI – Cat A Completed	-	-		
2b1	**Low Speed Controllability** **(Several speed increments to translational limit and 45 knots)**				
	Trimmed Flight Conditions – Forward	-	-	IGE	
	Trimmed Flight Conditions – Sideward	-	-	IGE	
	Trimmed Flight Conditions – Rearward	-	-	IGE	
2b2	**Critical Azimuth (Three relative wind directions)**				
	Direction #1	-	-	Hover	
	Direction #2	-	-	Hover	
	Direction #3	-	-	Hover	
2b3	**Control Response**				
2b3a	Longitudinal	-	-	Hover	
2b3b	Lateral	-	-	Hover	
2b3c	Directional	-	-	Hover	
2b3d	Vertical	-	-	Hover	
2c	**Longitudinal Handling Qualities**				
2c1	**Control Response (F/A Step inputs and Collective)**				
	Control Response – F/A	Light	Aft	3000	117
	Control Response – Collective	Heavy	Fwd	3000	60
2c2	**Static Stability (Minimum 2 speeds on each side of trim)**				
	Static Stability – Cruise/Climb	Heavy	Aft	3000	91
	Static Stability – Cruise/Climb	Heavy	Fwd	3000	103

Table VI (continued)

Quality Test Guide

Code	Manoeuvre	GW	CG	Hd (ft)	IAS (knots)
2c2	Static Stability - Autorotation	-	-	3000	
2c3	Dynamic Stability (Cruise or Climb. Minimum 2 speeds on each side of trim)				
2c3a	Dynamic Stability – Long period	-	-	3000	
2c3b	Dynamic Stability - Short Period- Speed #1	-	-	3000	
2c3b	Dynamic Stability - Short period- Speed #2	-	-	3000	
2c4	Manoeuvring Stability (Minimum 2 speeds on each side of trim)				
	Manoeuvring Stability - Speed 1 (30 deg)	Heavy	Aft	3000	60
	Manoeuvring Stability - Speed 2 (30 deg)	Heavy	Aft	3000	117
	Manoeuvring Stability - Speed 1 (45 deg)	Heavy	Aft	3000	60
	Manoeuvring Stability - Speed 2 (45 deg)	Heavy	Aft	3000	117
2d	Lateral/Directional Handling Qualities				
2d1	Control Response				
2d1a	Control Response - Lateral	Light	Aft	3000	60
2d1b	Control Response - Directional Speed 1	Light	Aft	3000	117
2d1b	Control Response - Directional Speed 2	Heavy	Aft	3000	60
2d2	Directional Static Stability				
	Directional Static Stability - Climb/Cruise	Heavy	Aft	3000	60
	Directional Static Stability - Climb/Cruise	Heavy	Aft	3000	60
	Directional Static Stability - Climb/Cruise	Heavy	Fwd	3000	117
	Directional Static Stability - Climb/Cruise	Heavy	Fwd	3000	117
	Directional Static Stability - Descent	Heavy	Aft	3000	102
	Directional Static Stability - Descent	Heavy	Aft	3000	102
	Directional Static Stability - Descent	Heavy	Aft	3000	102
	Directional Static Stability - Descent	Heavy	Aft	3000	102
2d3a	Dynamic Stability, Lateral/Directional Oscillations				
	Dynamic Stability - Climb/Cruise Speed 1	Light	Aft	3000	60
	Dynamic Stability - Climb/Cruise Speed 2	Light	Aft	3000	115
2d3b	Spiral Stability (Cyclic Only turns Left and Right turns until +/- 30° bank angle)				
	Spiral Stability - Cruise/Climb Left	Heavy	Aft	3000	60
	Spiral Stability - Cruise/Climb Right	Heavy	Aft	3000	60

All the simulation flights from the Table should be matched with recorded flights inside the tolerances stated in the Appendix 2 of AC 120-63 [9]. Here are presented parts of Appendix 2 in Table VII on various flight conditions:

Table VII

Table of validation tests – tolerances and flight conditions

Code	Tests	Tolerance	Flight Conditions and Comments
1c	Takeoff (All engines and OEI)	Airspeed ±3 kt Altitude ±20 ft (6.1m) Torque ±3% Rotor Speed ±1.5% Vertical Velocity ±100 fpm (0.5 m/sec) or 10% Pitch Attitude ±1.5 deg Bank Attitude ± 2 deg Heading ± 2 deg Longitudinal Control Position ± 10% Lateral Control Position ± 10% Directional Control Position ± 10% Collective Control Position ±10%	Ground/Takeoff and Initial Segment of Flight. Time history of takeoff flight path as appropriate to helicopter model simulated. Record data to at least 200ft (61m) AGL.
1d	Hover Performance	Torque ±3% Pitch Attitude ±1.5 deg Bank Attitude ±1.5 deg Longitudinal Control Position ±5% Lateral Control Position ±5% Directional Control Position ±5% Collective Control Position ±5%	In Ground Effect (IGE) Out of Ground Effect (OGE) Light/Heavy Gross Weights Snapshot Test
1e	Vertical Climb	Vertical Velocity ±100 fpm (0.5 m/sec) or 10% Directional Control Position ±5% Collective Control Position ±5%	From OGE Hover. Light/Heavy Gross Weights Snapshot Test
1i	Autorotational Entry	Rotor speed ± 3% Pitch Attitude ± 2 deg Roll Attitude ± 3 deg Yaw Attitude ± 5 deg Airspeed ± 5 kt Vertical Velocity ± 200 fpm (1 m/sec) or 10%	Cruise or Climb Time history of vehicle response to a rapid throttle reduction to idle.
2d1	Lateral and Directional Handling Qualities (a) Control Response Lateral	Roll Rate ± 10% or ± 3 deg/sec Roll Attitude Change ± 10% or 3 deg	Cruise Augmentation On/Off Step control input Off axis response must show correct trend for unaugmented cases.
2d1	(b) Control Response Directional	Yaw Rate ± 10% or ± 2 deg/sec Yaw Attitude Change ± 10% or ± 2 deg	Cruise Augmentation On/Off Step control input Off axis response must show correct trend for unaugmented cases.

Table VII (continued)

Table of validation tests — tolerances and flight conditions

2d2	Directional Static Stability	Lateral Control Position ± 10% of change from trim Roll Attitude ± 1.5 deg Directional Control Position ± 10% of change from trim Longitudinal Control Position ± 10% of change from trim Vertical Velocity ± 100 fpm (0.5m/sec) or 10%	Cruise or Climb/Descent Augmentation On/Off Steady heading sideslip Minimum of two sideslip angles on either side of the trim point. Snapshot test.
2d3	Dynamic Lateral and Directional Stability (a) Lateral-Directional Oscillations	± 0.5 sec or 10% of Period ± 10% of time to ½ or Double Amplitude or ± .02 of Damping Ratio ± 20% or ± 1 sec of Time Difference Between Peaks of Bank and Sideslip	Cruise or Climb Augmentation On/Off Two Airspeeds. Excite with cyclic or pedal doublet. Test should include six full cycles (12 overshoots after input completed) or that sufficient to determine time to ½ or Double Amplitude whichever is less. For non-periodic response, time history should be matched
2d3	(b) Spiral Stability	Correct Trend, ± 2 deg Bank or 10% in 20 sec	Cruise or Climb Augmentation On/Off Time history of release from pedal only or cyclic only turns in both directions.

In this thesis only a subset of QTG validation is presented. This subset consists of Hover performance, Autorotation performance and Lateral/Directional handling qualities. The Engine assessment, Ground operations, Takeoff, Level flight, Climb, Descent, Landing performance, Control system mechanical characteristics, Low airspeed handling qualities, Longitudinal handling qualities, Motion system and Visual system requirements of the AC 120-63 are not included in this thesis.

4.3   Proof-of-Match (POM)

The Proof-of-Match is used to validate the helicopter mathematical model. By the use of POM we compare on the same plot the parameters recorded during a flight test with the results obtained from the model simulation with the same initial conditions of the flight test. Differences between results obtained by simulator and recorded data are due to the errors and noise of the signals recorded by the instruments, and by the approximations and errors of the MLE method [7]. Because of the fact that the method used to obtain the helicopter model is an estimation likelihood method, the model results will be estimations of the parameters for a certain flight test case. For the model validation it is required that the parameters estimated have to be near the recorded parameters and should be inside certain tolerances according to the flight case. There are two types of input data by use of the POM software:

1. The initial conditions are stored in a Test Definition File (TDF),
2. The tolerances required for the parameters for each flight condition as stated in the AC 120-63 are stored in a Graphic Definition File (GDF) as shown in Figure 11.

Both TDF and GDF files are automatically generated by separated programs from the main POM software. Following the generation of these files, the operator can edit manually the values of initial conditions.

GDF Options

```
maxControl   = 100      [deg]
Long         = 5        [%] (max/min)
Coll         = 5        [%] (max/min)
Lat          = 5        [%] (max/min)
Ped          = 5        [%] (max/min)
P_rate       = 3        [deg/s] (max/min)
Q_rate       = 3        [deg/s] (max/min)
R_rate       = 3        [deg/s] (max/min)
Phi_att      = 1.5      [deg] (max/min)
Theta_att    = 1.5      [deg] (max/min)
Psi_att      = 2        [deg] (max/min)
Alpha_aoa    = 2        [deg] (max/min)
Beta_roll    = 2        [deg] (max/min)
Mach         = 0.003    [-] (max/min)
U_vel        = 3        [ft/s] (max/min)
V_vel        = 3        [ft/s] (max/min)
W_vel        = 1.67     [ft/s] (max/min)
Ax           = 3        [ft/s2] (max/min)
Ay           = 3        [ft/s2] (max/min)
Az           = 3        [ft/s2] (max/min)
Alt          = 20       [ft] (max/min)
EngTorque    = 3        [%] (max/min)
```

Figure 11 Sample of a Graphic Definition File input

TDF Options

```
23-Jun-2005 15:31:41
------------------------------------------------
        Manoeuver: Hover Performance (1d)
        Model Selected: Hover
        GE Model Selected: Hover GE
------------------------------------------------
dataFile            = 't909r19_m.dat'
manoeuver           =        '1d'       [from QTG_Check.xls]
startTime           =        0.00       [sec]
endTime             =        2.00       [sec]
TRIMf               = 'TrimAngAccel'     -> edit: PDOT,QDOT,RDOT
subTRIMf            = 'subTrimRate'      -> p/q/rdot = 0
ROLL_RATE           =                   [deg/s]
PITCH_RATE          =                   [deg/s]
YAW_RATE            =                   [deg/s]
X_ACCEL             =                   [ft/s2]
Y_ACCEL             =                   [ft/s2]
Z_ACCEL             =                   [ft/s2]
U_VEL               =                   [ft/s]
V_VEL               =                   [ft/s]
W_VEL               =                   [ft/s]
DENSITY_ALTITUDE    =                   [ft]
ROLL_ANGLE          =                   [deg]
SIDESLIP_ANGLE      =                   [deg]
HEADING_ANGLE       =                   [deg]
ANGLE_OF_ATTACK     =                   [deg]
PITCH_ANGLE         =                   [deg]
TRUE_AIRSPEED       =                   [ft/s]
MACH                =                   [-]
RATE_OF_CLIMB       =                   [ft/min]
PDOT                =                   [deg/s2]
QDOT                =                   [deg/s2]
RDOT                =                   [deg/s2]
```

Figure 12 Sample of a Test Definition File input

Figure 12 shows a sample of TDF for one flight case in a hover condition during the take off manoeuvre. In this file, the manoeuvre, the model and sub model (in this case the Ground Effect model) are shown. There are specified the start time and end time of the recorded test file. The parameter 'dataFile' specifies the number of the flight test and the record.

'TRIMf' and 'subTRIMf' are the functions used to trim the aircraft, to find the all parameters initial conditions.

The trim and sub-trim functions for the virtual helicopter have the following use:

1. Trim Functions: By selection of a certain trim function, the operator chose a set of parameters whose inputs can be controlled by slight adjustments of initial conditions.

'TrimRate'	edit: p, q, r
'TrimAccel'	edit: p, q, r, A_x, A_y, A_z
'TrimAngAccel'	edit: $\dot{p}, \dot{q}, \dot{r}$
'TrimSideslip'	edit: β, p, q, r
'TrimSideslipM'	edit: β, $Mach$, p, q, r
'TrimRoll'	edit: p, q, r, φ

2. subTrim Functions gives control of the operator by imposing the derivatives values of the initial condition to be zero or non-zero as requested.

'subTrimRate'	initial condition imposed $\dot{p}, \dot{q}, \dot{r} = 0$
'subTrimVelRate'	initial condition imposed $\dot{u}, \dot{v}, \dot{w}, \dot{p}, \dot{q}, \dot{r} = 0$
'subTrimClimb'	initial condition imposed $\dot{u}, \dot{v}, \dot{w}, \dot{p}, \dot{q}, \dot{r}, ROC = 0$

'subTrimClimbAngAccel' initial condition imposed u, v, w, $ROC = 0$ edit: $\dot{p},\dot{q},\dot{r}$

'subTrimRateROC'   initial condition imposed $\dot{p},\dot{q},\dot{r} = 0$ edit: $ROC \sim= 0$

'subTrimVelRateROC' initial condition imposed $\dot{u},\dot{v},\dot{w}, \dot{p},\dot{q},\dot{r} = 0$ edit: $ROC \sim= 0$

'subTrimClimbROC'   initial condition imposed $\dot{u},\dot{v},\dot{w}, \dot{p},\dot{q},\dot{r} = 0$ edit: $ROC \sim= 0$

Theoretically, any trim function can be used in combination with any sub-trim function, although the results are significantly different, and sometimes very far from the real helicopter behaviour. For this reason, the POM operator should choose the best combination of trim and sub-trim functions which gives the most appropriate validation of the theoretical model results with the helicopter results. This trial and error process is time consuming due to the large amount of flight test data in various manoeuvre configurations.

In the example shown in figure 12, the trim function "TrimAngAccel" gives to the operator the possibility to edit arbitrarily the initial conditions of $\dot{p},\dot{q},\dot{r}$. The function "subTrimRate" imposes the conditions $\dot{p},\dot{q},\dot{r}$ equal to zero and all the others parameters are not constrained. In this particular case, the trim function supersedes the sub-trim function, then the initial conditions of $\dot{p},\dot{q},\dot{r}$ might be edited by the operator.

The output data of the POM software is a Postscript file which shows the time history plots of the parameters, superposed on the same plot the model generated over the recorded parameter. In Figures 13, 14 and 15 are shown plots of the parameters of the case from the chosen example. In these plots, there are three types of lines: continuous green line is the recorded parameter during the test flight; dashed blue line is the simulated parameter by the POM software; dashed red lines are the tolerances limits specified in the GDF for each parameter.
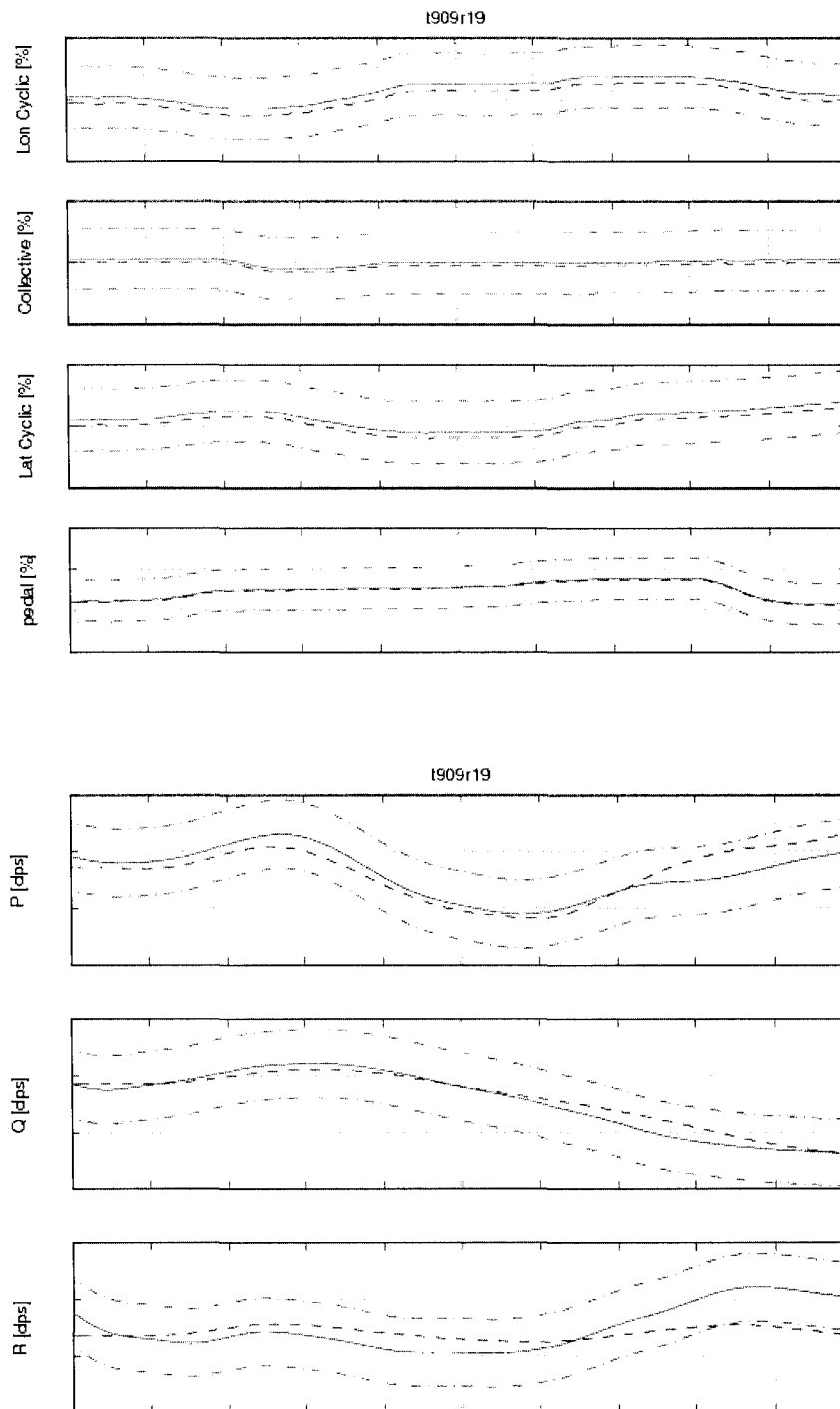
Figure 13 Sample of time history plots of controls and attitudes rates
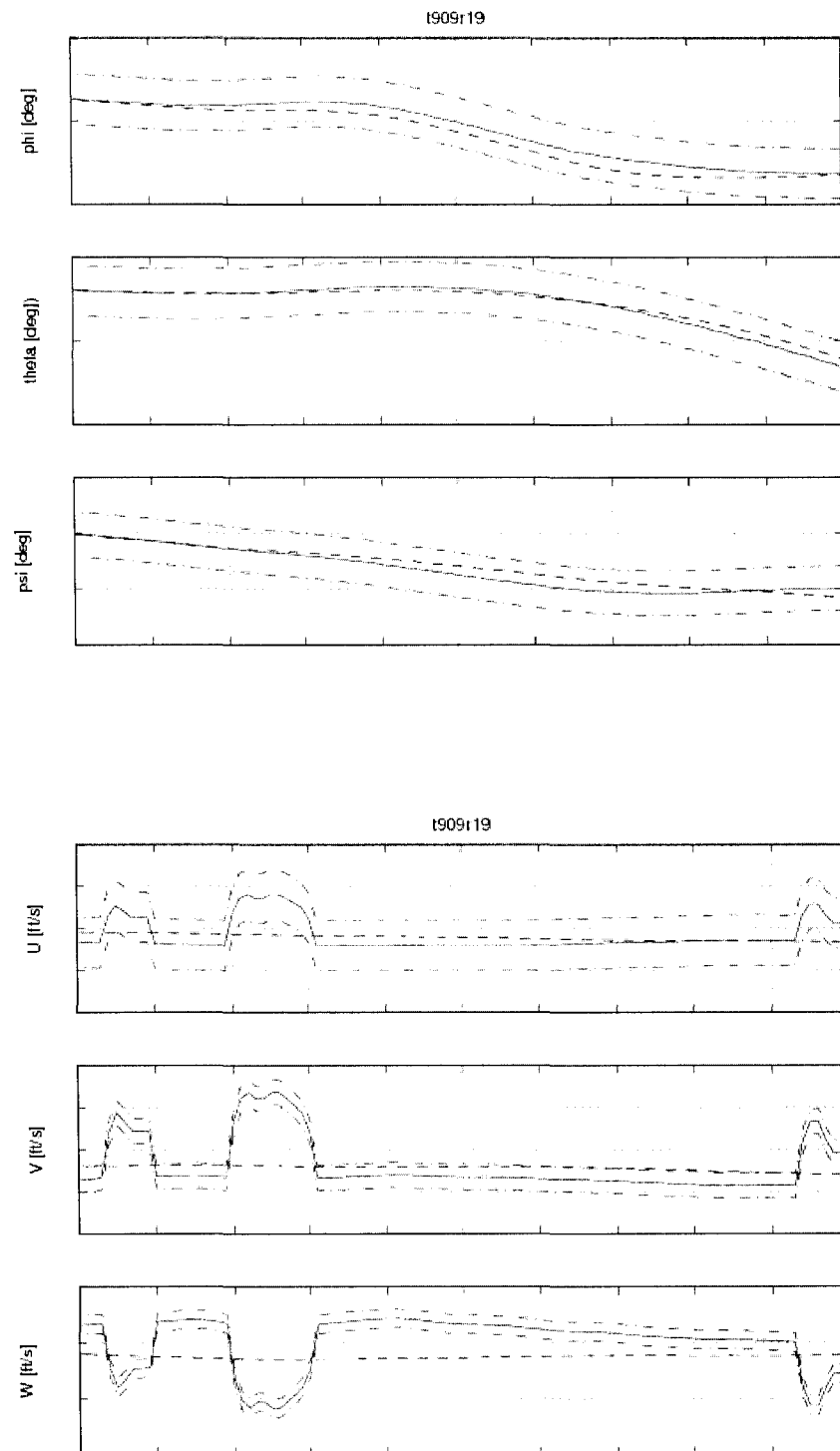
Figure 14 Sample of time history plots of Euler angles and body reference velocities
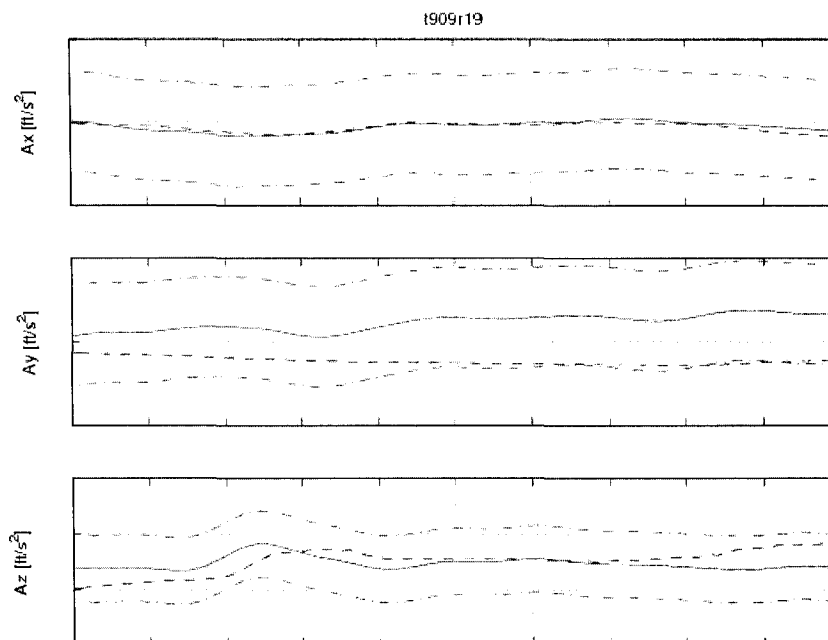
Figure 15 Sample of time history plots of accelerations

These plots are used for results visualisation and decisions making regarding the matching of the POM model with the real helicopter. The operator can change the initial conditions of the simulation and see the effect of changes in the parameters evolution. The most useful in this analysis is the plot of tolerances limits. The analyst can see if the simulated line is within the accepted limits. This is a very important information because the Advisory Circular for certain manoeuvres requires for validation a "snapshot" which generally accepted has a time of about 2-3 seconds.

The validation of several manoeuvres from the Quality Test Guide such as Lateral and Directional Handling Qualities, Hover In or Out of Ground Effect, Autorotation will be described in the following chapters.

CHAPTER 5

LATERAL AND DIRECTIONAL HANDLING QUALITIES VALIDATION

5.1 General considerations

In order to validate the model, we describe firstly the Up And Away (UAA) model. The UAA model simulates the helicopter's flight out of the ground effect (OGE) and consists mainly of level flight performance, vertical climb performance, climb and descent in trimmed flight, longitudinal and lateral motion. In this thesis, only the lateral motion results will be shown. The global model includes also the Autorotation and Ground Effect modules but these two modules were developed at a later time, since the helicopter's motion the in these two flight zones contains complex aerodynamics different than the aerodynamics of the helicopter engine powered and far from the ground.

5.2 Directional static stability – trimmed flight in cruise, climb or descent

For the directional static stability validation in trimmed flight, is required to match the flight test cases during cruise and climb/descent flight condition. The helicopter should have a steady heading sideslip and a minimum of two sideslip angles β on each side of the trim point. The matched cases may be "snapshot" tests. In this manoeuvre, the important parameters are the lateral and the longitudinal control position (cyclic stick) with a tolerance of ± 10%, roll attitude with a tolerance of ±1.5 deg, the directional control position (the pedals) with a tolerance of ±10% and the vertical velocity with a tolerance of ±100 ft/min (±1.67 ft/s).

Firstly, the trim function chosen was the "trimSideslipM" due to the fact that the sideslip angle β is an important parameter. The sub-trim functions giving the best results were "subtrimClimbROC" and "subtrimVelRateROC" due to the importance of vertical velocity and to the possibility to edit the rate of climb. The cases to match were considered both for the same altitude of 3000 ft, but at two different airspeeds: 102 knots and 112 knots. The helicopter loadings in these cases were "Heavy" and "Light" and the CG position was aft in both cases. The sideslip angles of the helicopter during the flight tests were ± 5 deg, ±10 deg and ±15 deg (pedal left/right).

In Figures 17-22, an example of time histories plots is shown for one of the cases, which didn't match the required QTG for validation on the first POM run. The helicopter's loading was in configuration "Heavy/Aft" at cruise flight (constant altitude 3000 ft) at a speed of 112 knots and zero sideslip angle. The initial ROC was -36 ft/min, which is equivalent to a slight descent of the helicopter at the beginning of the record.
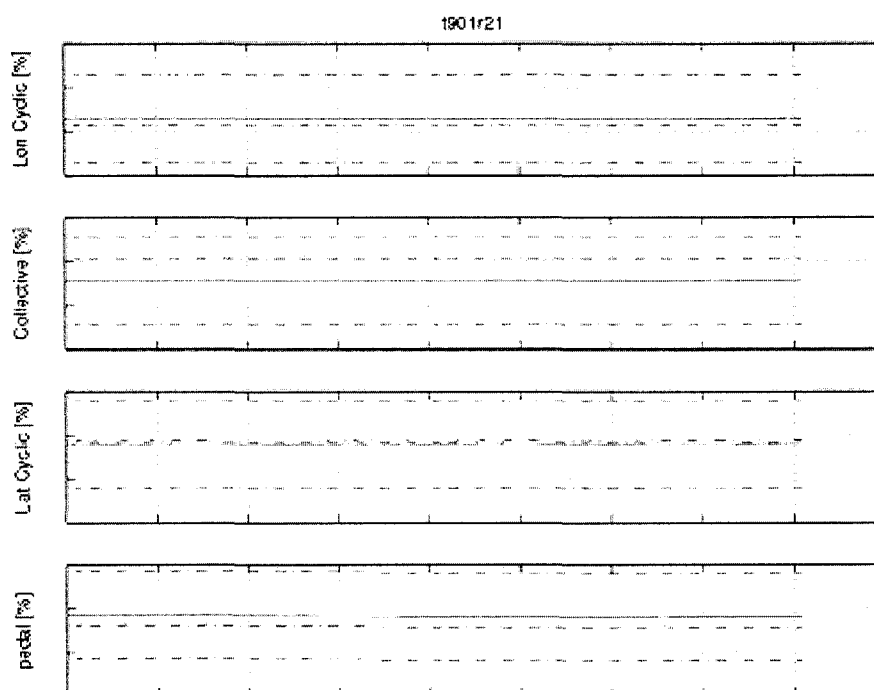
Figure 16 Flight test t901r21 controls time history
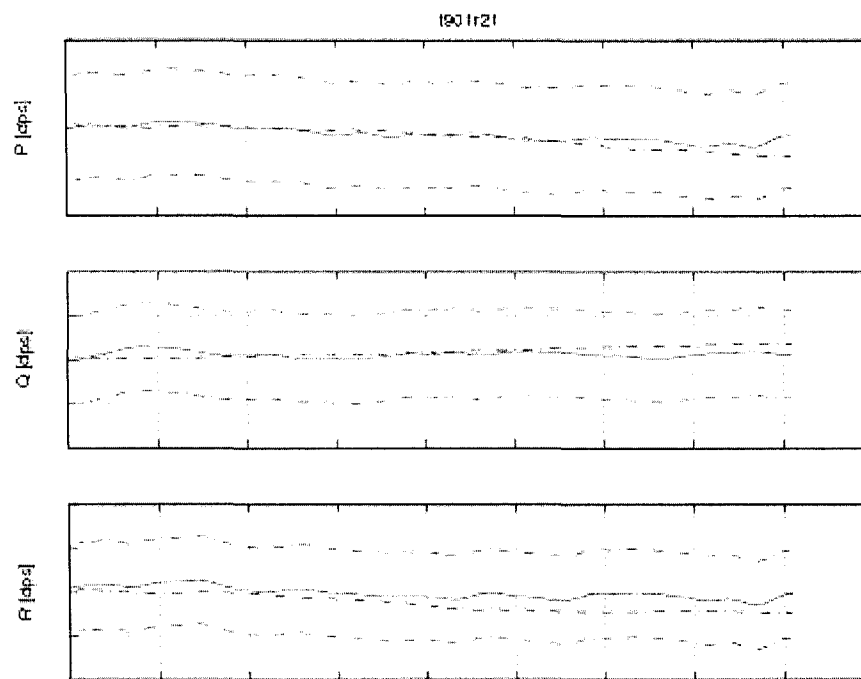
t901r21

Figure 17 Flight test t901r21 attitude rates time history
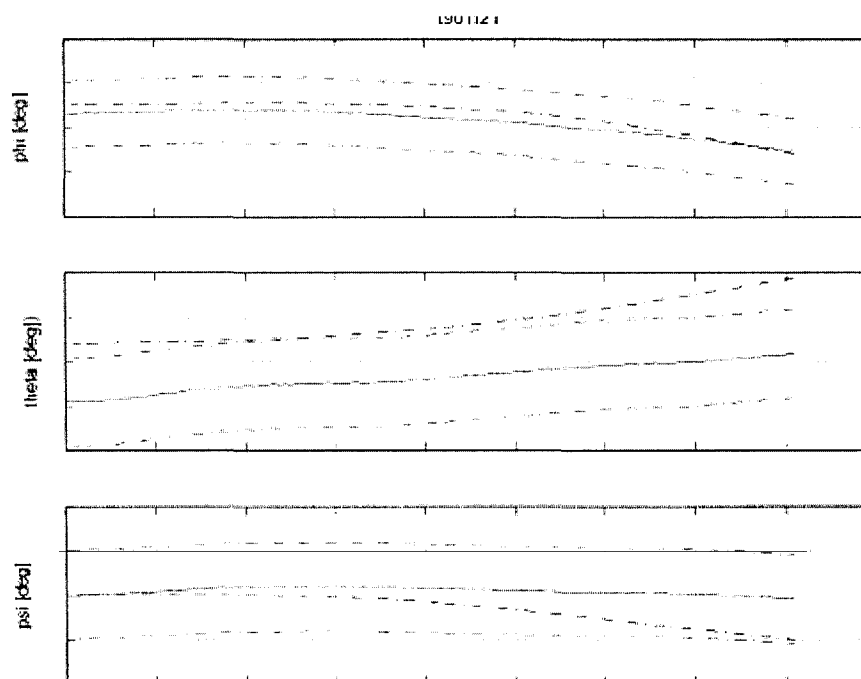
t901r21

Figure 18 Flight test t901r21 Euler angles time history
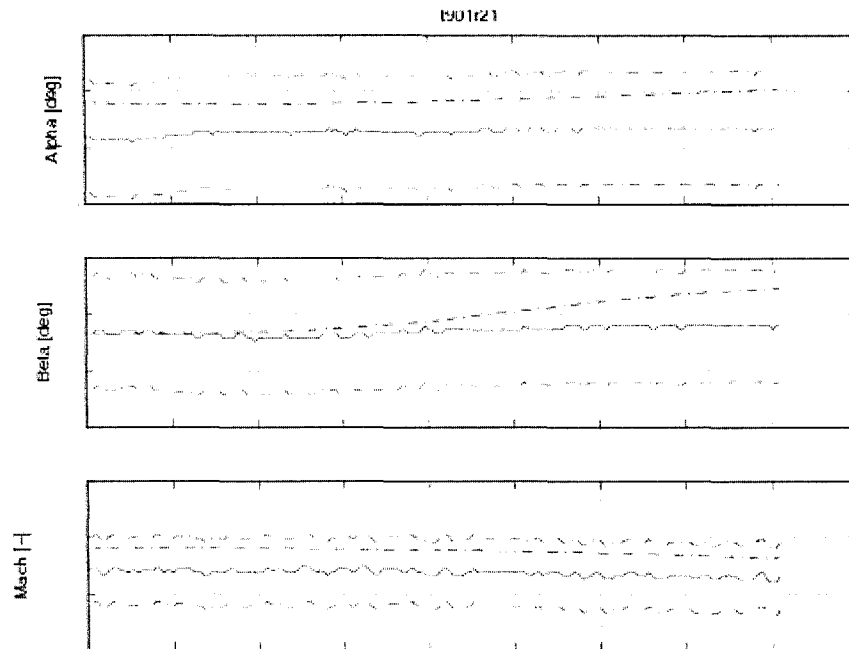
Figure 19 Flight test t901r21 α, β, and airspeed (Mach number) time history
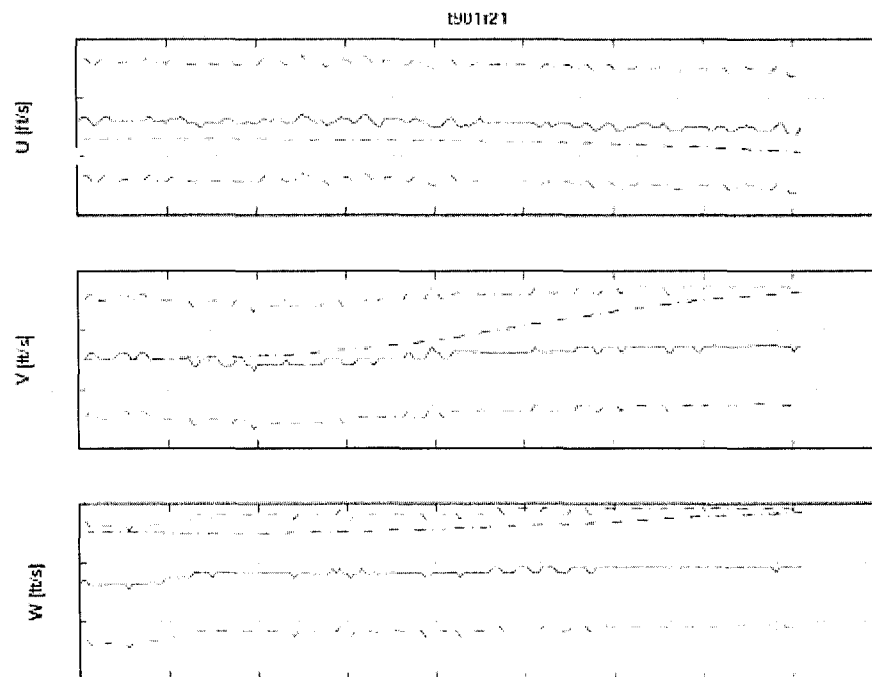
Figure 20 Flight test t901r21 speeds in body reference system time history
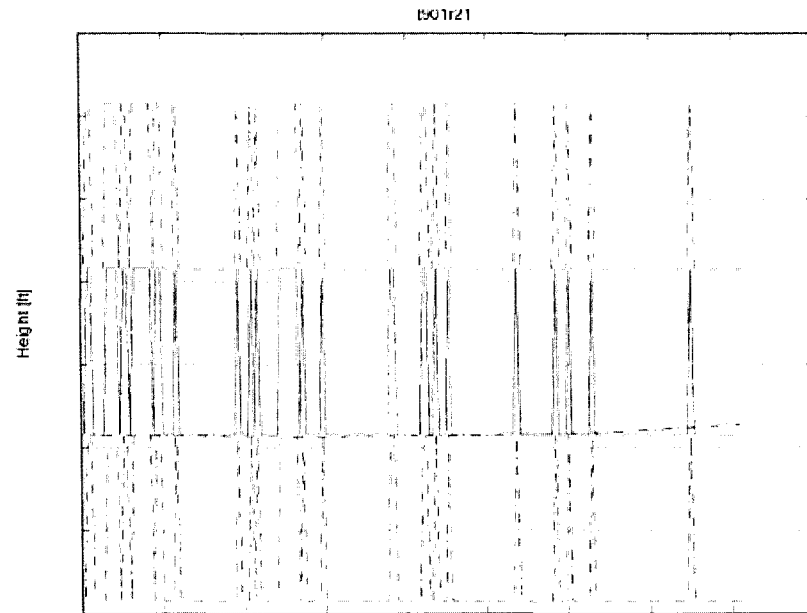
Figure 21 Flight test t901r21 altitude time history

From Figure 18, we see that the pitch angle θ calculated by the model is outside tolerances limits than the recorded θ parameter. From Figure 20 the vertical speed w of the model was found to be higher than the recorded vertical speed w. The other parameters are within tolerances. Using the above information we found the differences in α, θ and w between the helicopter POM model and flight test as in Figure 22:
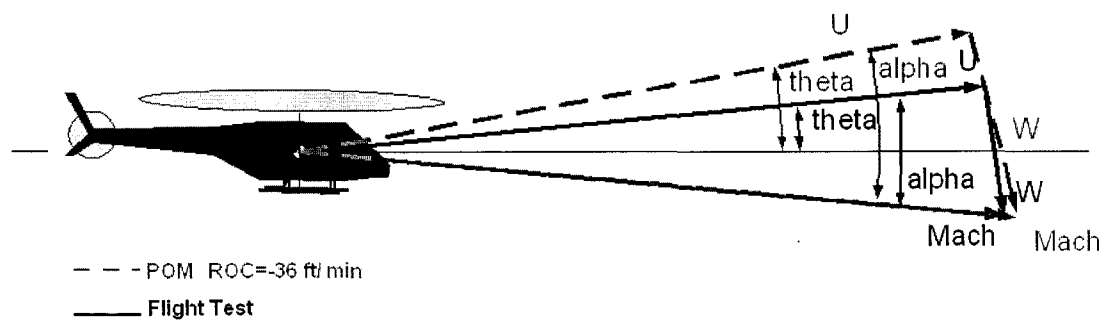
Figure 22 Differences between the simulation model and the flight test during cruise

To match the pitch angle θ within the required tolerances there is a need of an adjustment of the initial ROC by forcing the simulated helicopter to descend. The function "subtrimVelRateROC" allows editing the parameter Rate Of Climb (ROC) by adding an arbitrary value by the operator as shown in Figure 23:

TDF Options
02-Mar-2005 12:18:45

```
dataFile              = 't901r21_m.dat'
startTime             =    0.03      [sec]
endTime               =    4.08      [sec]
TRIMf                 = 'TrimSideslipM'    -> edit: beta,mach,p,q,r
subTRIMf              = 'subTrimVelRateROCu/v/w/p/q/rdot = 0 edit: ROC' = 0
ROLL_RATE             =              [deg/s]
PITCH_RATE            =              [deg/s]
YAW_RATE              =              [deg/s]
X_ACCEL               =              [ft/s2]
Y_ACCEL               =              [ft/s2]
Z_ACCEL               =              [ft/s2]
U_VEL                 =              [ft/s]
V_VEL                 =              [ft/s]
W_VEL                 =              [ft/s]
PRESSURE_ALTITUDE     =              [ft]
ROLL_ANGLE            =              [deg]
SIDESLIP_ANGLE        =              [deg]
HEADING_ANGLE         =              [deg]
ANGLE_OF_ATTACK       =              [deg]
PITCH_ANGLE           =              [deg]
TRUE_AIRSPEED         =              [ft/s]
MACH                  =         .004  
RATE_OF_CLIMB         = -36.73-300 [ft/min]
PDOT                  =              [deg/s2]
QDOT                  =              [deg/s2]
RDOT                  =              [deg/s2]
```

Figure 23 Edit of the parameter ROC

The modification of the helicopter initial conditions should have a direct effect on the pitch angle θ and vertical speed w as shown in next Figure 24:

— — — POM ROC = -336 ft/min
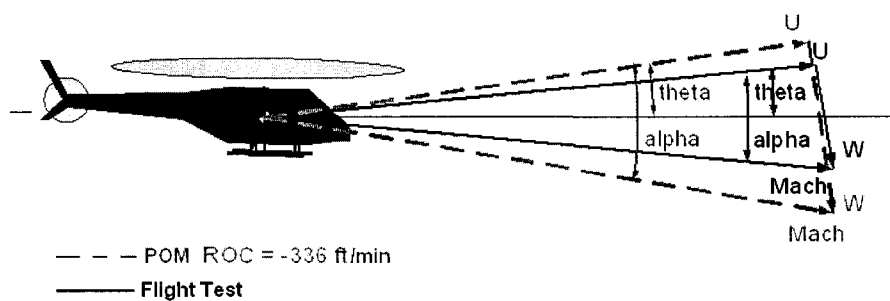
———— Flight Test

Figure 24 Modification of the helicopter's ROC with a negative value

The results obtained by the TDF input file modification and following the POM running are plotted in Figures 25 - 28:
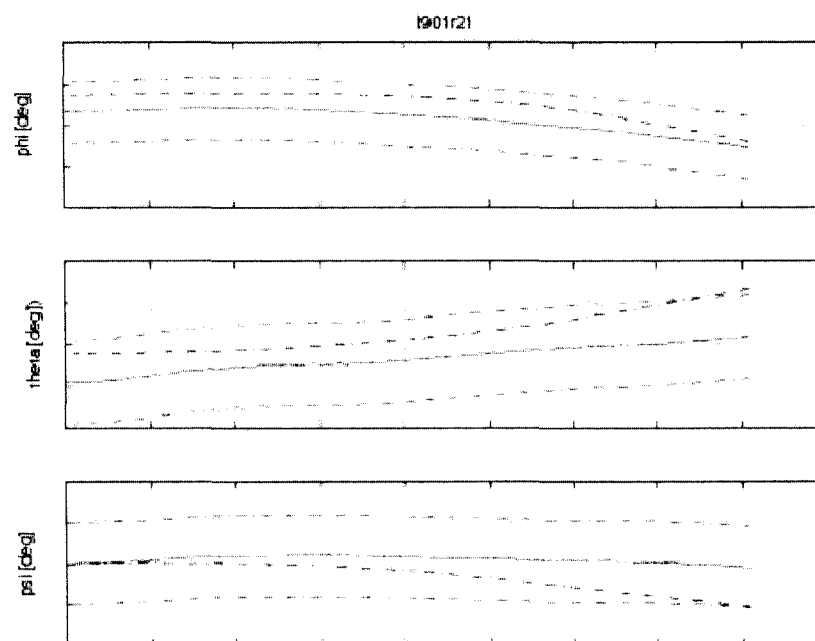
Figure 25   Flight test t901r21 Euler angles time history of the descending virtual helicopter
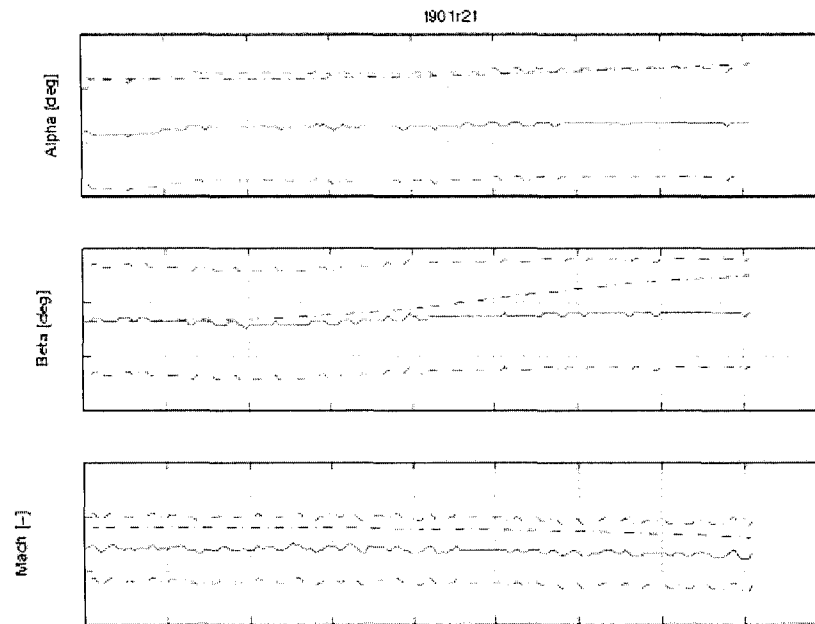
Figure 26 Flight test t901r21 α, β and airspeed (Mach number) time history of the descending virtual helicopter
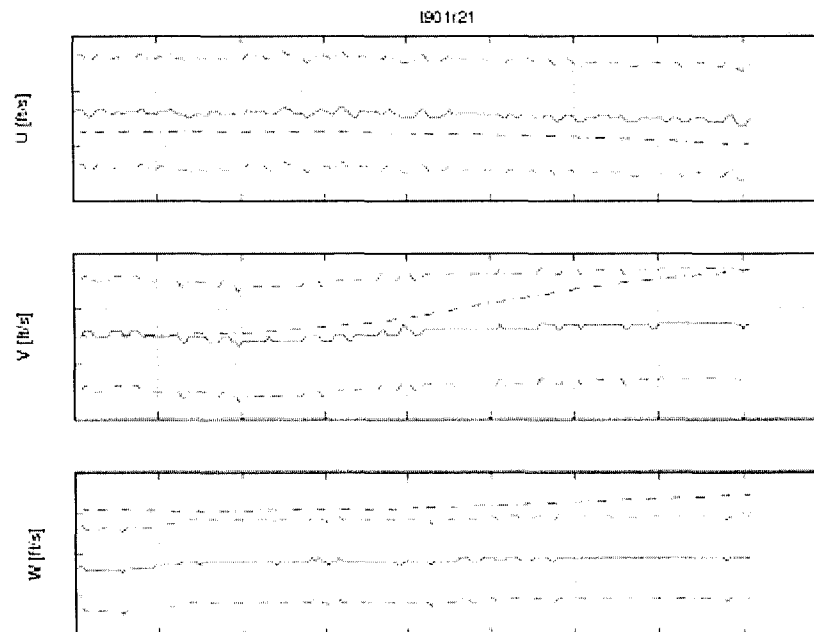
Figure 27 Flight test t901r21 speeds in body reference system time history of the descending virtual helicopter

t901r21

Height [ft]
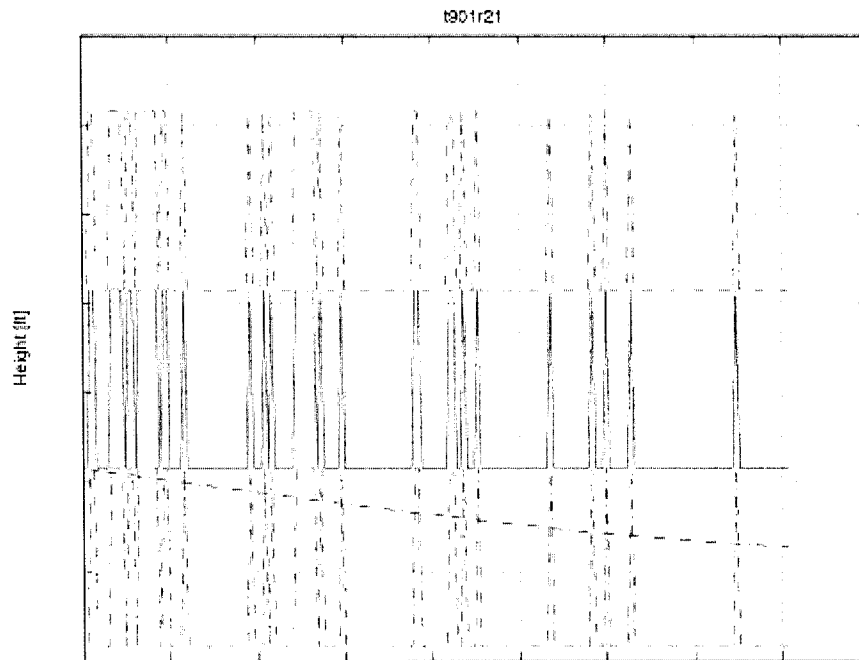
Figure 28 Flight test t901r21 altitude time history of the descending virtual helicopter

The results are still not satisfactory since the pitch angle θ is within the tolerances limits but w speed is outside the tolerances limits. This value of the vertical speed w higher than the recorded value is due to the virtual helicopter rate of descent -336 ft/min, since the z axis is positive downwards, any descent of the virtual helicopter will increase vertical speed w value. The second way to match the θ and w parameters is to climb the virtual helicopter, so that the climb rate will have the value of +336 ft/min. The results of the second run of the POM and with the modified ROC value is shown in Figures 29 - 32:
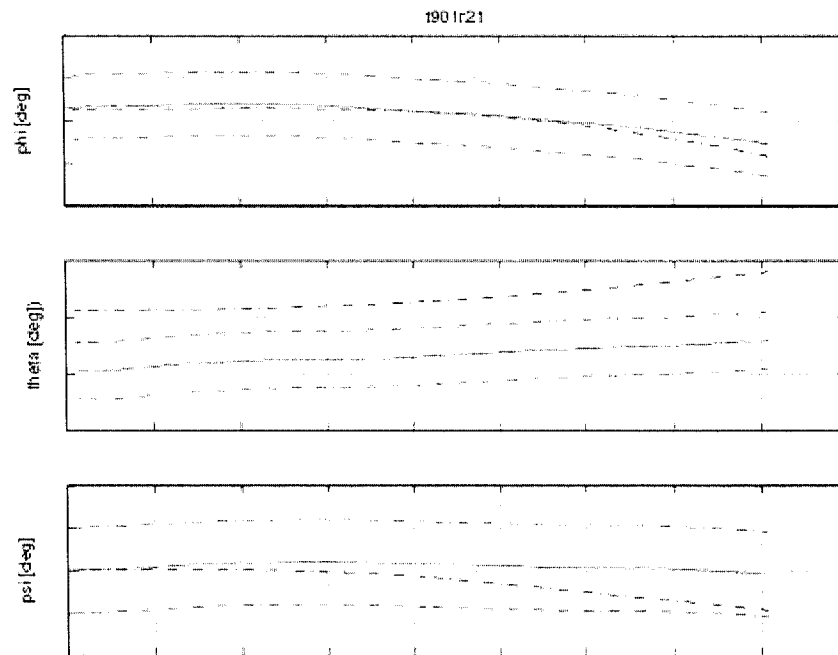
Figure 29   Flight test t901r21 Euler angles time history of the climbing virtual
helicopter

In Figure 29, the pitch angle θ is outside the tolerances values and the second run of this POM version is still unsatisfactory.
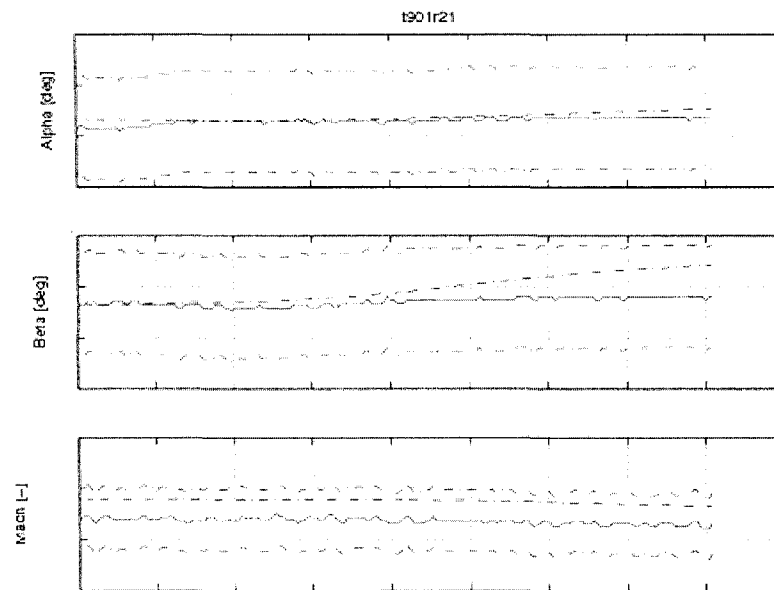
Figure 30 Flight test t901r21 α, β, and airspeed (Mach number) time history of the climbing virtual helicopter
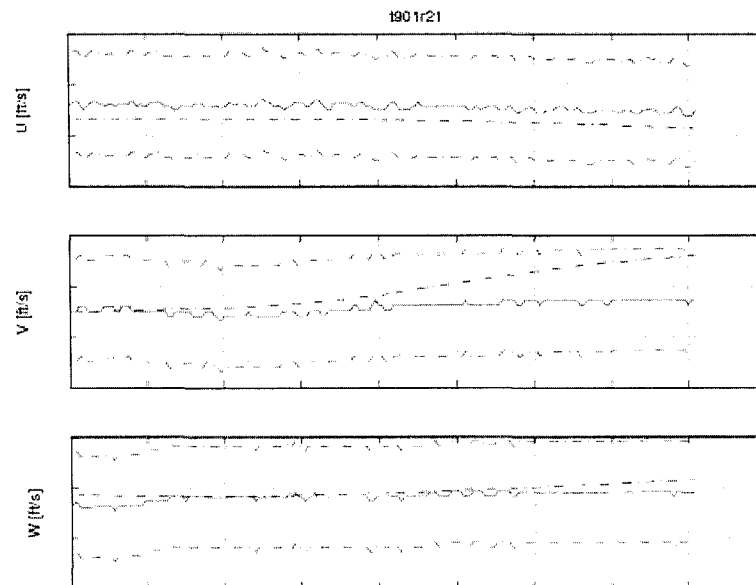
Figure 31 Flight test t901r21 speeds in body reference system time history of the climbing virtual helicopter
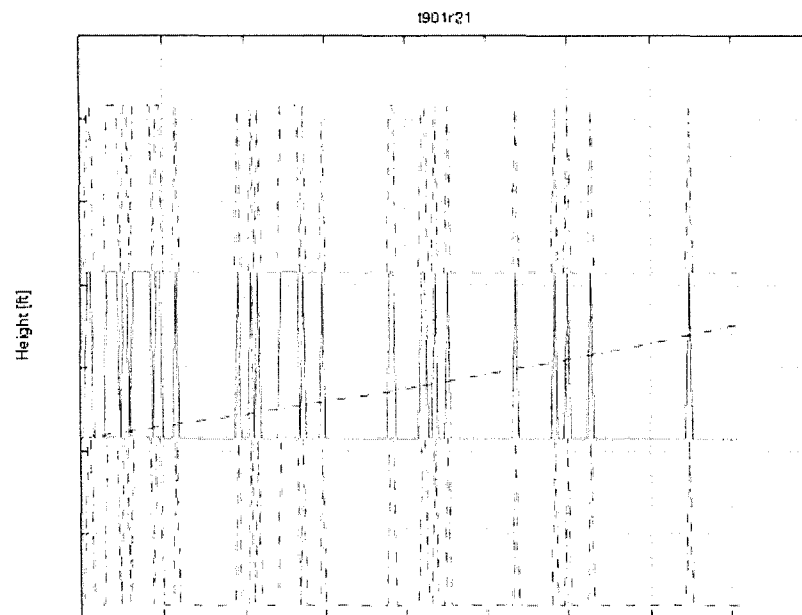
Figure 32 Flight test t901r21 altitude time history of the climbing virtual helicopter

From figures 29 - 32 following the second run, the differences between the virtual helicopter trajectory and the real helicopter trajectory are as shown in the Figure 33:
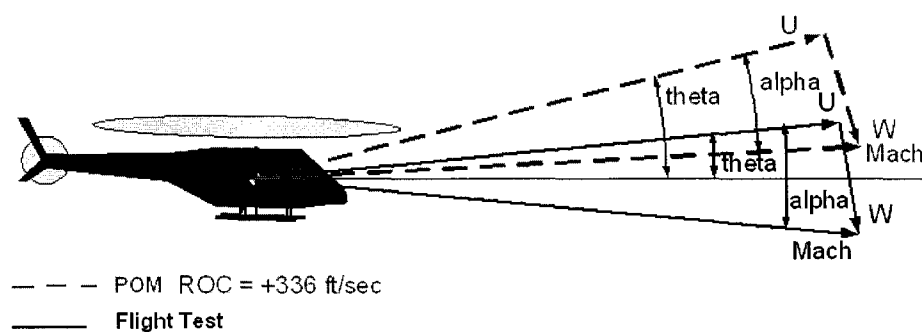
Figure 33 Modification of the helicopter rate of climb by a positive value

The conclusion is that in this stage of the model development, there is a need for adjustments in the actual POM model. From the analysis of this case in three different situations, it can be predicted that the vertical speed w value is calculated by the trim

function erroneous. The above presented analysis is part of the process of "trial and error" adjustments following the mathematical model generation. This process requires very large quantities of flight test data to be validated, which are equivalent to large amounts of man-hours.

Following this first analysis, which conclusions were confirmed by running 40 different flight condition cases in various configurations (Light/Heavy, CG Aft/Forward, Low speed, High speed), a new POM version was issued with a new set of trim and sub-trim functions. The new POM version gave better results, which enabled us to fulfill all the QTG requirements and to validate the Directional Static Stability chapter 2d2 from Table V. In Figure 34 the same case t901r21, with no ROC correction made to pass the QTG list requirements is shown:
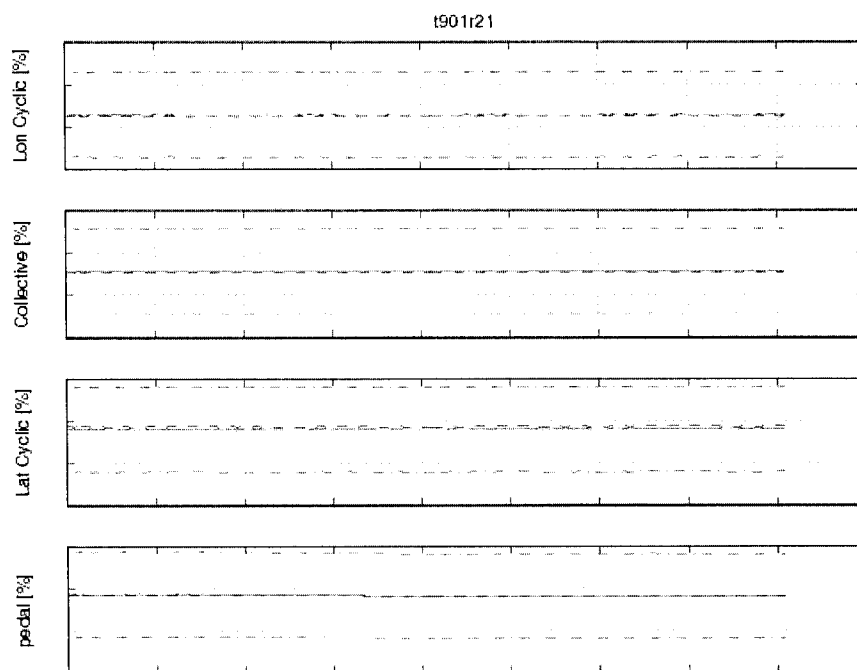
Figure 34 Flight test t901r21 controls time history
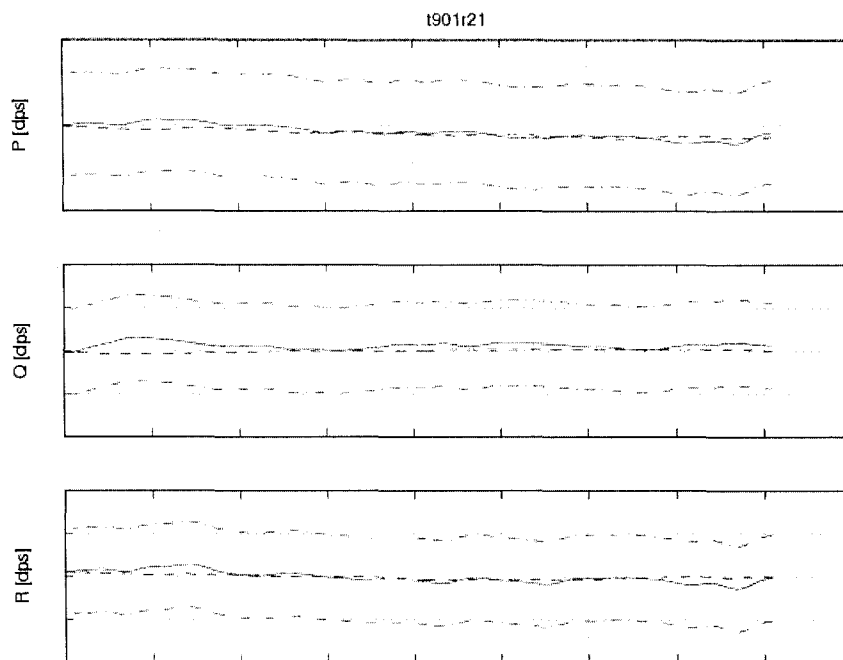
t901r21

Figure 35 Flight test t901r21 attitude rates time history
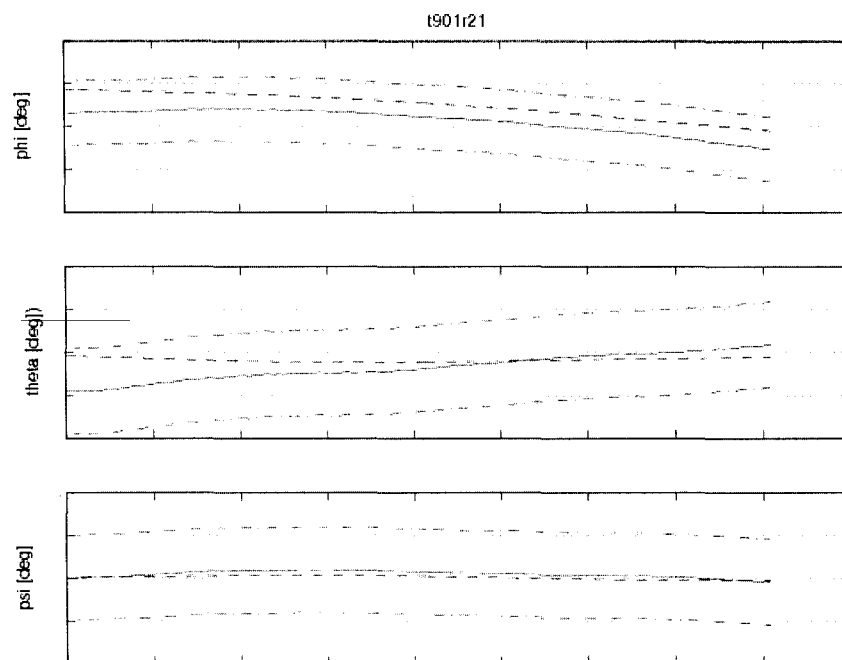
t901r21

Figure 36 Flight test t901r21 Euler angles time history
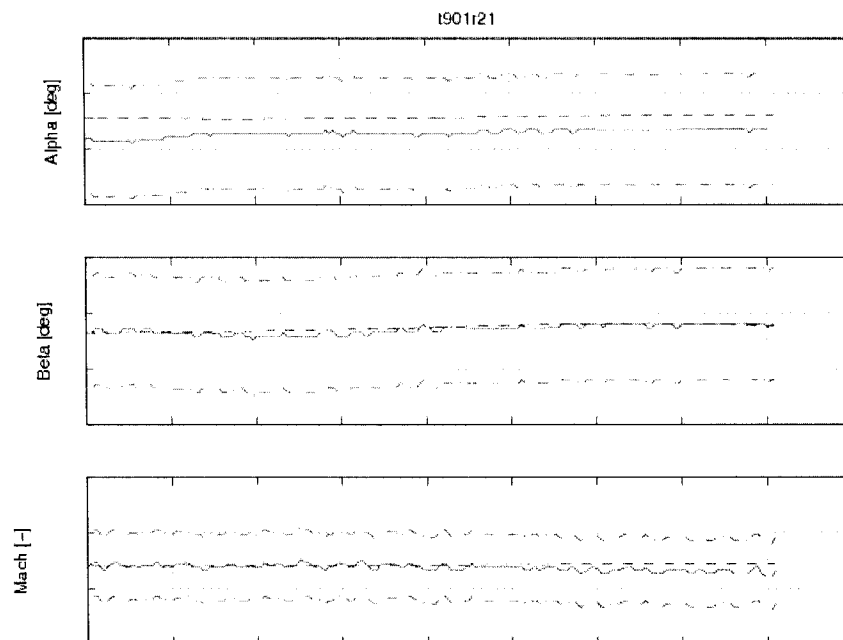
Figure 37 Flight test t901r21 α, β and airspeed (Mach number) time history
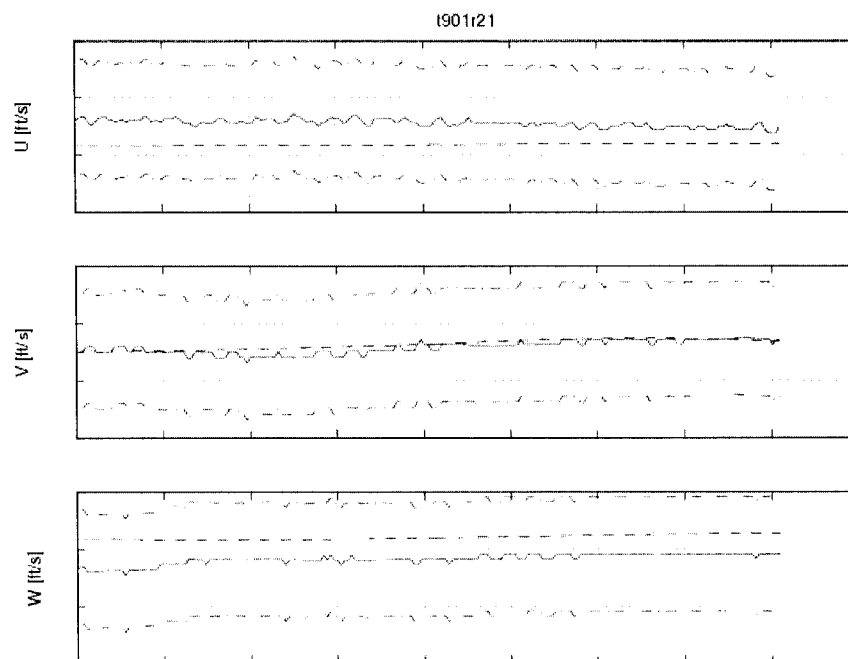
Figure 38 Flight test t901r21 speeds in body reference system time history

5.3 Lateral control response

For the lateral control response validation, there is the requirement to match the flight cruise cases for two airspeeds. The helicopter should have an input step in lateral control and the off axis response should show the correct trend. In this manoeuvre, the main parameters are the lateral control position (cyclic stick), the roll attitude with a tolerance of ± 3 deg, and the roll rate with a tolerance of ± 3 deg/sec. The other parameters are not mandatory; still the fitness of them is important. Firstly, the trim function chosen was the "trimSideslipM" due to the well fitness in the steady flight. The sub-trim functions giving the best results were "subtrimClimbROC" and "subtrimVelRateROC" due to the initial conditions imposed to the speeds to be zero and to the possibility of rate of climb editing.

In Figures 39 - 43 is shown one of the best fits, the case t892r72, in which the helicopter has a loading Heavy-Forward (HF). The test was recorded at an altitude of 3000 ft and airspeed of 60 knots. The pilot moved the lateral cyclic stick to the right and kept the control in this position for several seconds. Figures 39 – 43 shows the output of the POM software first version uncorrected.
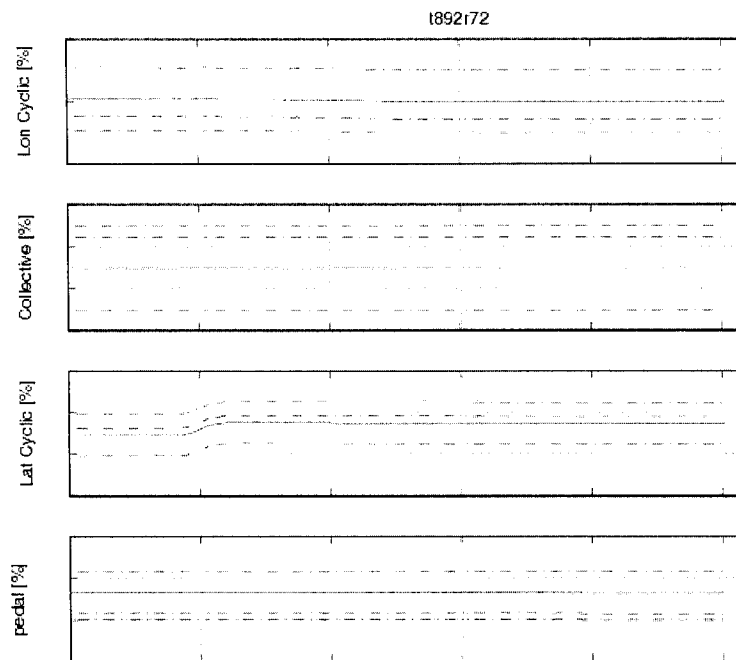
t892r72

Figure 39 Flight test t892r72 controls time history of uncorrected model
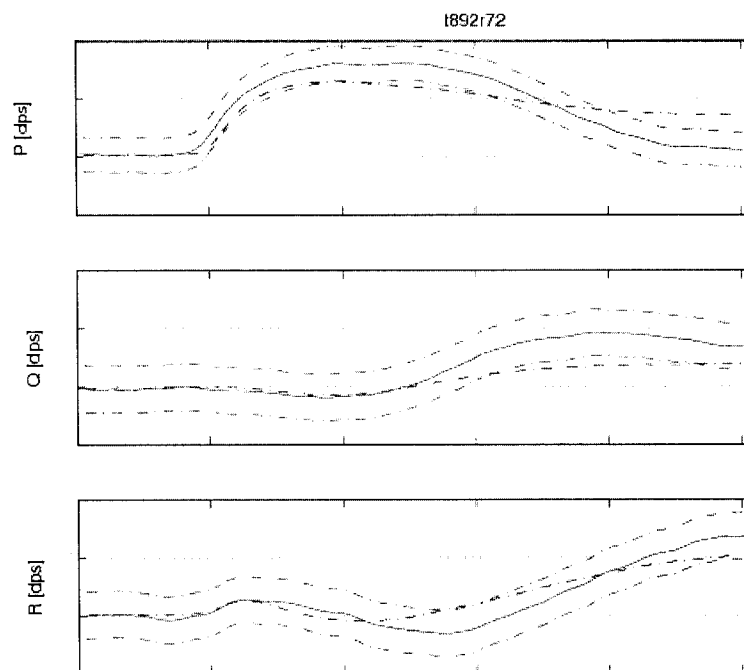
t892r72

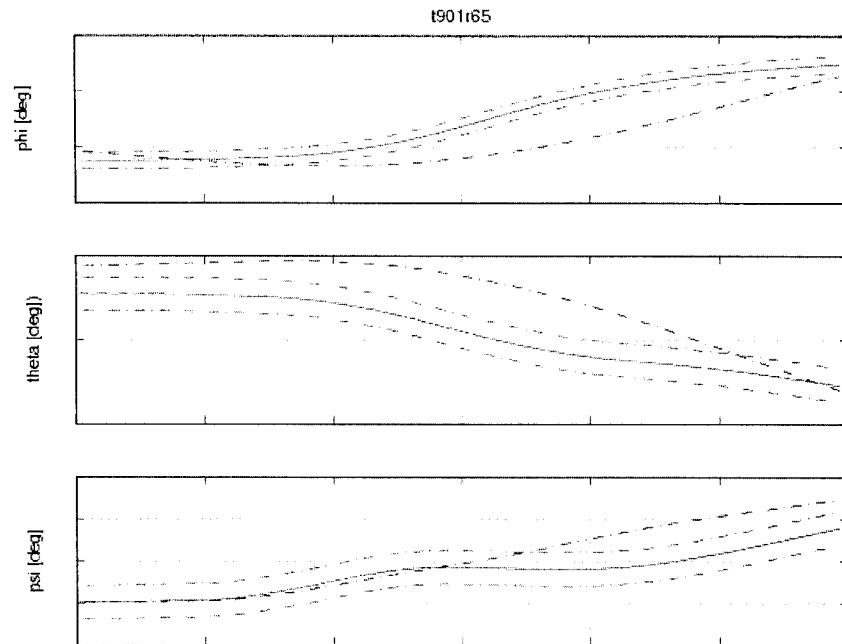**Figure 40 Flight test t892r72 attitudes rates time history of uncorrected model**
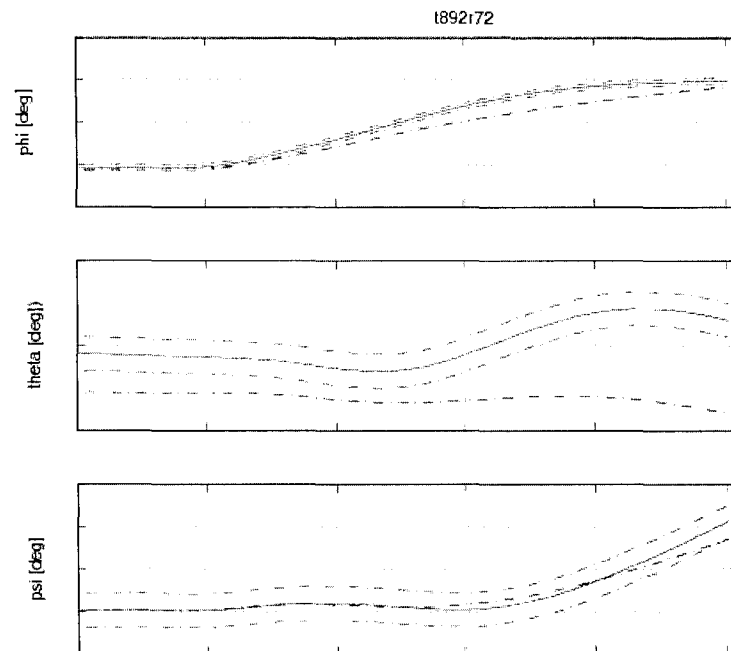
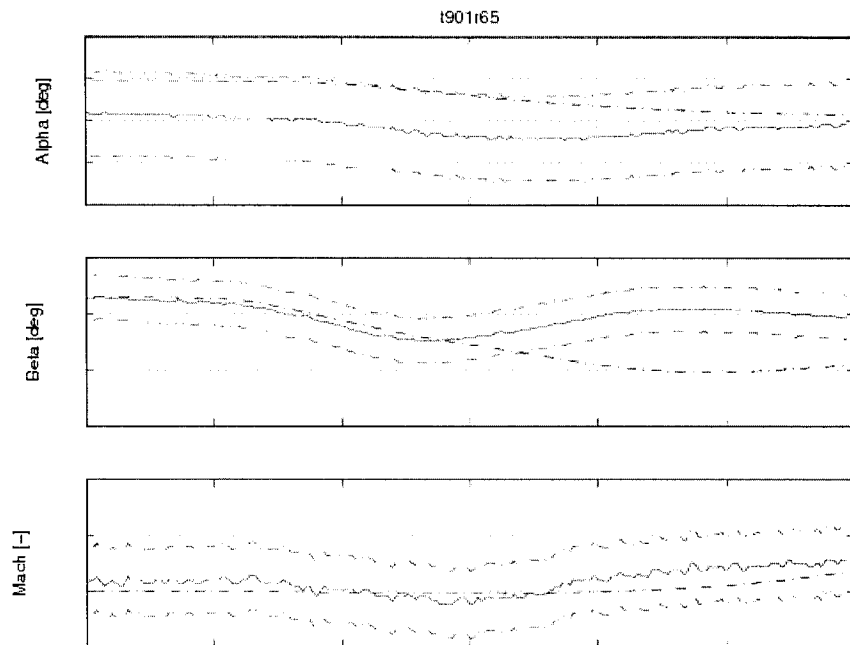Figure 41 Flight test t892r72 Euler angles time history of uncorrected model
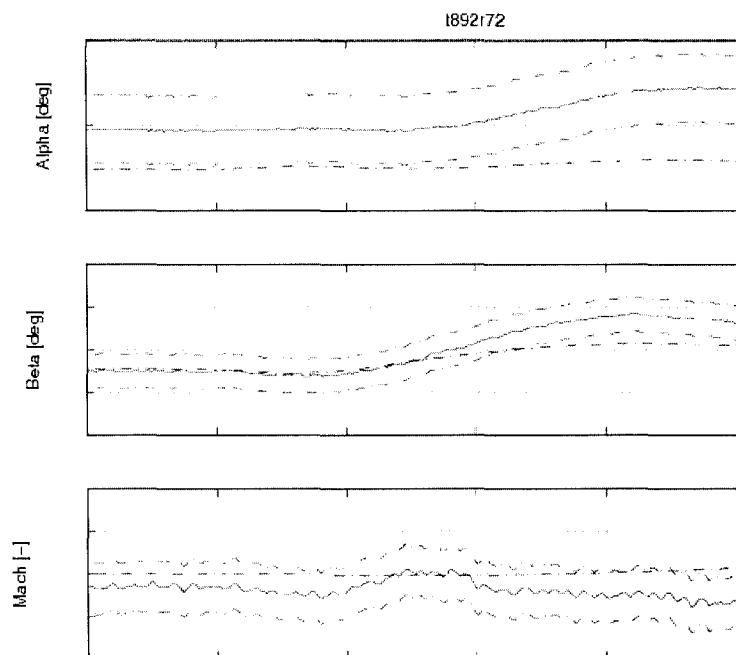
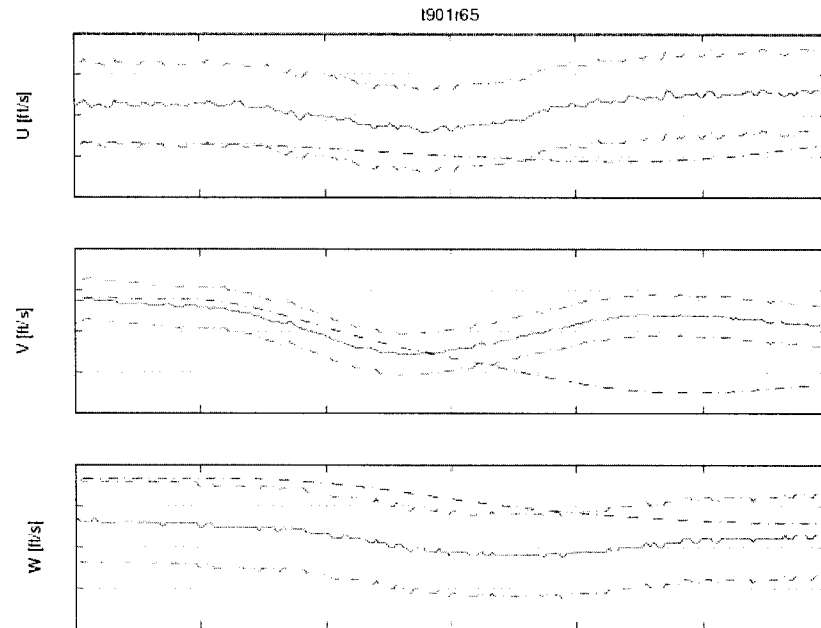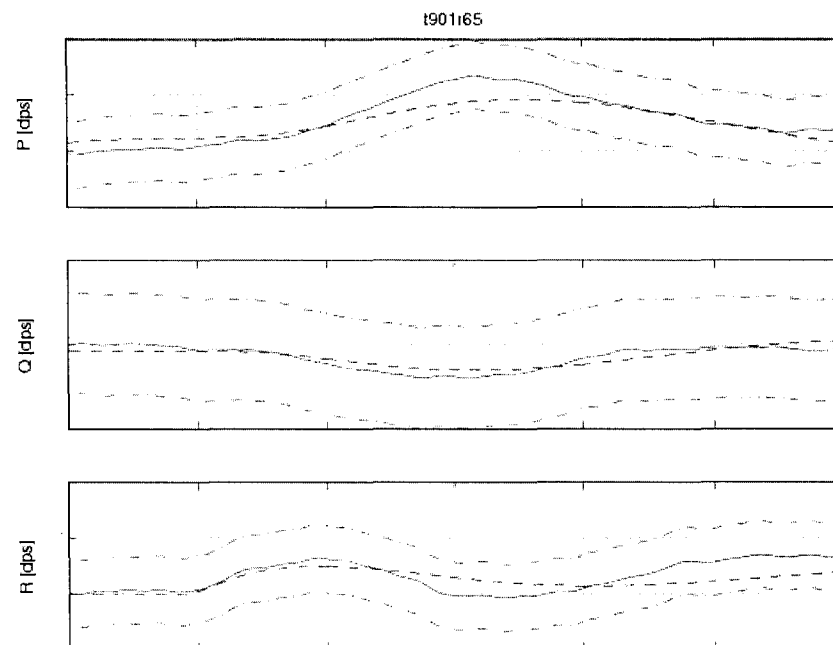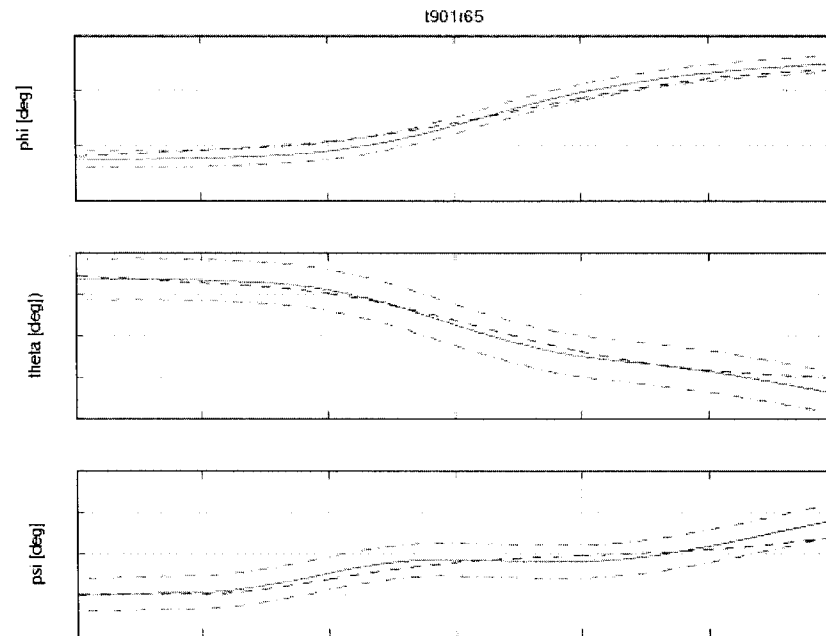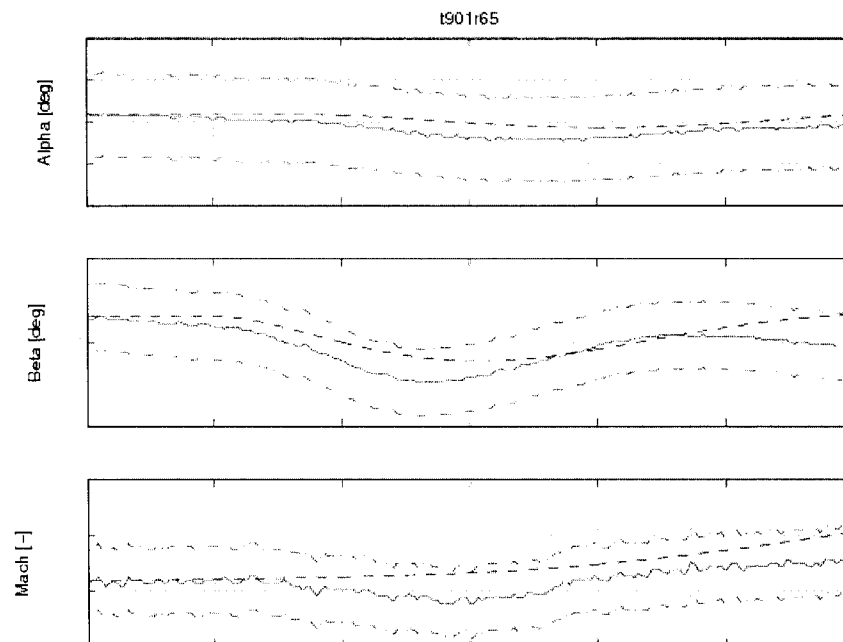Figure 42   Flight test t892r72 α, β and Mach number time history of uncorrected model
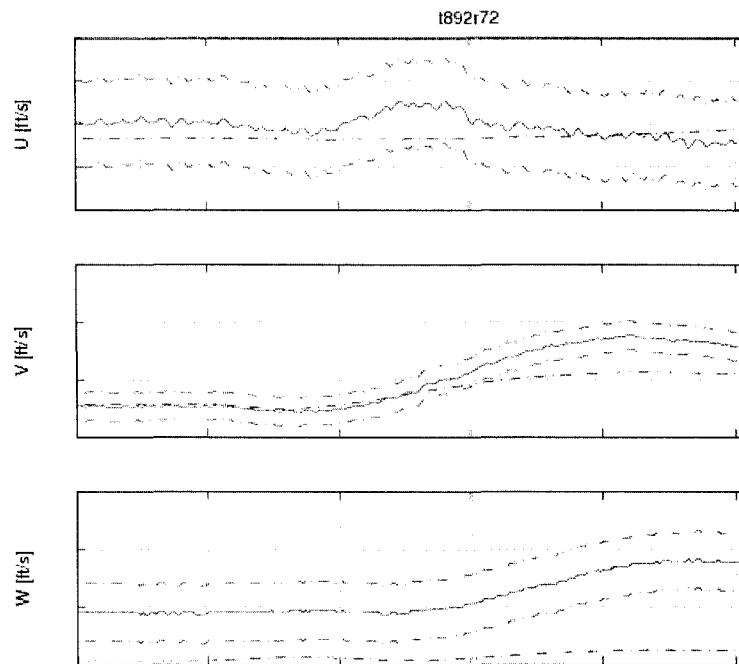
Figure 43   Flight test t892r72 speeds in body reference system time history of uncorrected model

This case was not matched, as well as all the cases solved with this POM version. Following the model's adjustments and corrections, the new POM version matched sufficiently cases to be accepted by the QTG requirements. The results obtained for the same case with the new POM version are shown in Figures 44 – 49.
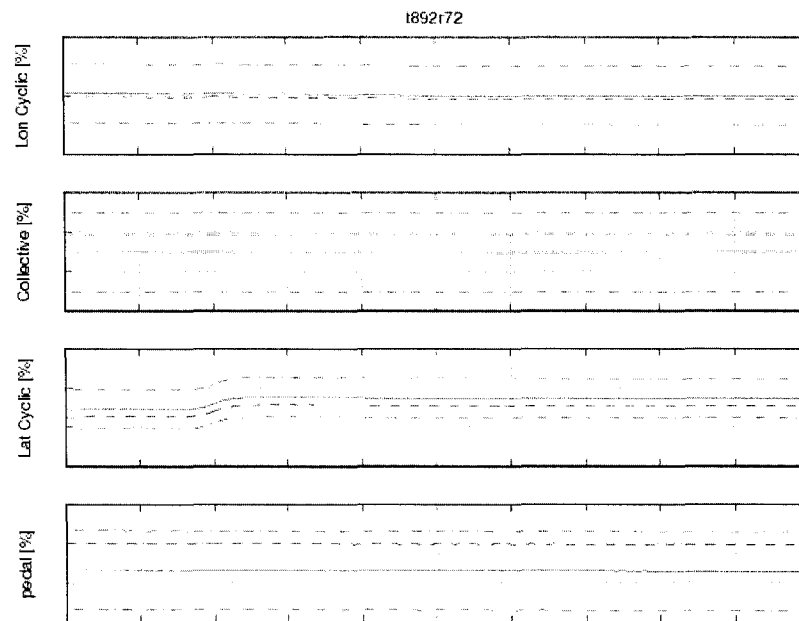
t892r72

Figure 44 Flight test t892r72 controls time history of corrected model
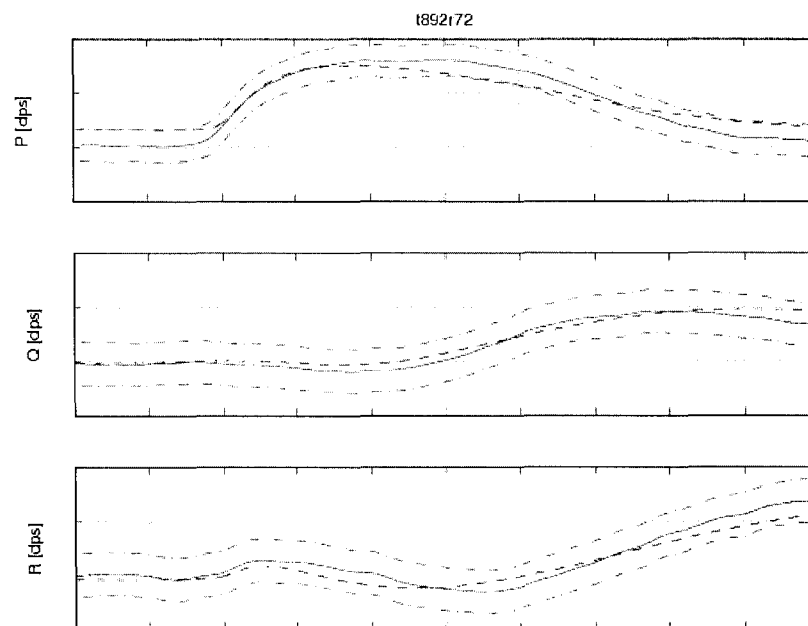
t892r72

Figure 45 Flight test t892r72 attitude rates time history of corrected model
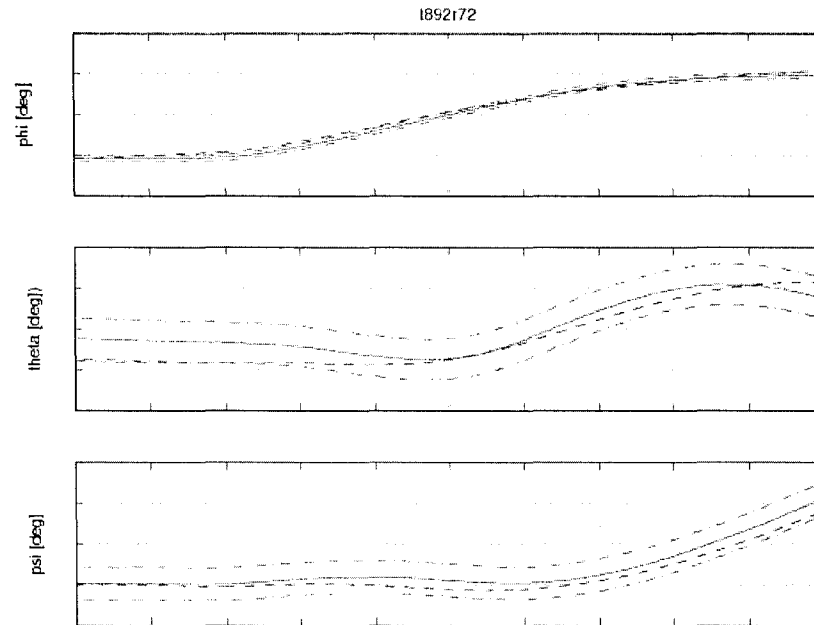
Figure 46 Flight test t892r72 Euler angles time history of corrected model
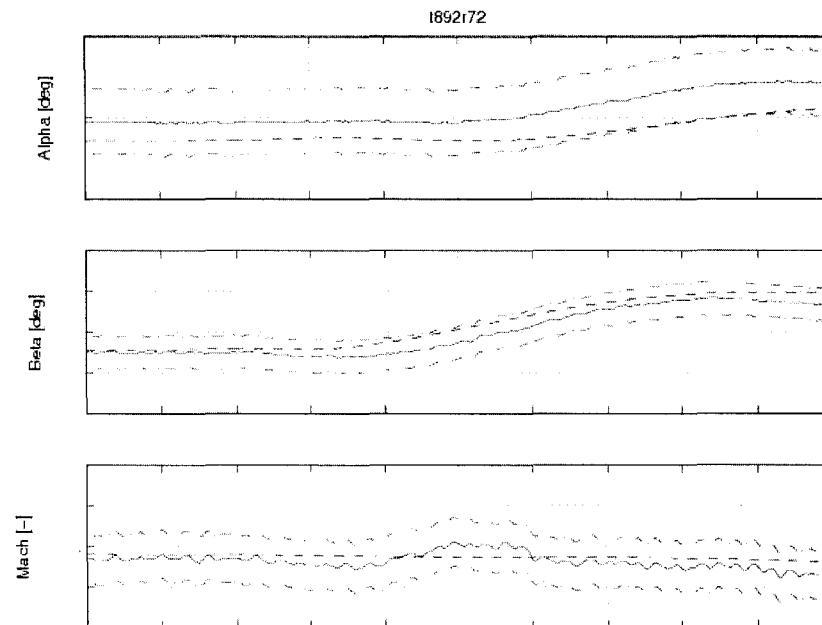
Figure 47 Flight test t892r72 α, β and Mach number time history of corrected model
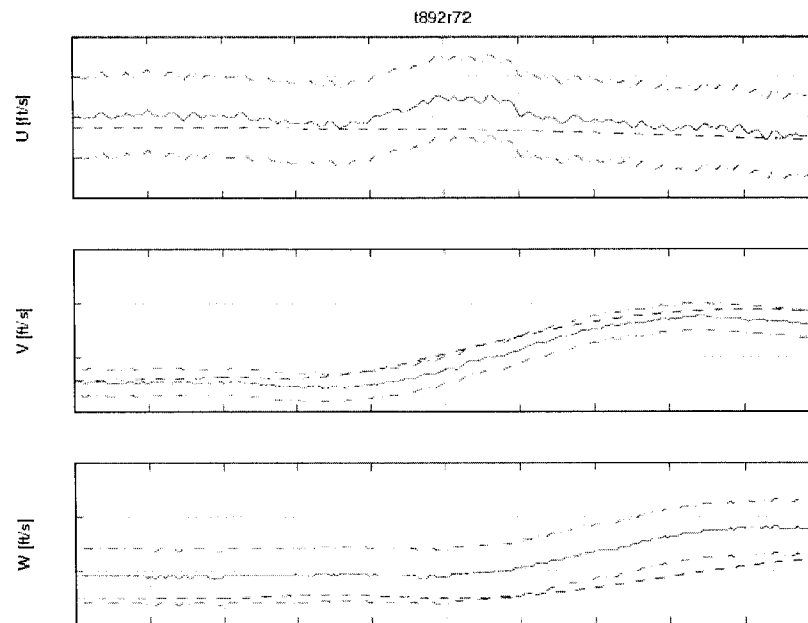
t892r72

Figure 48   Flight test t892r72 speeds in body reference system time history of corrected model
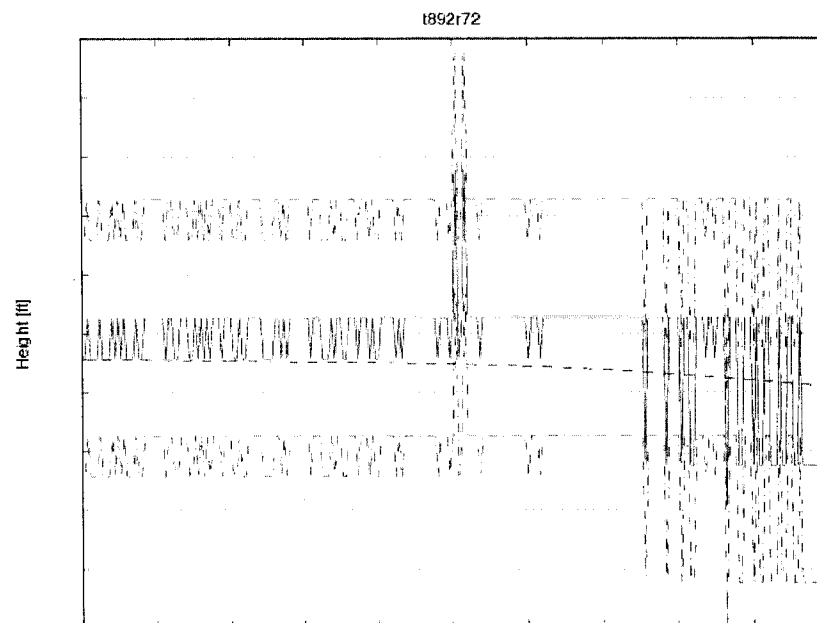
t892r72

Figure 49 Flight test t892r72 density altitude time history of corrected model

5.4 Directional control response

For the validation of the directional control response, the cases during cruise flight for two airspeeds have to match. The helicopter should have an input step given in directional control (pedals) and the off axis response of the helicopter should show the correct trend. In this manoeuvre, the main parameters are the pedals, the yaw attitude with a tolerance of ± 2 deg, and the yaw rate with a tolerance of ± 2 deg/sec. The other parameters are not mandatory; still the fitness of them is important. Firstly, the trim function chosen was the "trimSideslipM" due to the well fitness in the steady flight. The sub-trim functions giving the best results were "subtrimClimbROC" and "subtrimVelRateROC" due to the initial conditions imposed on the speeds to be zero and to the possibility of rate of climb editing.

In the following figures one of the best fits is shown, the case t901r65, in which the helicopter has a loading Heavy-Aft (HA). The test was recorded at an altitude of 3000 ft and airspeed of 112 knots. The pilot moved the pedal to the right and kept the control in this position for several seconds. Figures 50 - 54 shows the results given by the first version uncorrected of the POM software.
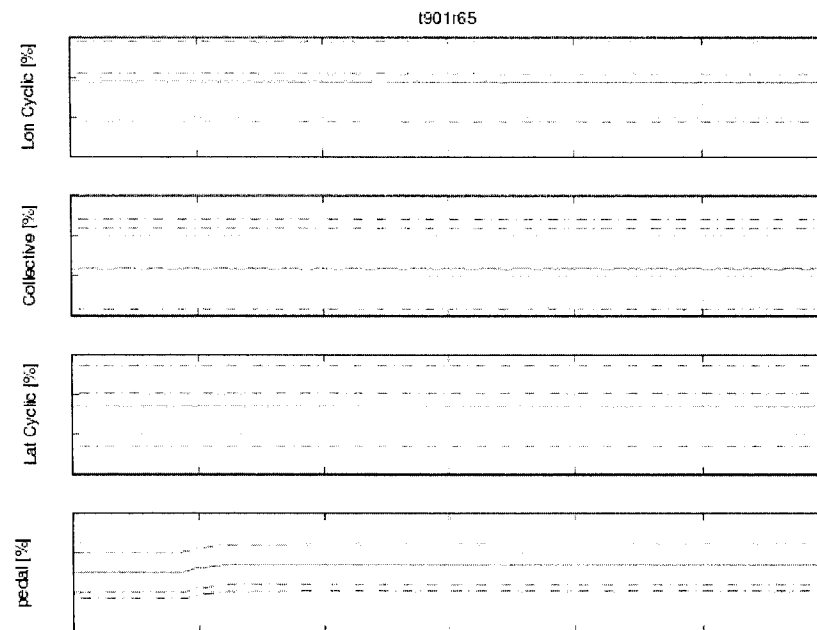
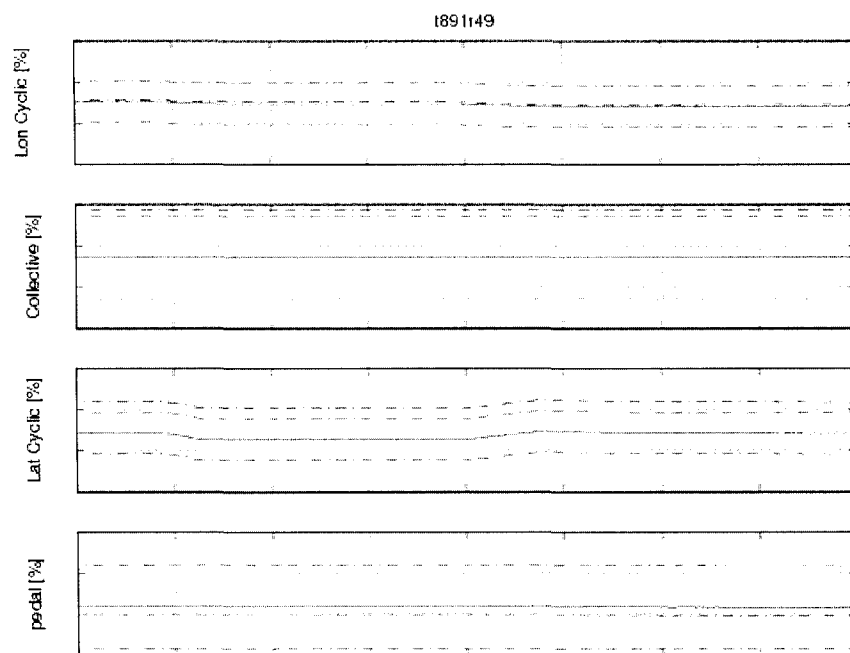

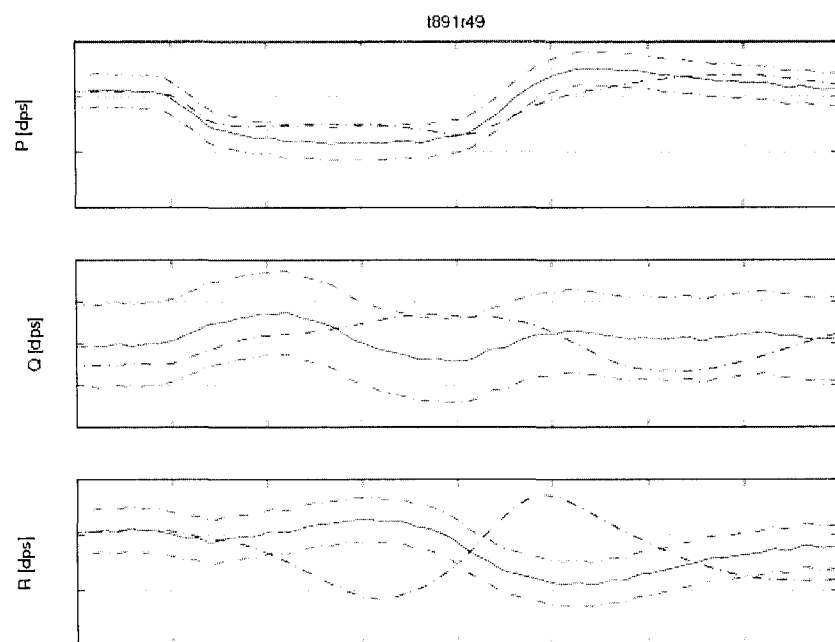Figure 50 Flight test t901r65 controls time history of uncorrected model
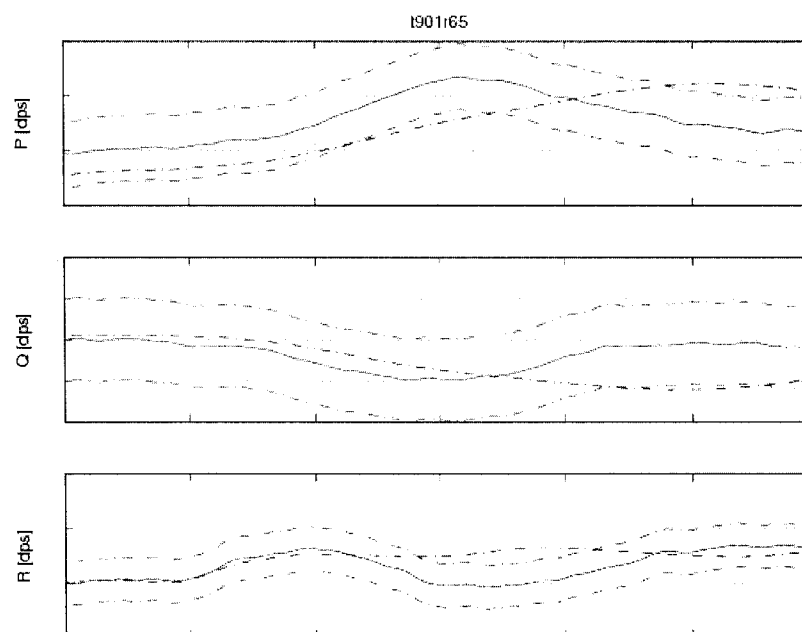
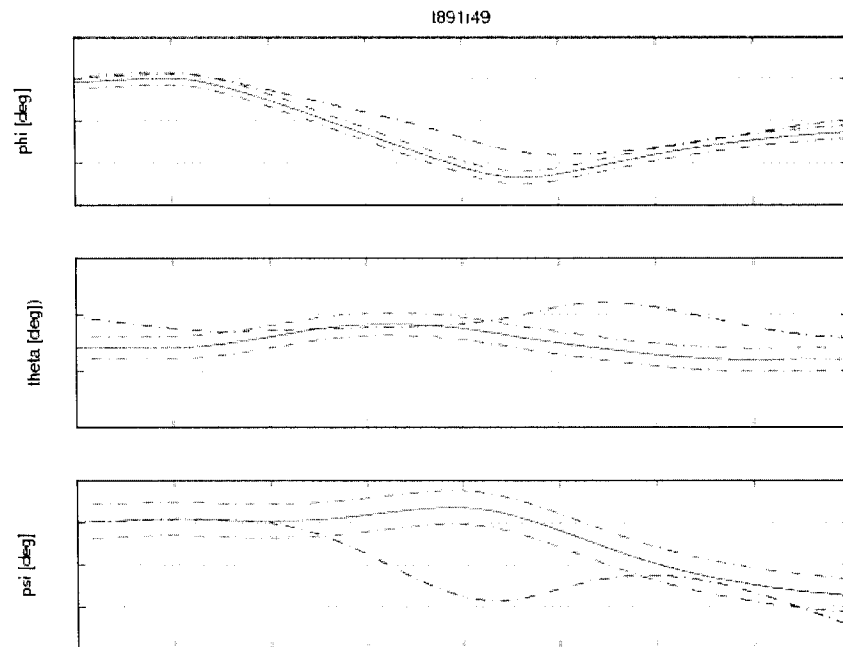Figure 51 Flight test t901r65 attitudes rates time history of uncorrected model

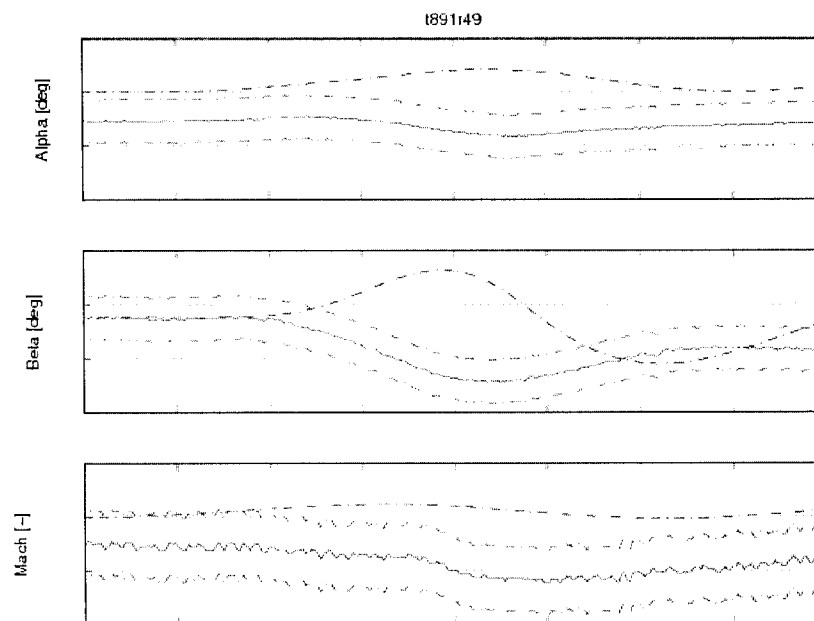Figure 52 Flight test t901r65 Euler angles time history of uncorrected model

Figure 53   Flight test t901r65 α, β and Mach number time history of uncorrected model
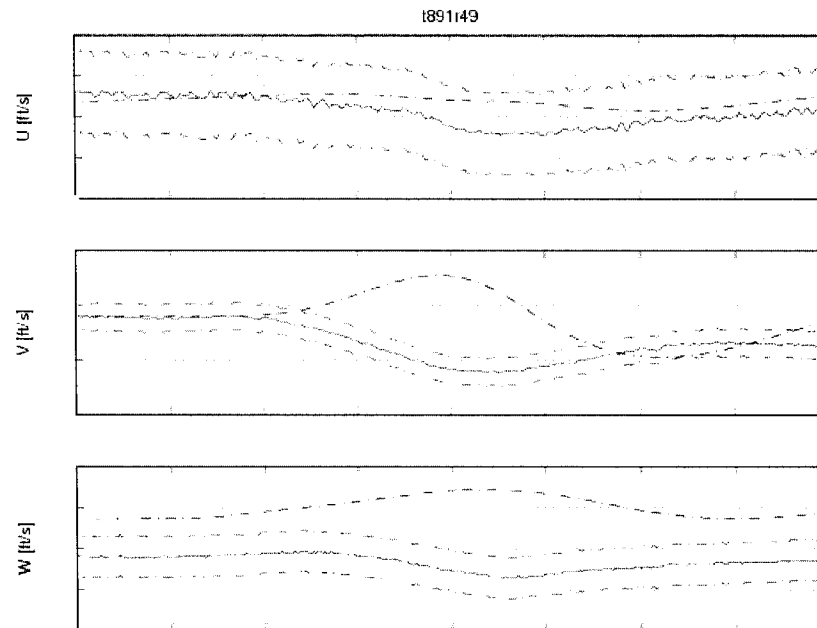
t901r65

Figure 54   Flight test t901r65 speeds in body reference system time history of uncorrected model

This case was not matched, as well as all the cases run with uncorrected initial POM version. Following the model adjustments and corrections, the new POM version matched sufficiently cases to be accepted by the QTG requirements. The results obtained for the same case with the new POM version are shown in Figures 55 – 60.
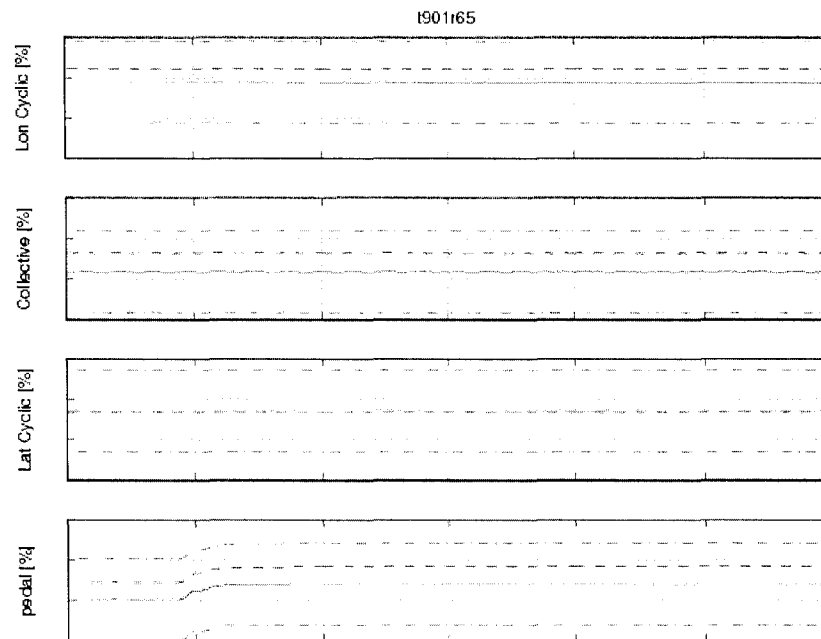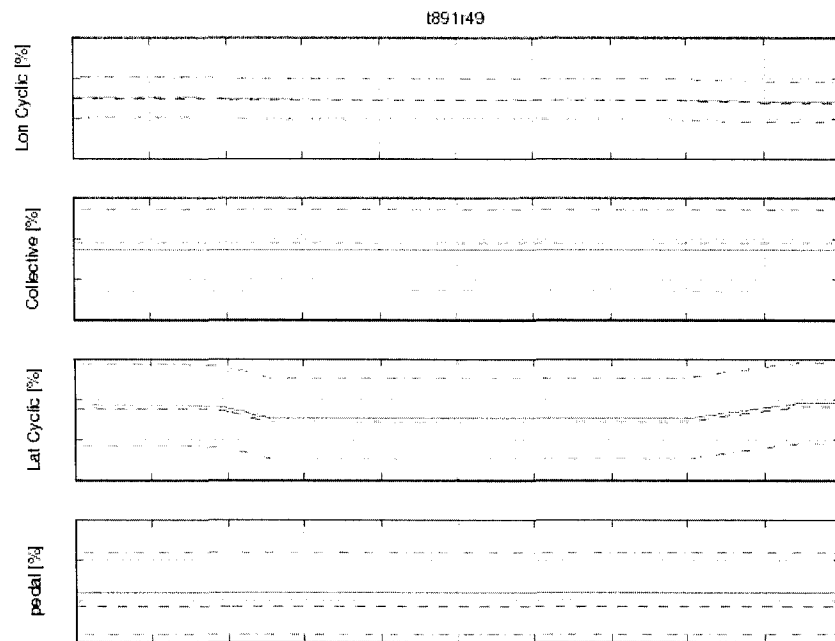
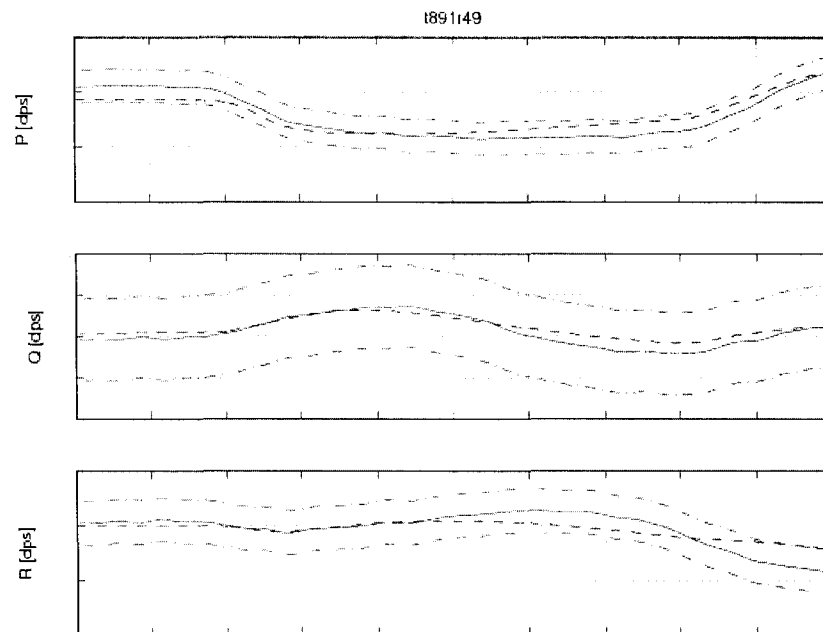Figure 55 Flight test t901r65 controls time history of corrected model

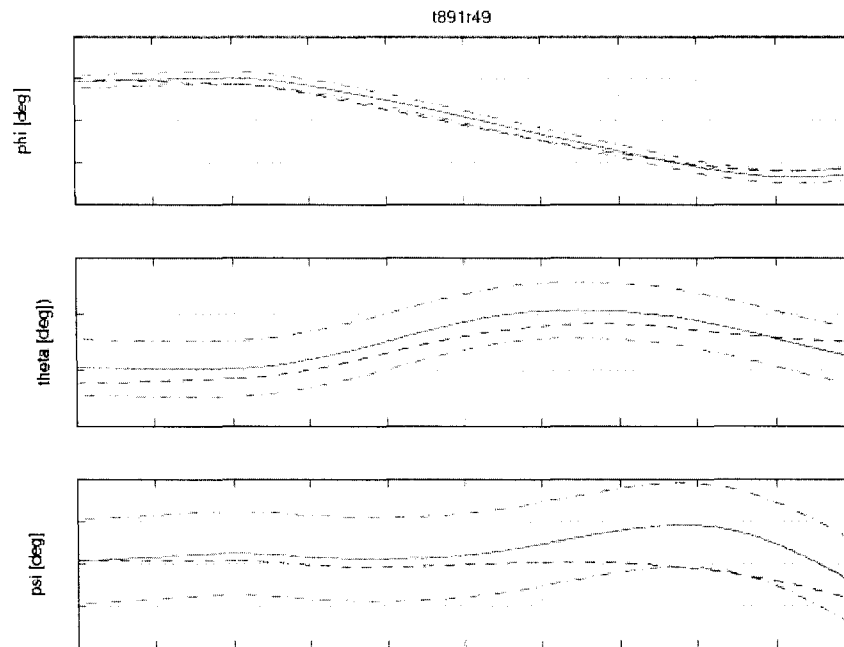Figure 56 Flight test t901r65 attitude rates time history of corrected model

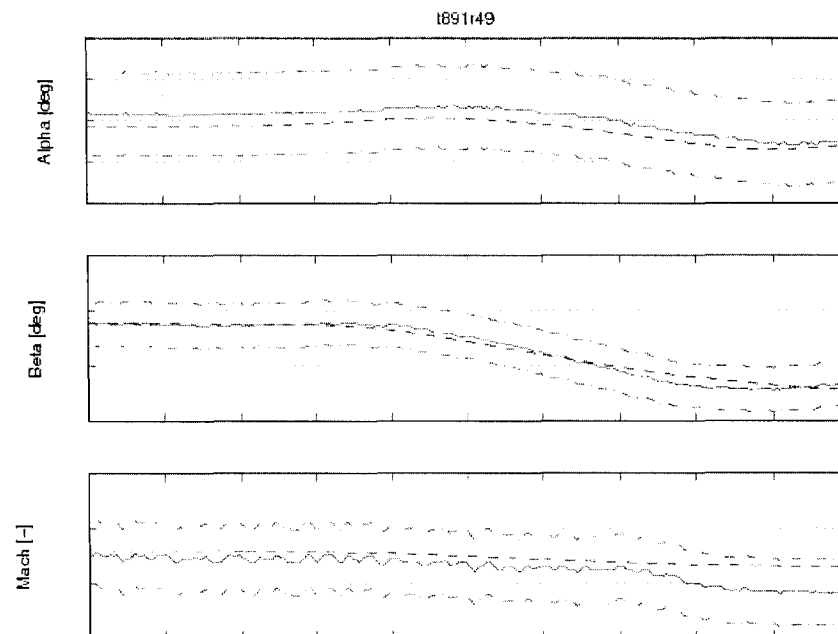Figure 57 Flight test t901r65 Euler angles time history of corrected model

Figure 58 Flight test t901r65 α, β and Mach number time history of corrected model
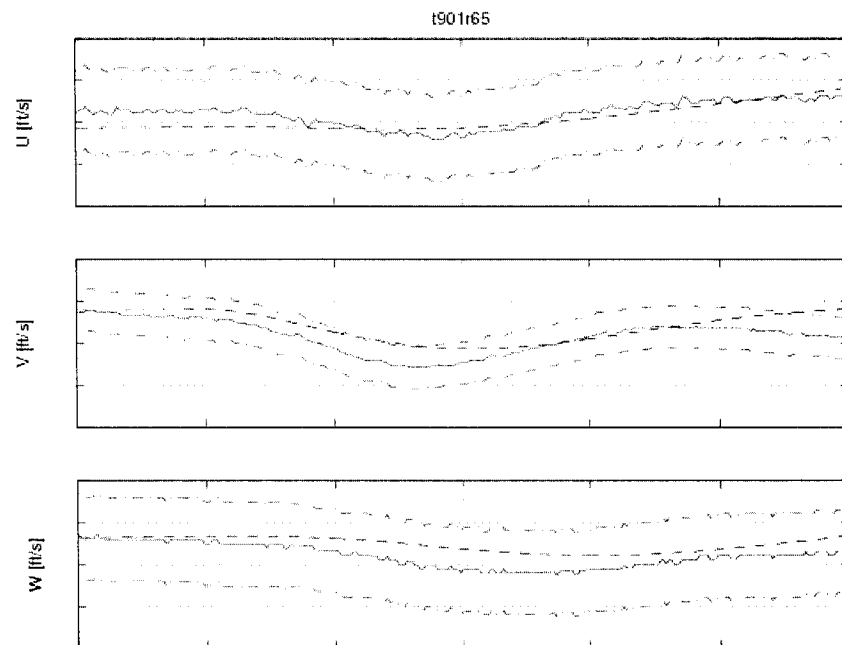
Figure 59   Flight test t901r65 speeds in body reference system time history of corrected model
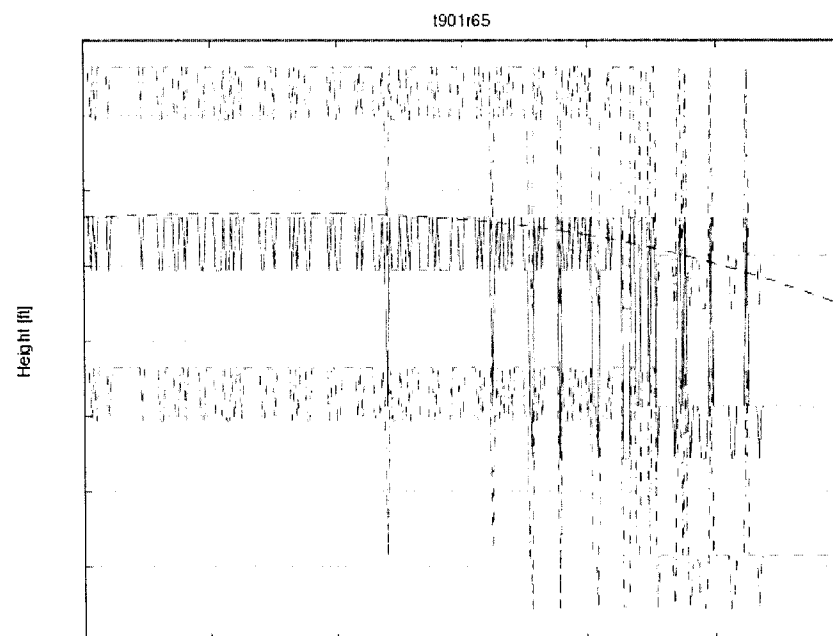
Figure 60 Flight test t901r65 density altitude time history of corrected model

5.5 Dynamic lateral and directional stability – spiral stability

For the spiral stability validation, the cruise or climb cases are required to match. The helicopter should have an input step only in directional control (pedals) or only in lateral cyclic only, in both directions (left and right) and the response of the helicopter should show the correct trend. To avoid entering in an uncontrolled spiral mode, the manoeuvre should be stopped and reversed in the initial trim position in which the helicopter could reach a 30 deg bank angle. In this manoeuvre, the important parameters are pedals or lateral cyclic and bank attitude within a tolerance of ± 2 deg. The other parameters are not mandatory; still the fitness of them is important. The trim function chosen was the "trimSideslipM" due to the well fitness in the steady flight. The sub-trim functions giving the best results were "subtrimClimbROC" and "subtrimVelRateROC" due to the initial conditions imposed to the speed rates to be zero and to the possibility of editing the rate of climb.

In Figures 61 - 65 one of the best fits is shown, the case t891r49, in which the helicopter has a Light-Aft (LA) loading. The test was recorded at an altitude of 3000 ft and airspeed of 112 knots. The pilot moved the cyclic stick to the left and kept the control in this position for several seconds until the helicopter reached a 30 deg bank angle. Figures 61 - 65 shows the results obtained by the first uncorrected POM version.

Figure 61 Flight test t891r49 controls time history of uncorrected model

Figure 62 Flight test t891r49 attitudes rates time history of uncorrected model

Figure 63 Flight test t891r49 Euler angles time history of uncorrected model

Figure 64   Flight test t891r49 α, β and Mach number time history of uncorrected model
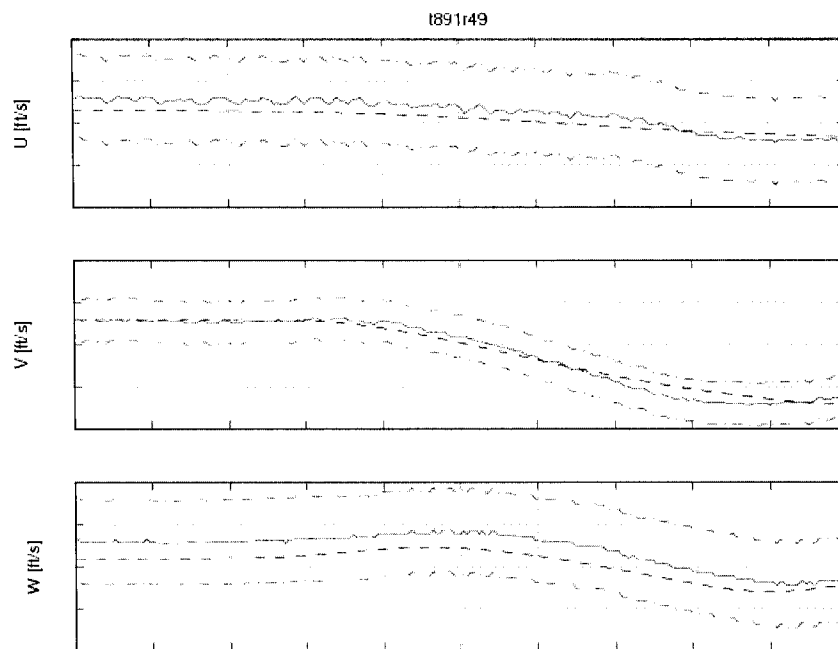
Figure 65   Flight test t891r49 speeds in body reference system time history of
uncorrected model

This case was not matched, as well as all the cases obtained with this POM version. Following the model adjustments and corrections, the new POM version matched sufficiently cases to be accepted by the QTG requirements. The results obtained for the same case with the new POM version are shown in Figures 66 – 71.
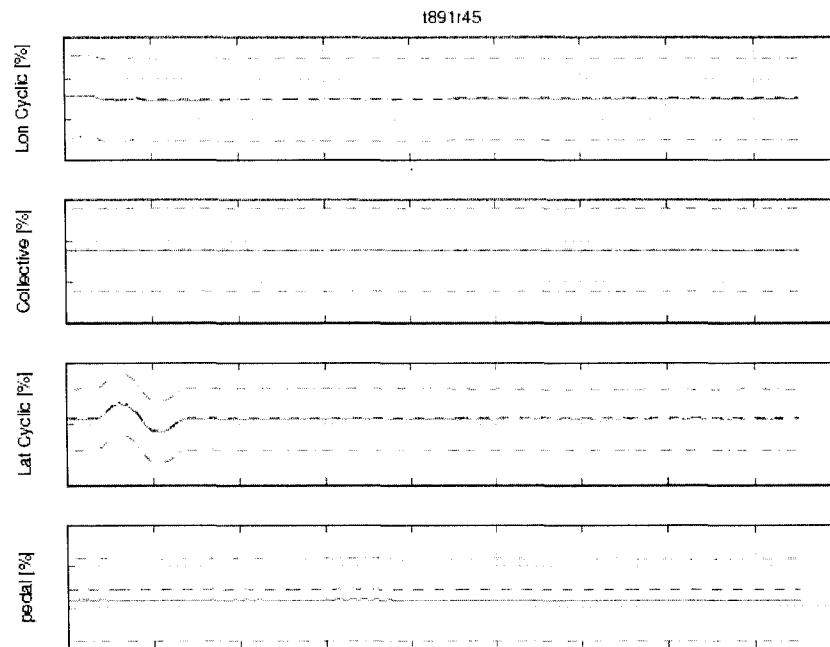
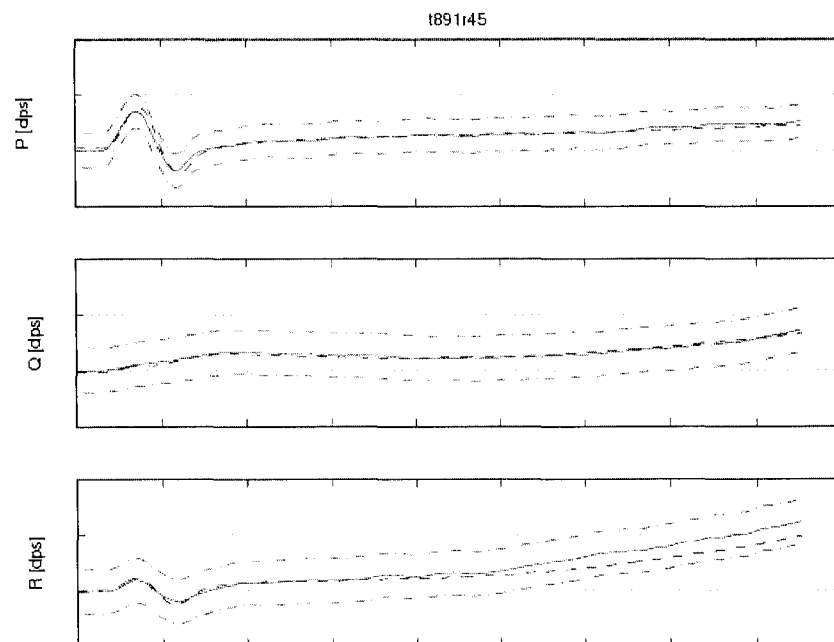Figure 66 Flight test t891r49 controls time history of corrected model

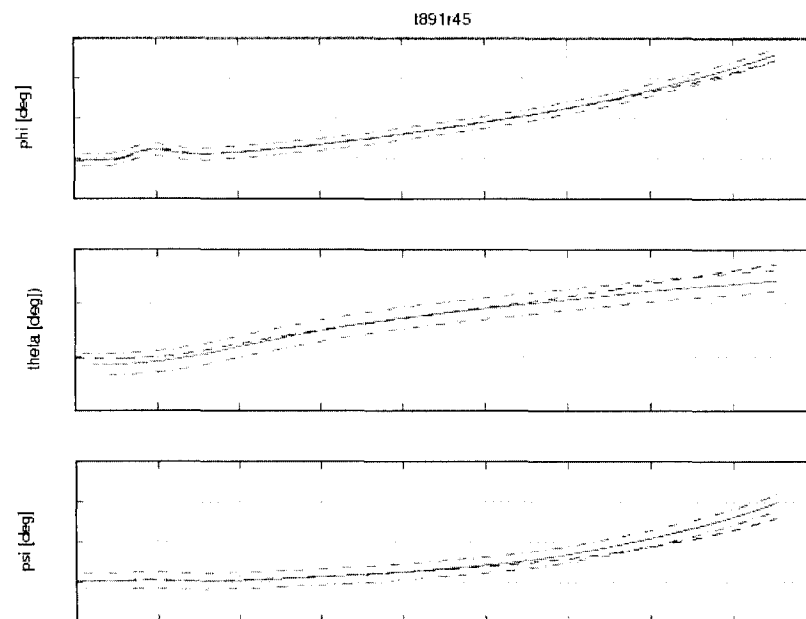Figure 67 Flight test t891r49 attitude rates time history of corrected model

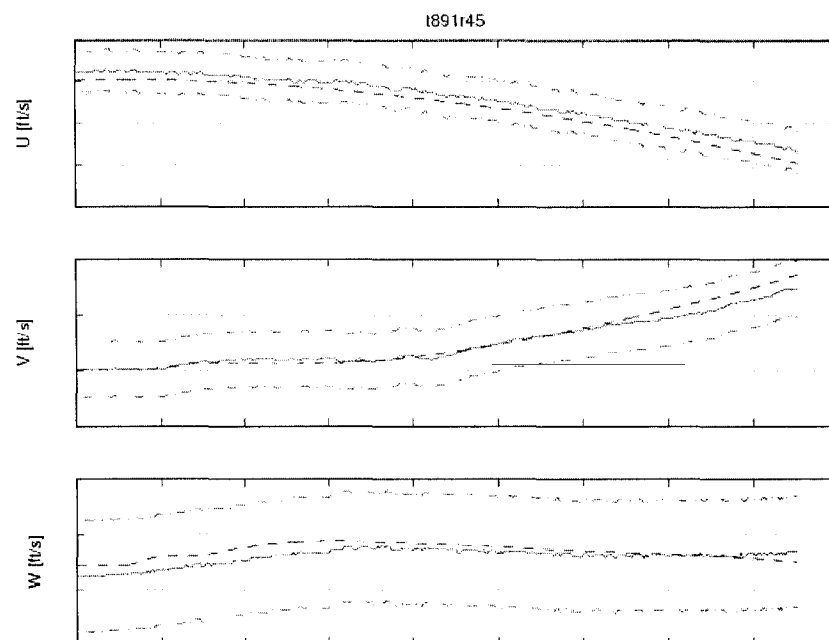Figure 68 Flight test t891r49 Euler angles time history of corrected model

Figure 69 Flight test t891r49 α, β, and Mach number time history of corrected model

Figure 70   Flight test t891r49 speeds in body reference system time history of corrected model
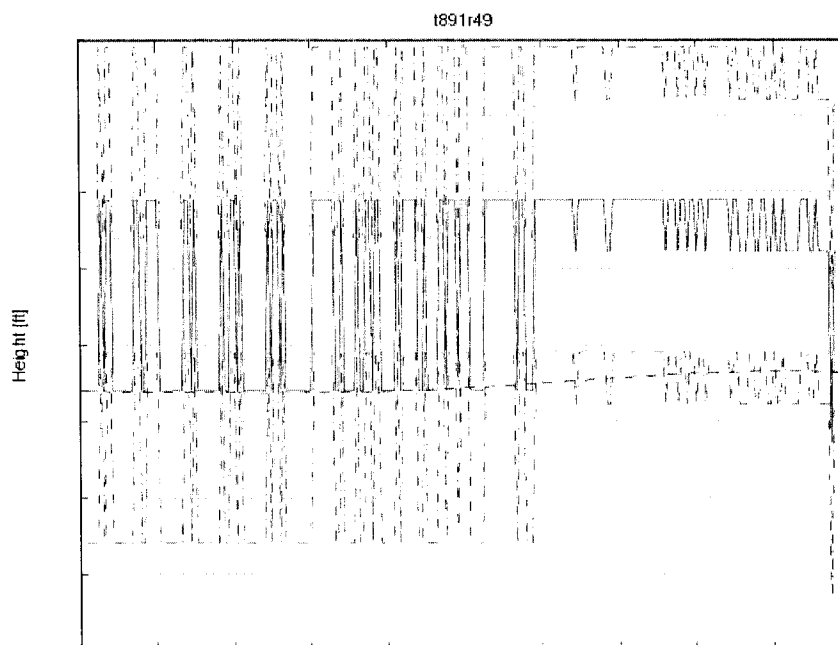
Figure 71 Flight test t891r49 density altitude time history of corrected model

5.6   Dynamic lateral and directional stability – lateral and directional oscillations

For the lateral and directional oscillations validation, the cruise or climb cases are required to match for two different airspeeds. The helicopter oscillations should be excited by use of a lateral cyclic stick or pedals doublet. Test should include six full cycles (12 overshoots following input) or enough cycles to determine time to half or double amplitude, whichever is less. For a non-periodic response, time history should be matched.   In this manoeuvre, the main parameters are the period of oscillations within a tolerance of ±0.5 sec or 10%, the time to half or double amplitude within a tolerance of 10% and the time differences between peaks of bank and sideslip angle of 20% or ±1 sec. The chosen trim function was "trimSideslipM" due to the well fitness in the steady flight. The sub-trim functions giving the best results were "subtrimClimbROC" and "subtrimVelRateROC" due to the initial conditions imposed to the speed rates to be zero and to the possibility of editing the rate of climb.

In the following figures, one of the best fits is shown the case t891r45, in which the helicopter has a Light-Aft loading (LA). The test was recorded at an altitude of 3000 ft and airspeed of 65 knots. The pilot moved the cyclic stick by a lateral doublet to excite lateral-directional oscillations. In Figures 72 - 76 the helicopter response for this configuration was non-periodic. In these figures, the results of the latest corrected POM version are shown. The model has a perfect match with the recorded parameters.

Figure 72 Flight test t891r45 controls time history of corrected model

Figure 73 Flight test t891r45 attitudes rates time history of corrected model

Figure 74 Flight test t891r45 Euler angles time history of corrected model

Figure 75   Flight test t891r45 speeds in body reference system time history of corrected model
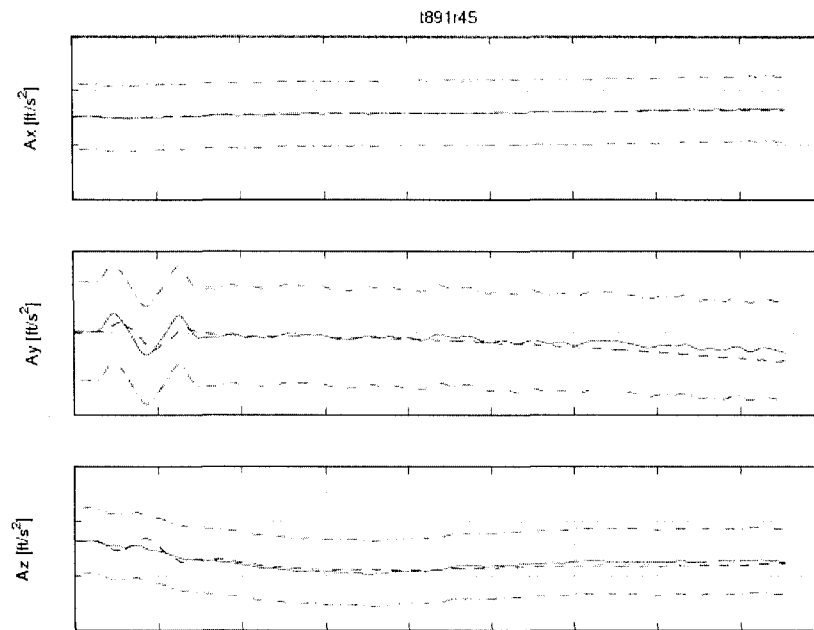
Figure 76   Flight test t891r45 accelerations in body reference system time history of corrected model

For the model certification, is required at least two cases in two different air-speeds to be matched. All the cases matched in the POM were for helicopter in Light-Aft (LA) configuration. In the following figures, two cases in different configurations than LA are shown, which are not perfectly matched, so that do not satisfy the certification requirements.

The case t892r55 shown in Figures 77 - 79 is a lateral dynamic oscillation excitation due to a doublet input in the pedal for a Heavy-Forward (HF) helicopter configuration with airspeed of 112 knots. From the figures, it can be seen that the oscillations period matches the AC requirements which states that the tolerances applied for the first overshoot are ±10% of the first period. The amplitude of the oscillations of the model is almost half of the amplitude of the real helicopter which is outside of the tolerances stated in the AC of ±10% for the first overshoot and ±20% for subsequent overshoots,

especially in the yaw rate *r* plot. The same unmatching issue can be seen in the vertical acceleration A_z plot.
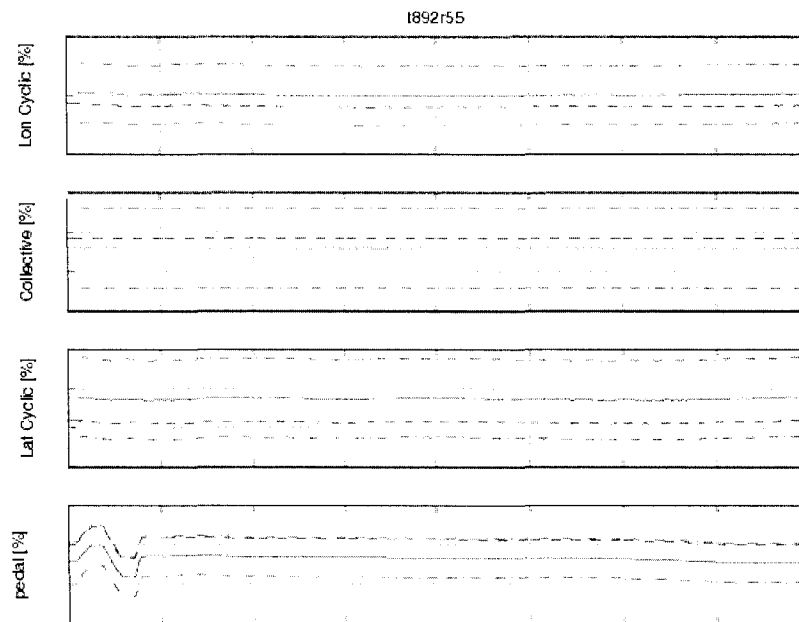
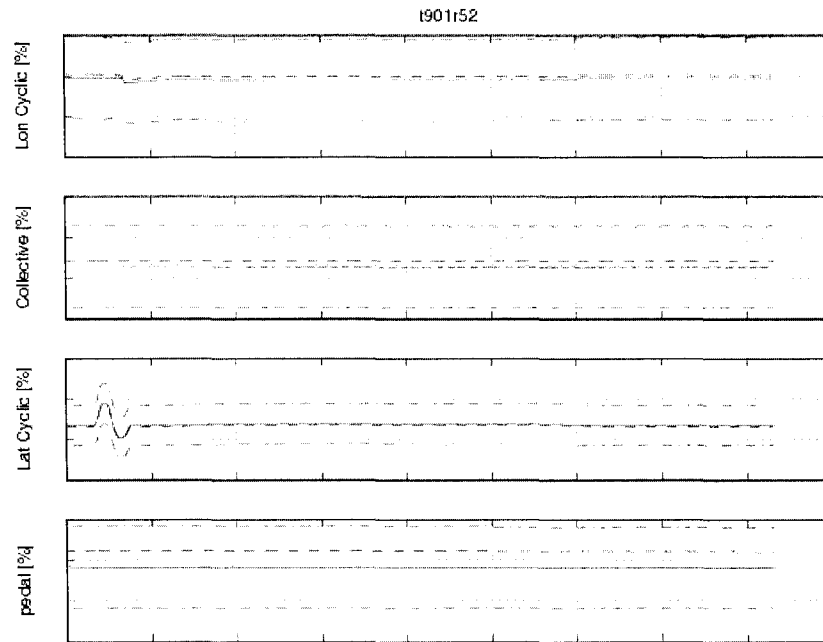
Figure 77 Flight test t892r55 controls time history
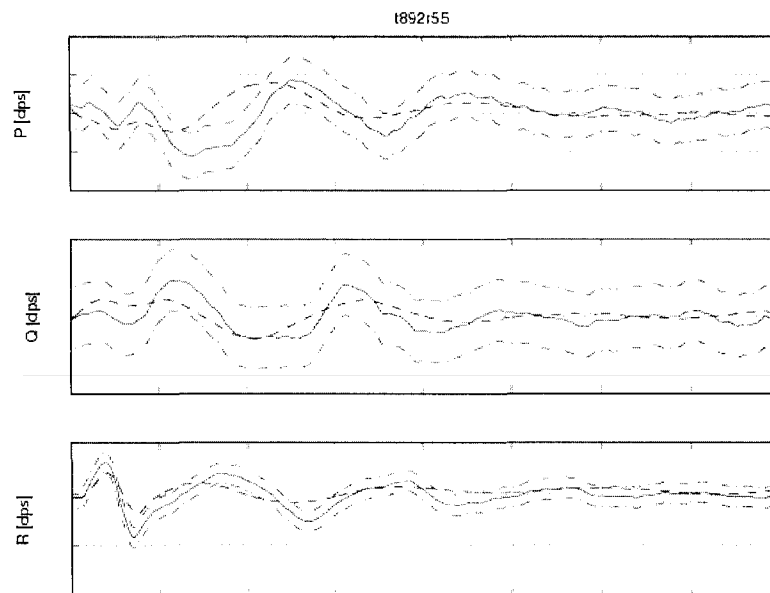
Figure 78 Flight test t892r55 attitude rates time history
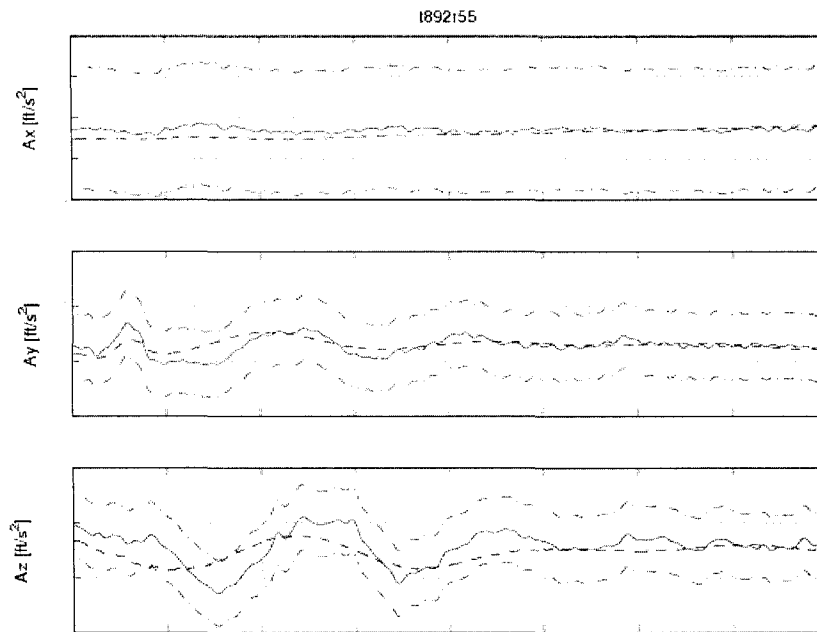
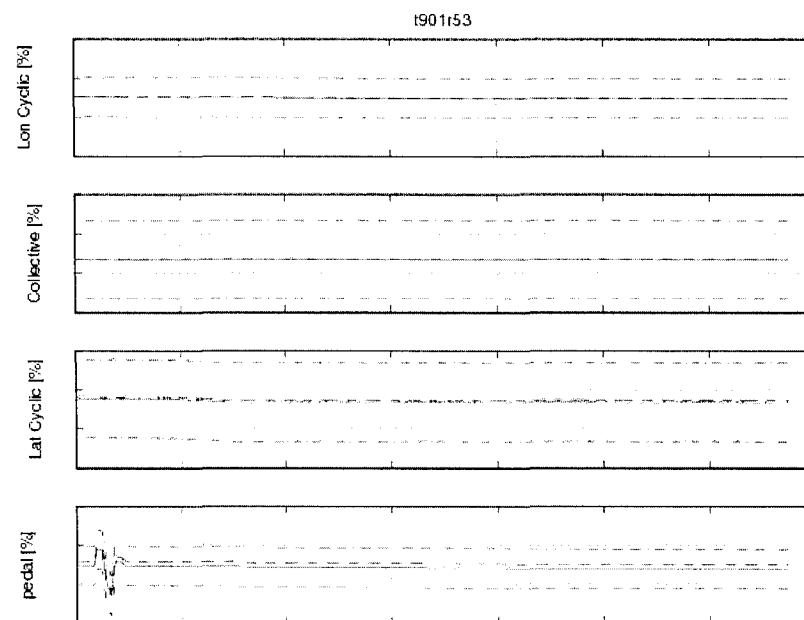Figure 79 Flight test t892r55 accelerations time history

From Figures 78 and 79, the helicopter in the HF configuration at high airspeed has an underdamped Dutch roll. There is a difference of 1 second between the simulated helicopter period and the flight test data, which is out of the tolerance of ±0.5 sec required by the AC [9]. The simulated helicopter oscillations amplitudes are much smaller than the real helicopter oscillation amplitudes, which show that the model damping ratio ζ is higher than the helicopter damping ratio.

In Figures 80 – 83, the case t901r52 of lateral dynamic oscillations excitation by an input doublet in cyclic stick in the lateral direction, for a helicopter in the Heavy-Aft configuration is shown. In Figures 84 - 87 the case t901r53 of lateral dynamic oscillations excitation by an input doublet in pedals, for a helicopter in the same Heavy-Aft configuration is shown.

Figure 80 Flight test t901r52 controls time history
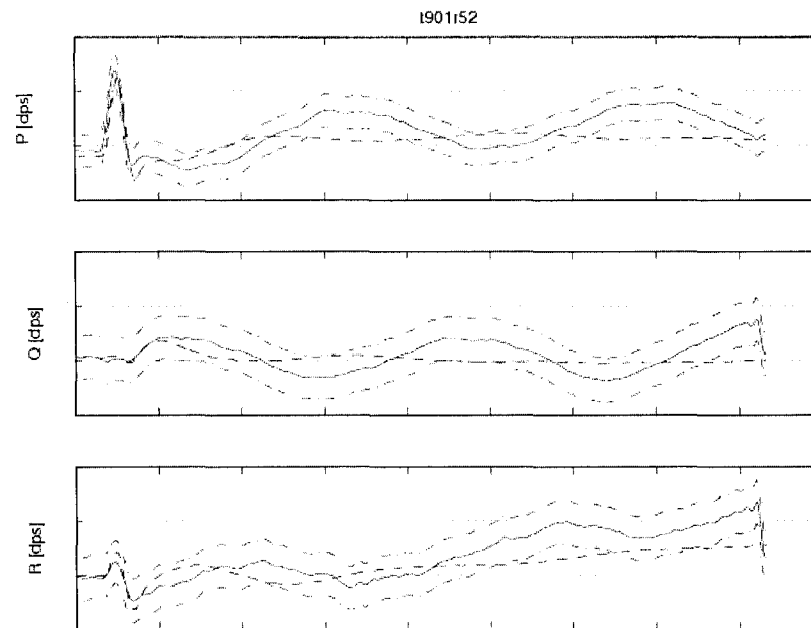
Figure 81 Flight test t901r52 attitudes rates time history
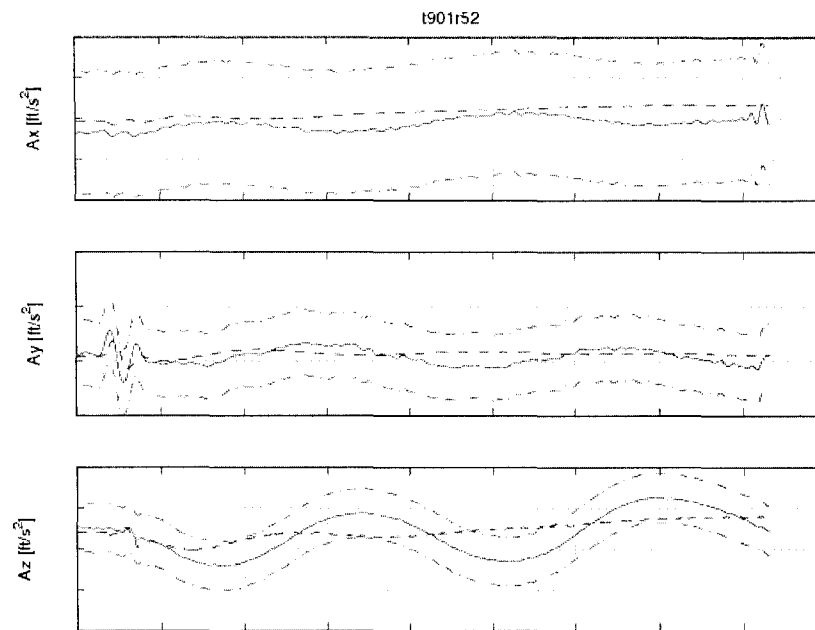
Figure 82 Flight test t901r52 accelerations time history
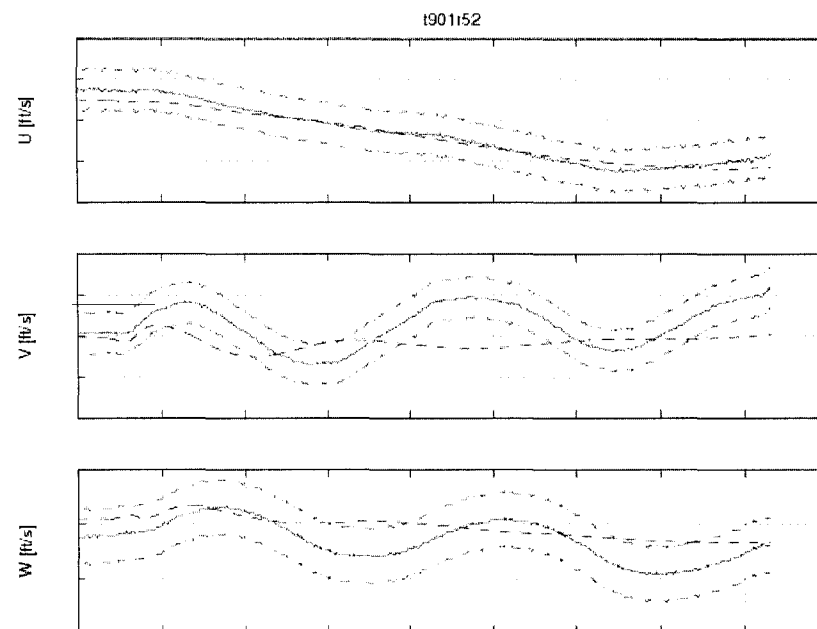
Figure 83 Flight test t901r52 speeds in body reference system time history

Figure 84 Flight test t901r53 controls time history
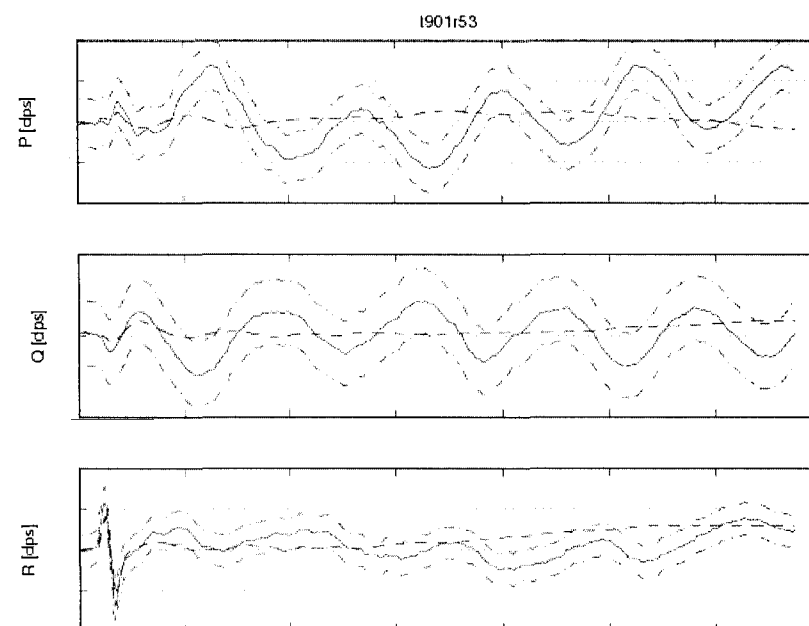
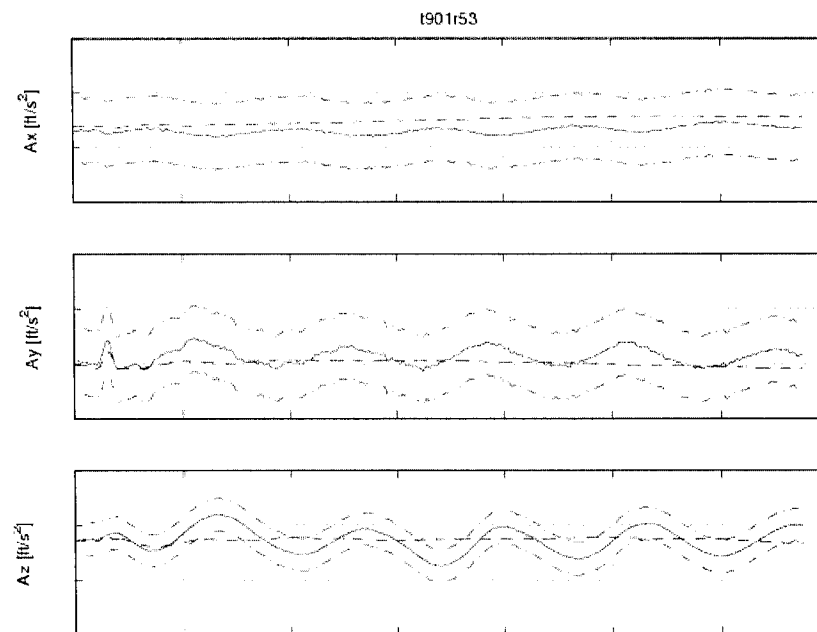Figure 85 Flight test t901r53 attitudes rates system time history

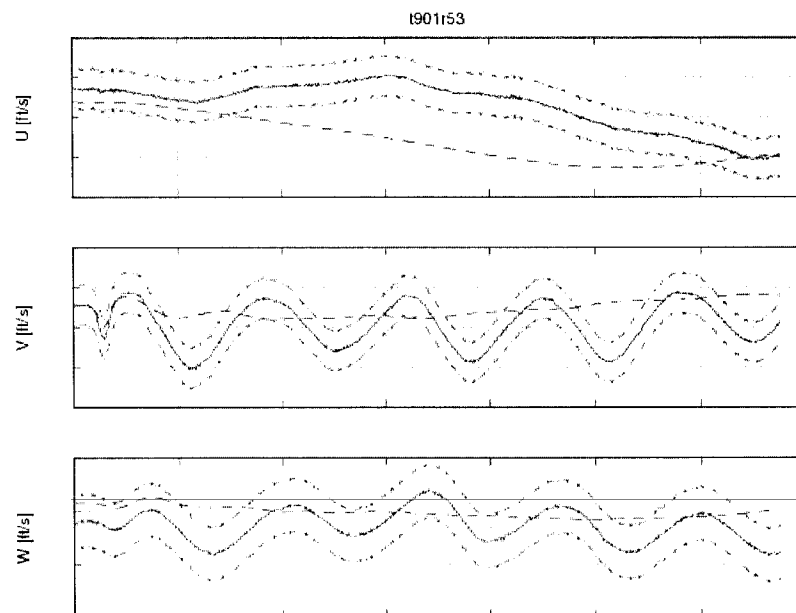Figure 86 Flight test t901r53 accelerations time history

Figure 87 Flight test t901r53 speeds in body reference system time history

In both cases, an excitation of the Dutch roll oscillations exists, in the first case is given by a lateral cyclic doublet and in the second case is given by a pedal doublet. Both cases took place at a high airspeed and in this configuration the oscillations of the helicopter have a period greater than the simulated helicopter which is out of the tolerance of ±0.5 seconds required by the AC [9]. The damping ratio of the helicopter is very small compared to the very strong damping of the simulated helicopter.

These three cases show that the models built for the configurations Heavy-Aft and Heavy-Forward at high airspeeds needs more adjustments to satisfy the requirements of the FAA helicopter certification. From the point of view of FAA certification it is sufficient that the model Light-Aft in two different airspeeds (low and high airspeed) to be matched, which in this point of the certification procedure, the model can be considered satisfactory for the purpose of this project.

CHAPTER 6

HOVER PERFORMANCE VALIDATION

6.1 General considerations

The hover model is a separate model from the UAA model because of its specific aerodynamics characteristics, firstly because there is no translational airspeed. These aerodynamics characteristics are very different when the helicopter is in the proximity of the ground. When the helicopter flies far from the ground (OGE) its sustentation is given by the air wake created by the main rotor according to the momentum theory [3], [4], [5]. The momentum theory treats the rotor as an actuator disk through which a uniform flow passes. For a given gross weight it is required a certain airspeed of the wake which is named "induced velocity" of the air wake.

Blade element theory overcomes some of the restrictions inherent in the momentum theory as it is based upon the idea that the rotor blades function as high aspect ratio wings constrained to rotate around a central mast as the rotor system advances through the air. In Figure 88 the momentum theory and blade element theory for the helicopter out of ground effect and in ground effect is shown.

The induced velocity is given by the blades collective pitch angles and is controlled by the collective stick. To maintain the helicopter in the air, the pilot must displace the collective stick in a certain position. In the proximity of the ground which is defined as the altitude less than one main rotor diameter, the air wake of the main rotor forms a cushion under the helicopter [3].

This cushion of air allows the helicopter to be maintained in the air with a smaller "induced velocity", equivalent to a smaller blades collective pitch angle, and to a lower

position of the collective stick. The phenomenon shown in figure 88 is called "In Ground Effect (IGE)" and a separate mathematical model is necessary to simulate its apparition. The POM software uses an "IF function" to make the difference between the UAA model and Hover model when TAS is smaller than 7 knots arbitrary chosen. There is another "IF function" to make the difference between the In Ground Effect model (IGE) and Out of Ground Effect model (OGE) when radar altitude RALT is less than 40 ft arbitrary chosen (the main rotor diameter is 37 ft).
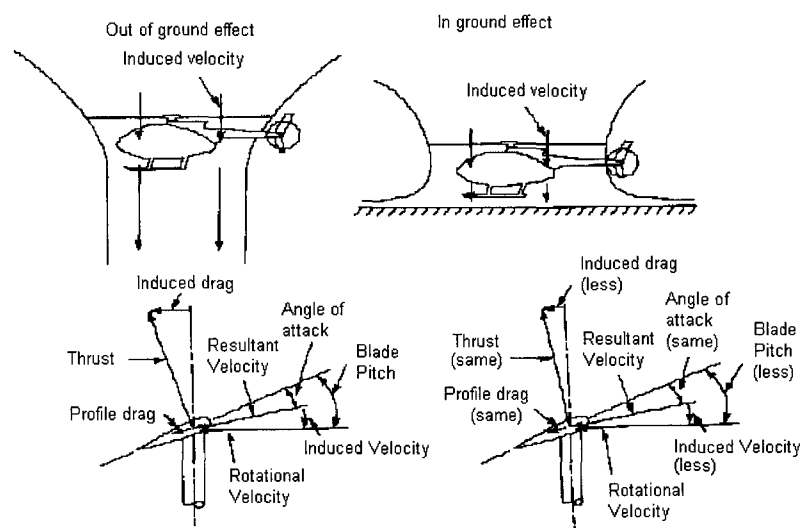
Figure 88 Aerodynamic effect of the ground proximity (In Ground Effect)

In Figure 89 the POM logic the model for the simulated flight test is shown:
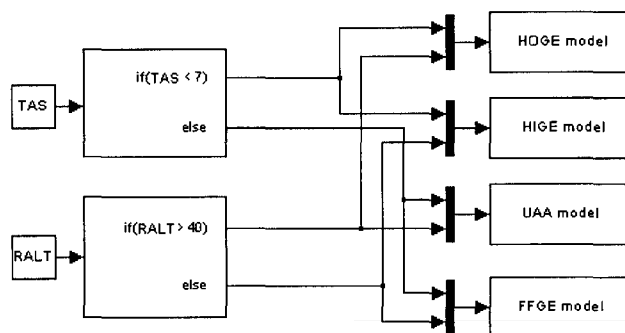
Figure 89 POM logic of Hover IGE, OGE, FFGE and UAA model

6.2 Hover performance In Ground Effect (IGE) validation

For the validation of the hover performance there is the requirement to match two gross weights (Light and Heavy) in both flight conditions IGE and OGE. The matching may be a "snapshot", which means 2-3 seconds of matching may be acceptable. The parameters required by the AC to match are the pitch attitude θ within a tolerance of $\pm$ 1.5 degrees, the bank attitude with a tolerance of $\pm$ 1.5 degrees and all the controls (longitudinal position of cyclic stick, lateral position of cyclic stick, collective stick position, pedals position) within a tolerance of $\pm$ 5% of range motion. The trim function chosen was the "trimAngAccel" because this function allows editing the initial condition for angular accelerations $Pdot$, $Qdot$ and $Rdot$ ($\dot{p},\dot{q},\dot{r}$). The sub-trim function giving the best results was "subtrimRate" in which the rates attitudes are the only constraints.

In Figures 90 - 94 the case t894r51 of hover performance in ground effect, for the helicopter in light gross weight configuration is shown:
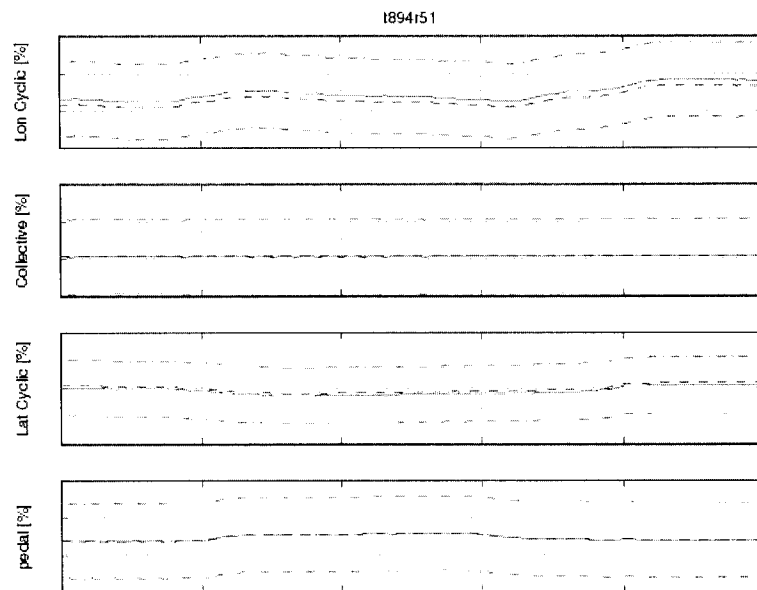
Figure 90 Flight test t894r51 controls time history
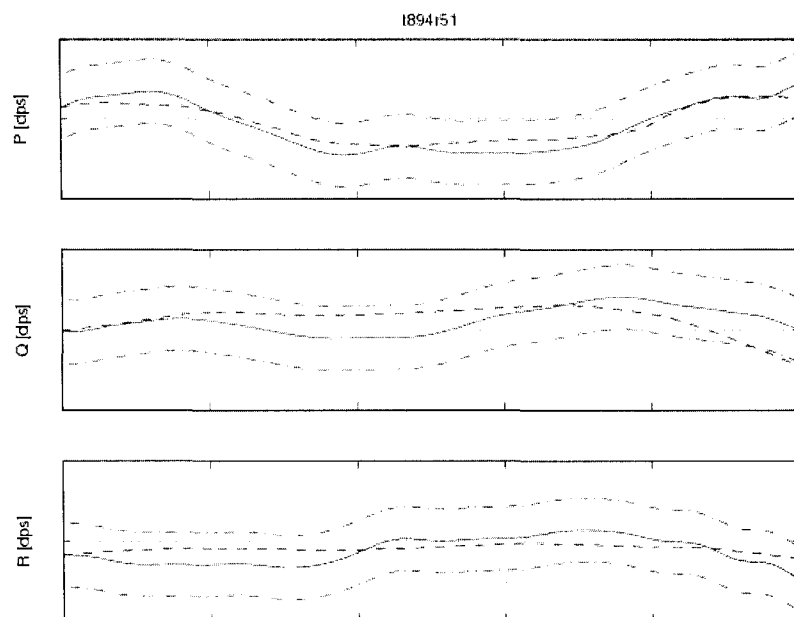
Figure 91 Flight test t894r51 attitude rates time history
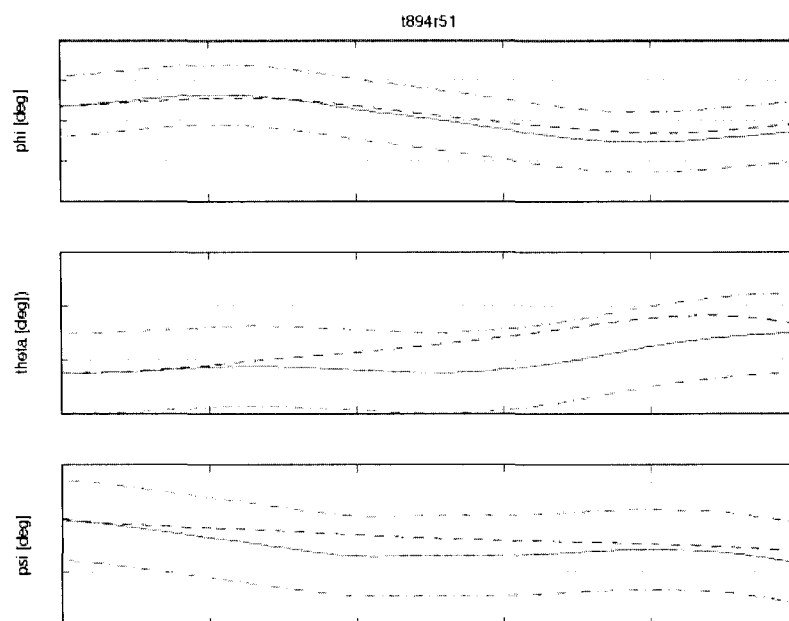
Figure 92 Flight test t894r51 attitude angles time history
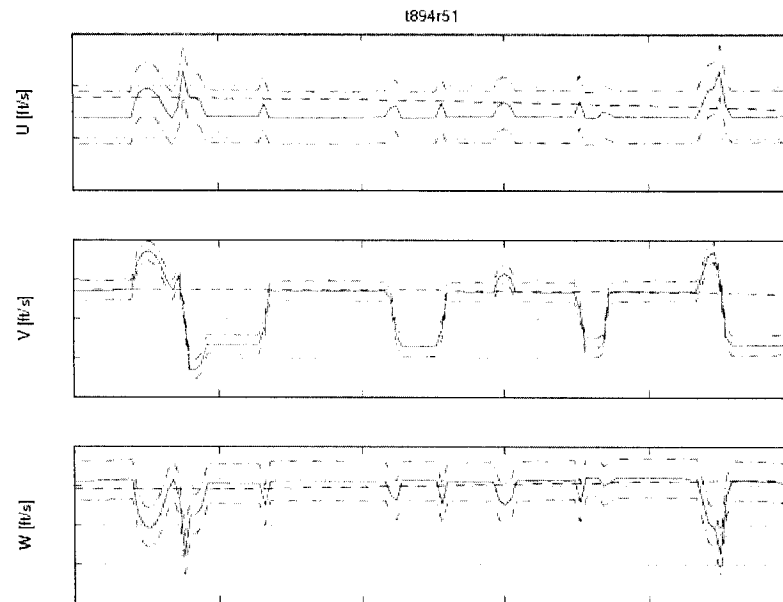
t894r51

Figure 93 Flight test t894r51 speeds in body reference system time history
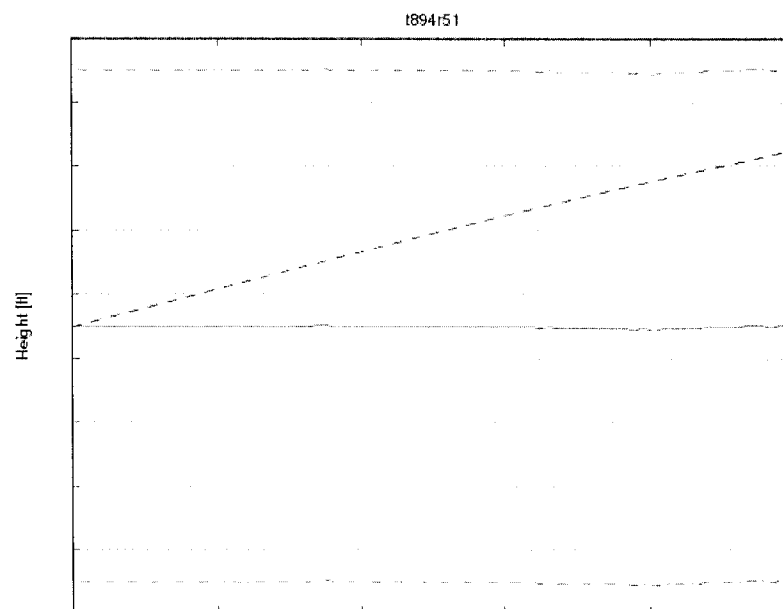
t894r51

Figure 94 Flight test t894r51 radar altitude time history

In Figures 95 – 99, the case t893r39 for the hover performance in ground effect, for the helicopter in heavy gross weight configuration is shown:
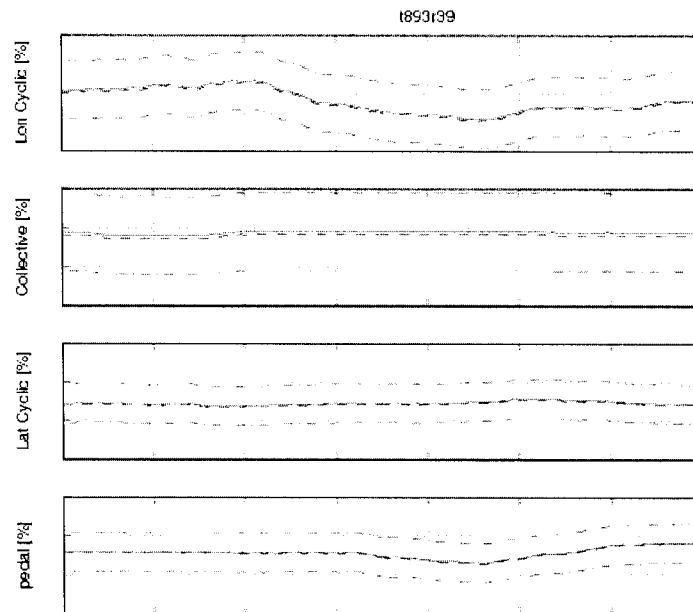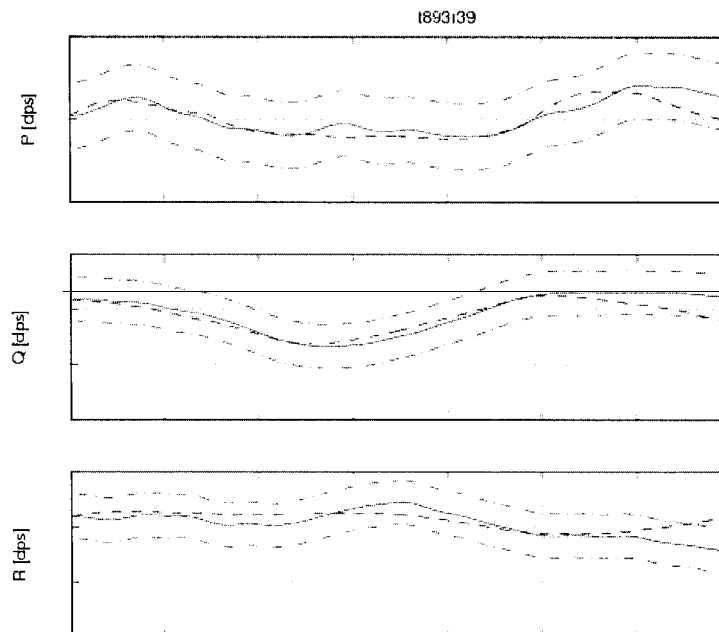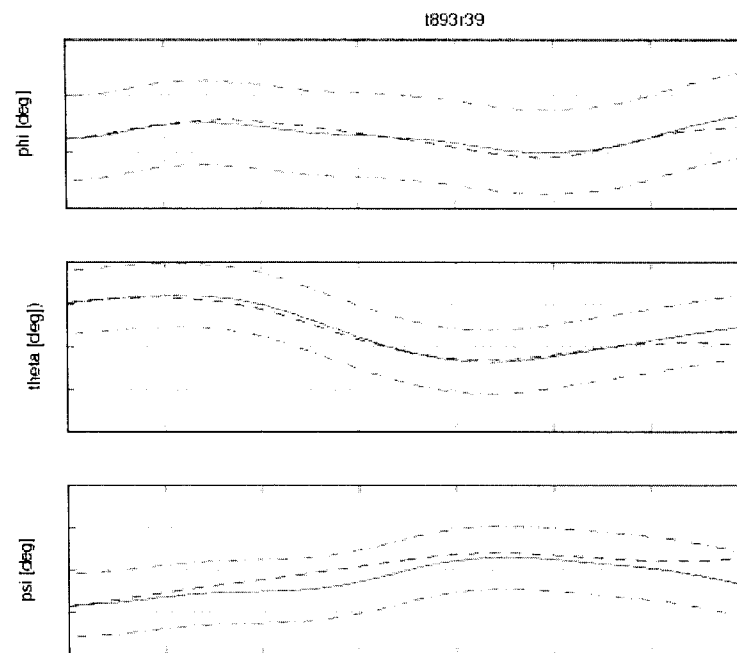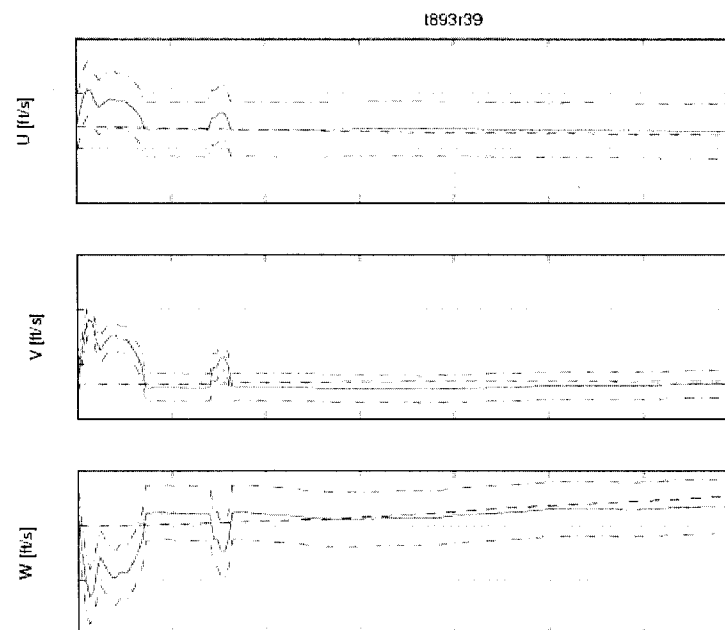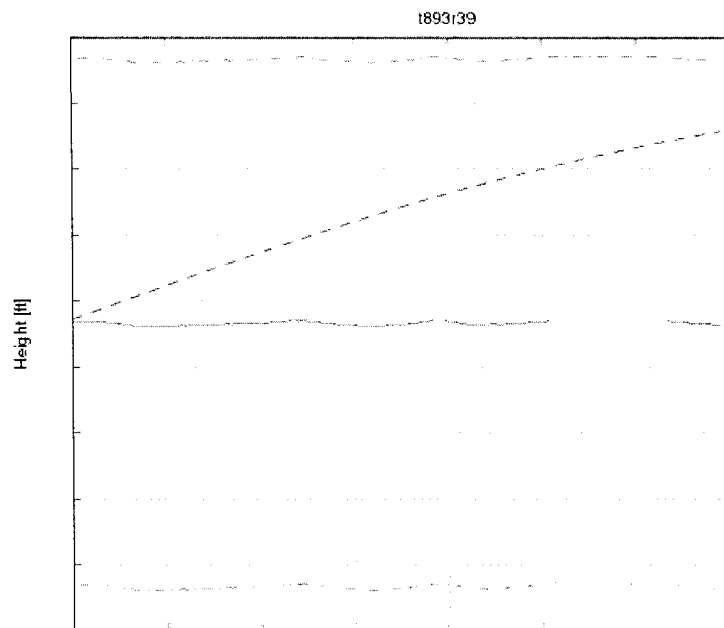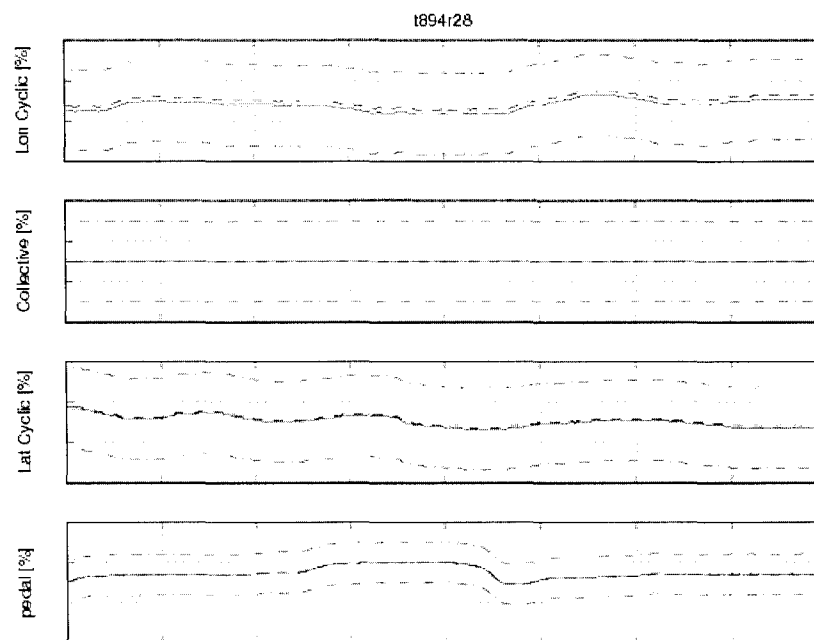

Figure 95 Flight test t893r39 controls time history

Figure 96 Flight test t893r39 attitude rates time history

Figure 97 Flight test t893r39 Euler angles time history

Figure 98 Flight test t893r39 speeds in body reference system time history

Figure 99 Flight test t893r39 helicopter altitude time history

The two simulation cases in light and heavy gross weight configuration matched perfectly with the flight test, and the certification requirements of the AC for the hover IGE chapter (Table V, 1d) are satisfied.

6.3   Hover performance Out of Ground Effect (OGE) validation

The same requirements for the IGE are applied also for the OGE model. In Figures 100
– 104, the case t894r28 for the hover performance out of ground effect, for the
helicopter in light gross weight configuration is shown:
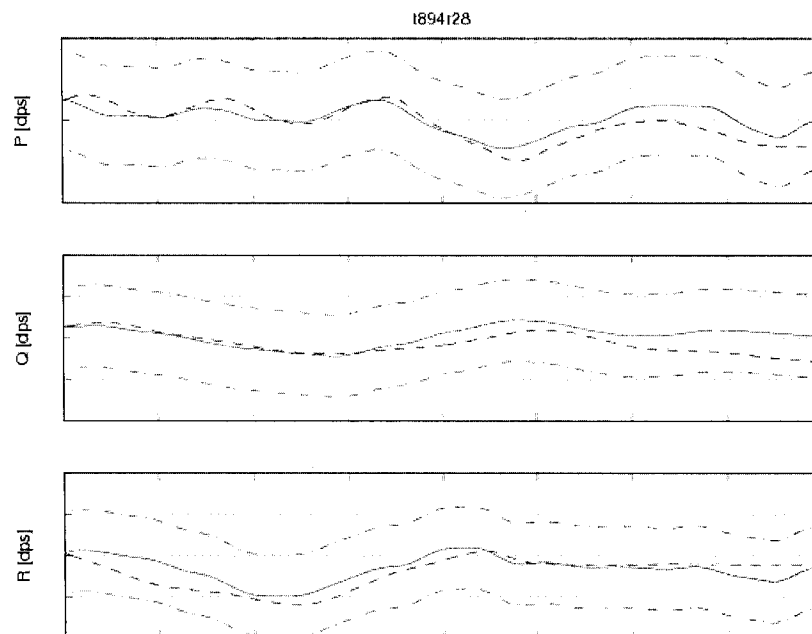

Figure 100 Flight test t894r28 controls time history

t894r28
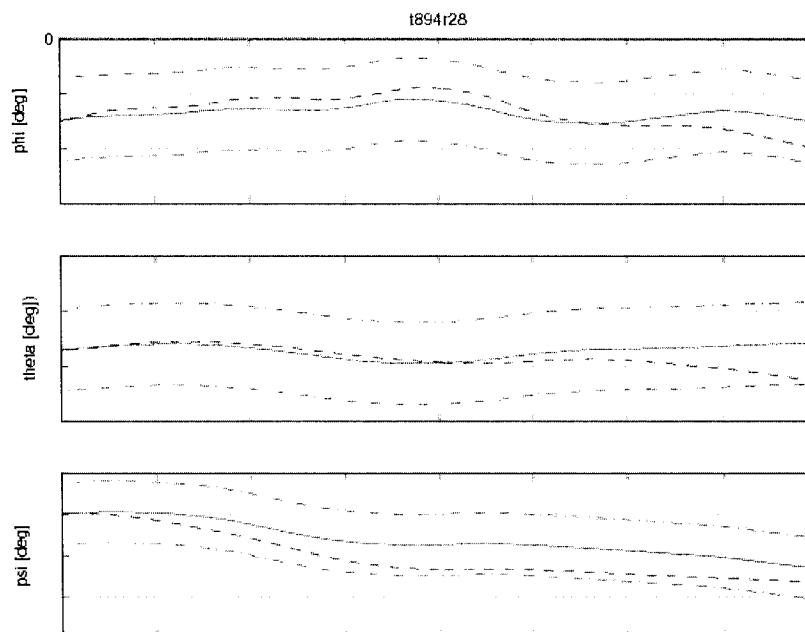
Figure 101 Flight test t894r28 attitude rates time history

t894r28

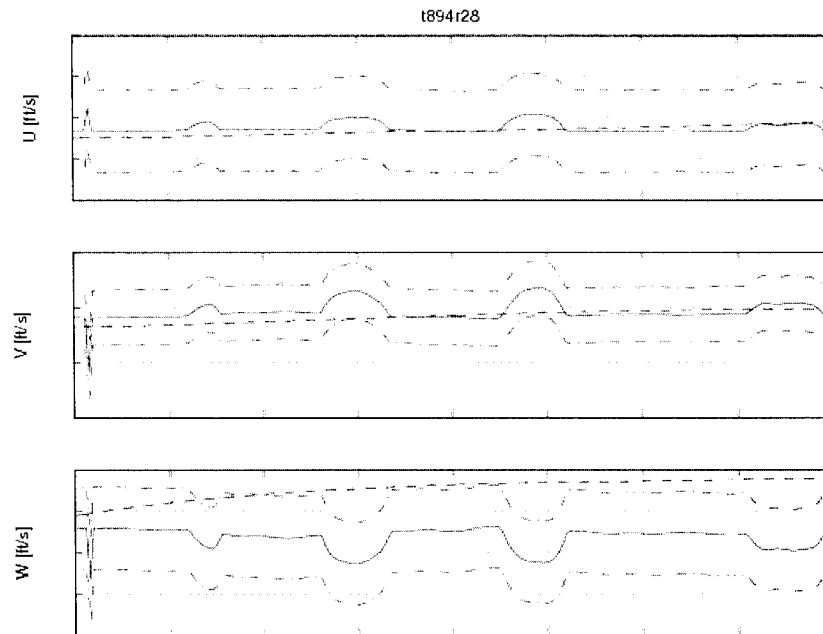Figure 102 Flight test t894r28 Euler angles time history

t894r28

Figure 103 Flight test t894r28 speeds in body reference system time history
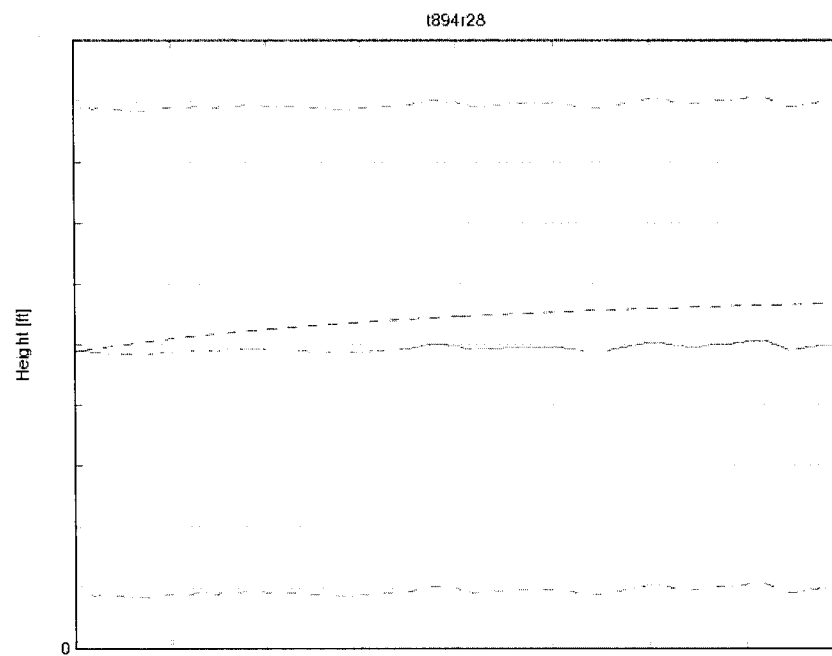
t894r28

Figure 104 Flight test t894r28 radar altitude time history

In Figures 105 – 108, the case t893r43 for the hover performance out of ground effect, for the helicopter in heavy gross weight configuration is shown:
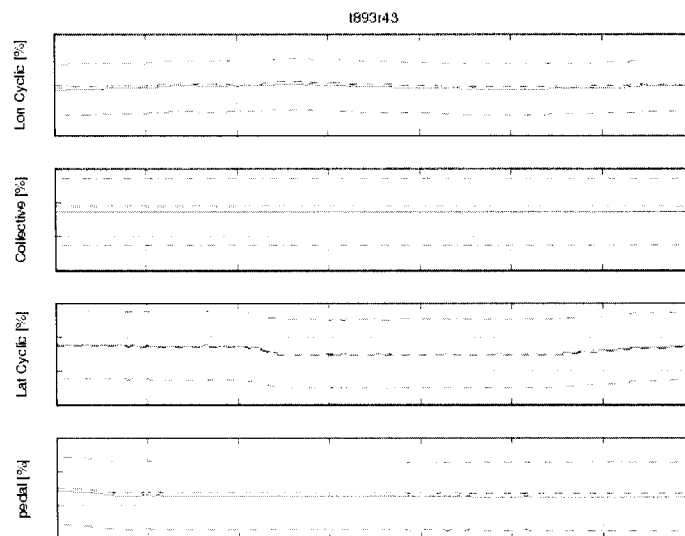

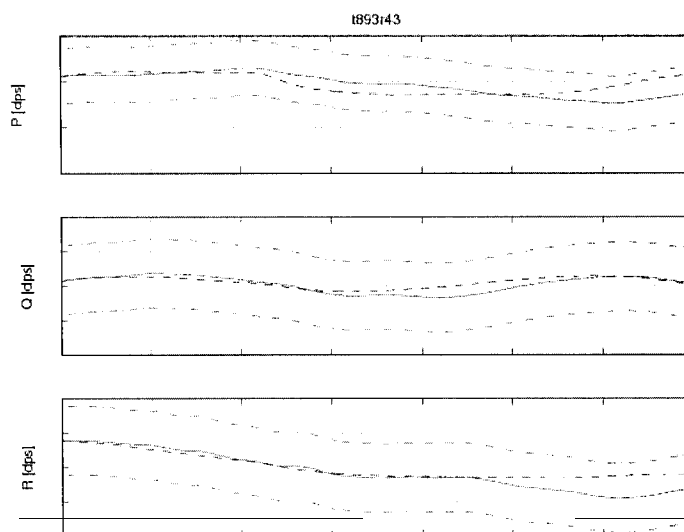Figure 105 Flight test t893r43 controls time history

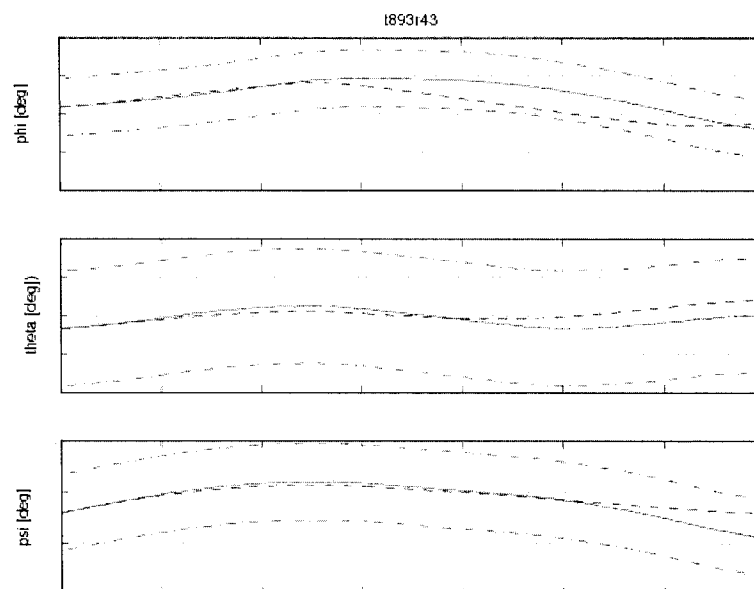Figure 106 Flight test t893r43 attitude rates time history

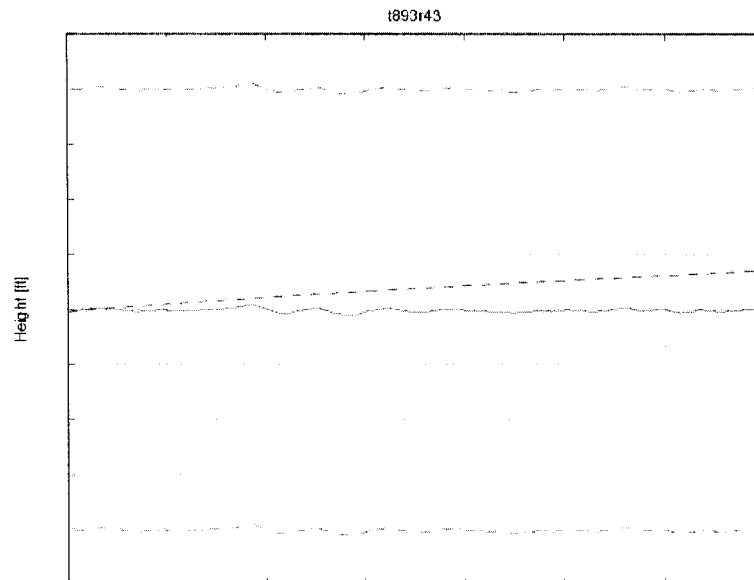Figure 107 Flight test t893r43 Euler angles time history

Figure 108 Flight test t893r43 radar altitude time history

6.4 Control response in Hover Out of Ground Effect validation

The requirements for the control response validation are divided into four categories:

1. *Longitudinal control*: the main parameters are the pitch rate (q) within a tolerance of ± 2 deg/sec and the pitch attitude (θ) within a tolerance of ± 1.5 deg.

2. *Lateral control*: the main parameters are the roll rate (p) within a tolerance of ± 3 deg/sec and the roll attitude (φ) within a tolerance of ± 3 deg.

3. *Directional control*: the main parameters are the yaw rate (r) within a tolerance of ± 2 deg/sec and the yaw attitude (heading change ψ) within a tolerance of ± 2 deg.

4. *Vertical control*: the main parameter is the normal acceleration (a_z) within a tolerance of ± 0.1 g.

In all these cases, is required that the control input should be a step function and the response of the helicopter must show the correct trend of the movement.

For the validation of each control manoeuvre only one case is shown. In Figures 109 - 113 the case t896r94 for the longitudinal control response hover performance out of ground effect, for the helicopter in heavy - forward gross weight configuration is shown:
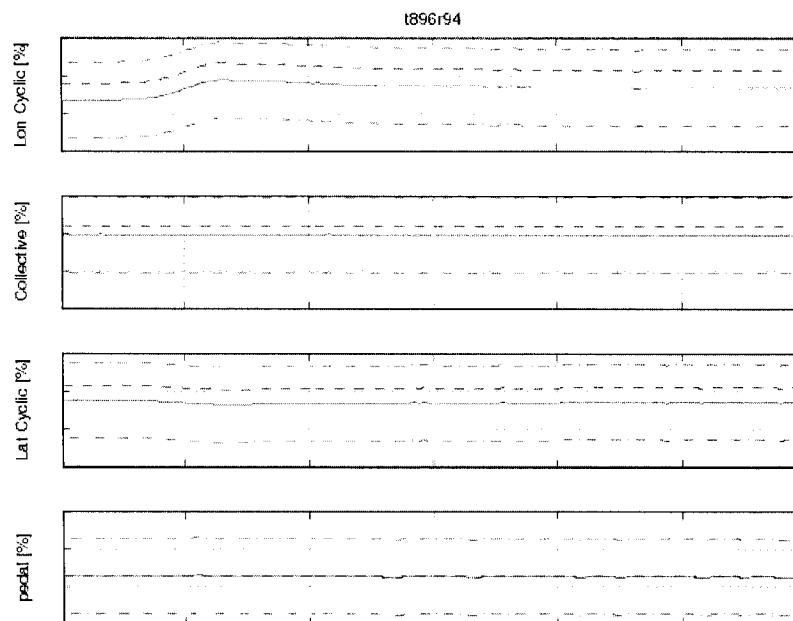
t896r94

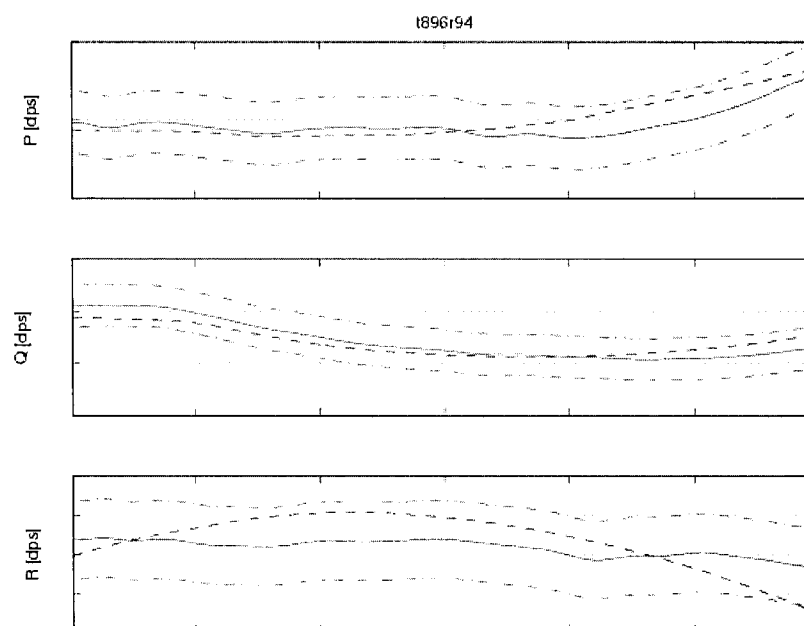Figure 109 Flight test t896r94 controls time history

t896r94

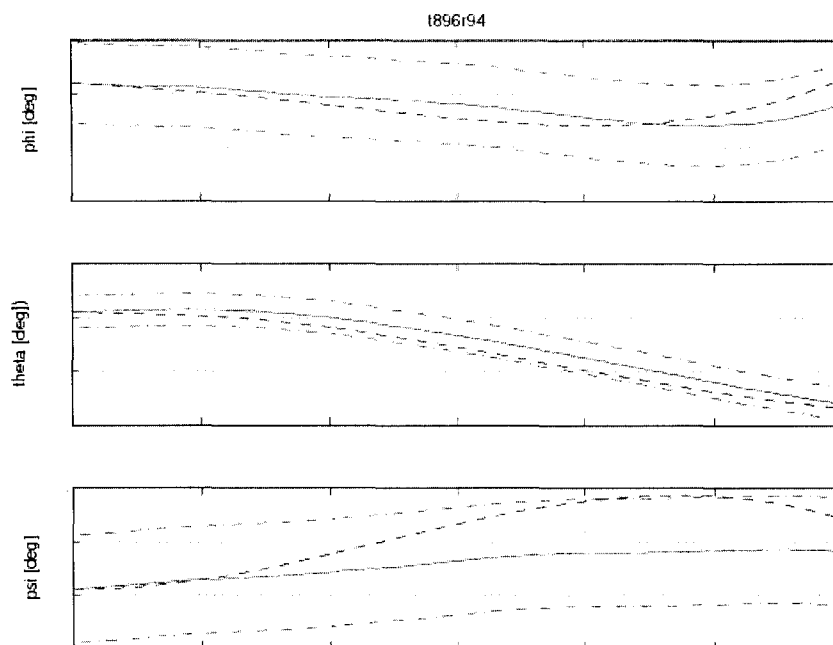Figure 110 Flight test t896r94 attitude rates time history

Figure 111 Flight test t896r94 attitude angles time history

Figure 112 Flight test t896r94 accelerations in body reference system time history
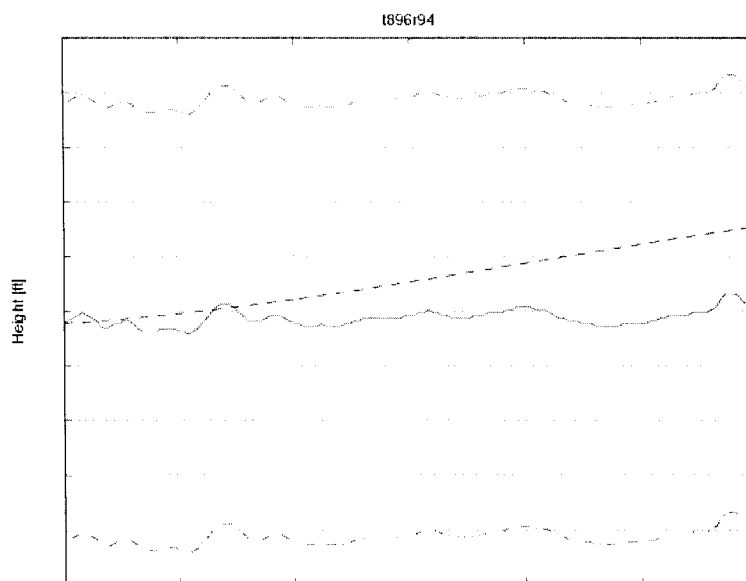
Figure 113 Flight test t896r94 radar altitude time history

In Figures 114 – 118, the case t896r97 of lateral control response hover performance out ground effect, for the helicopter in heavy - forward gross weight configuration is shown:

Figure 114 Flight test t896r97 controls time history

Figure 115 Flight test t896r97 attitude rates time history
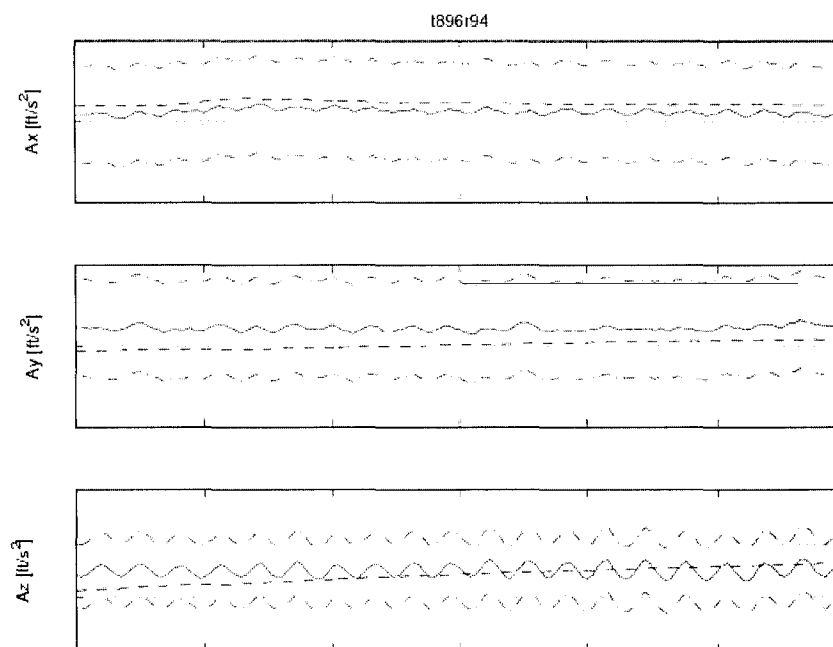

Figure 116 Flight test t896r97 Euler angles time history

t896r97

Figure 117 Flight test t896r97 accelerations time history
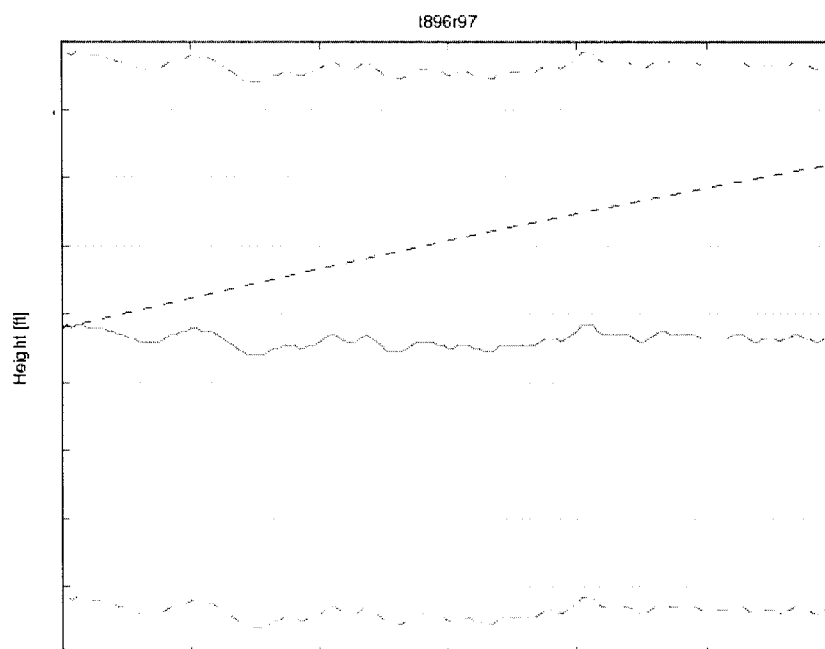
t896r97

Figure 118 Flight test t896r97 radar altitude time history

In Figure 119 – 122, the case t896r99 for directional control (pedal) response hover performance out of ground effect, for the helicopter in heavy - forward gross weight configuration is shown:
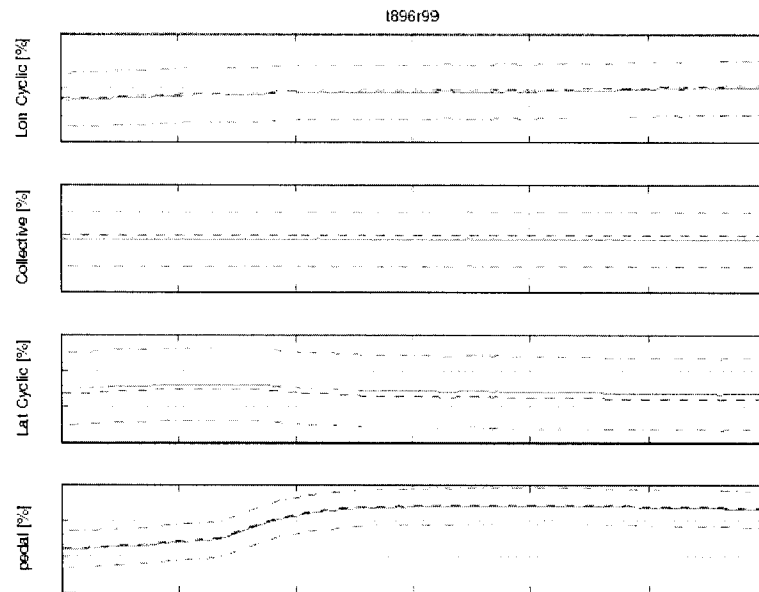
Figure 119 Flight test t896r99 controls time history
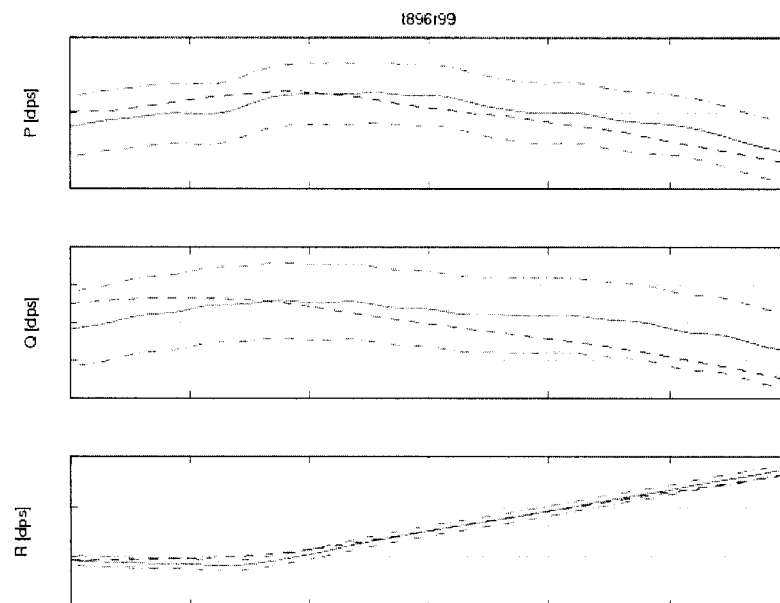
Figure 120 Flight test t896r99 attitude rates time history
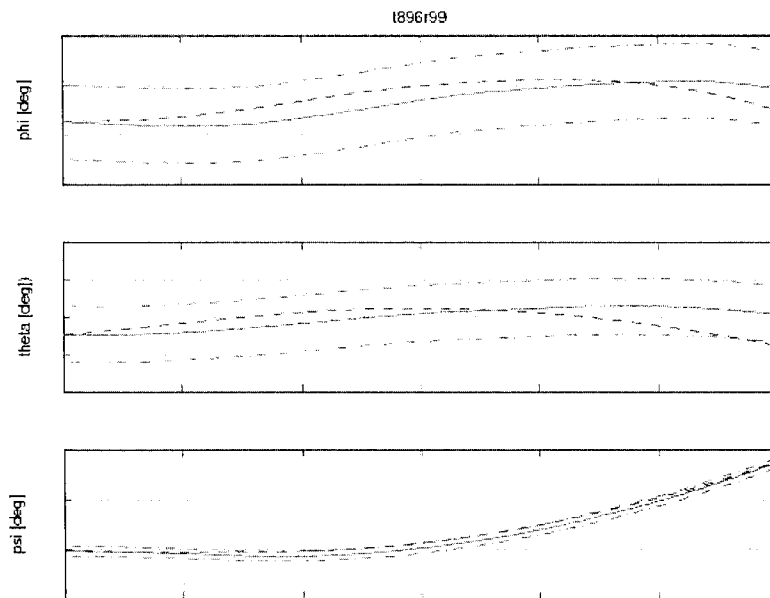
t896r99

Figure 121 Flight test t896r99 attitude angles time history
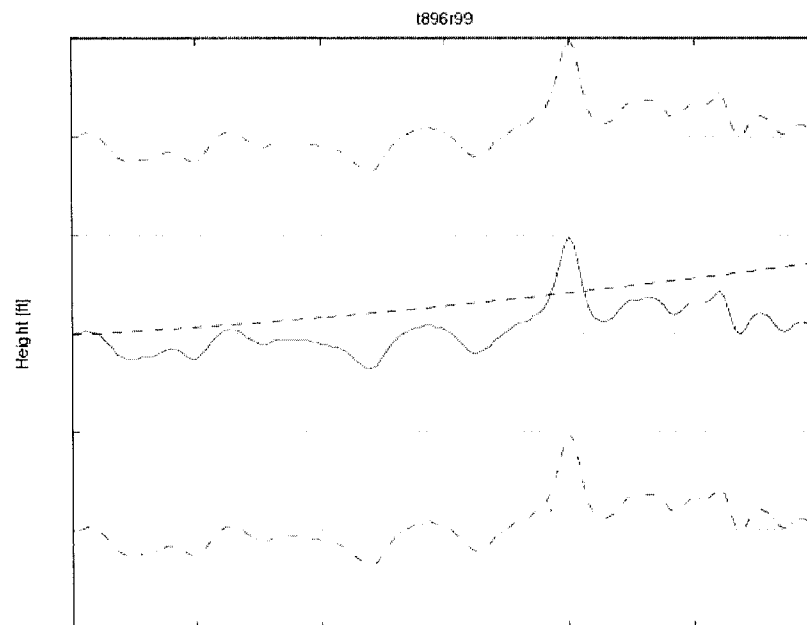
t896r99

Figure 122 Flight test t896r99 radar altitude time history

In Figures 123 – 127, the case t896r100 for vertical control (collective stick) response hover performance out ground effect, for the helicopter in heavy - forward gross weight configuration is shown:
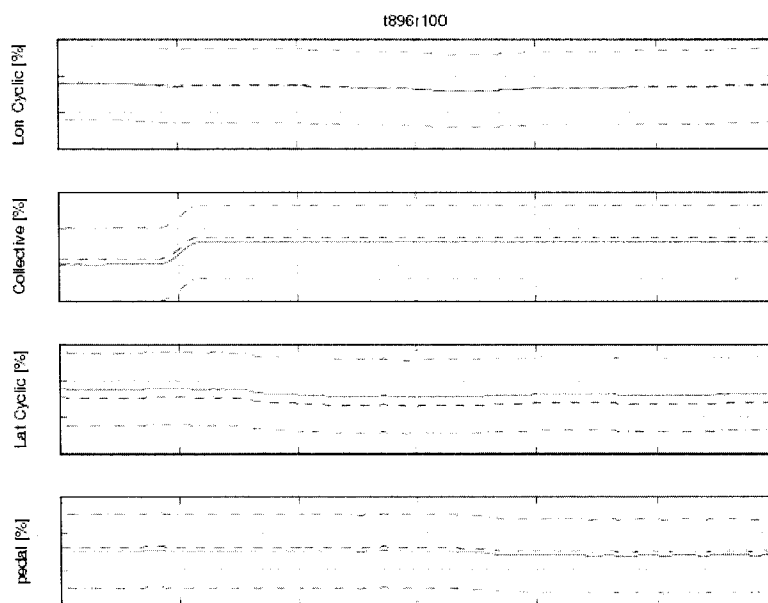
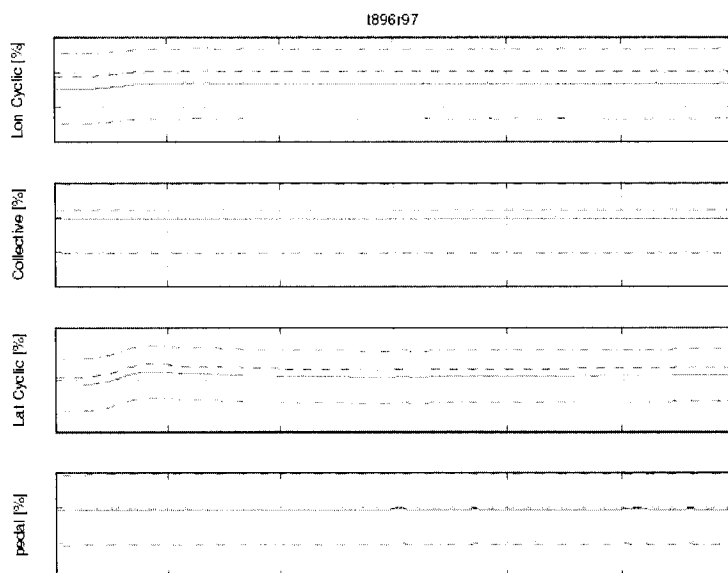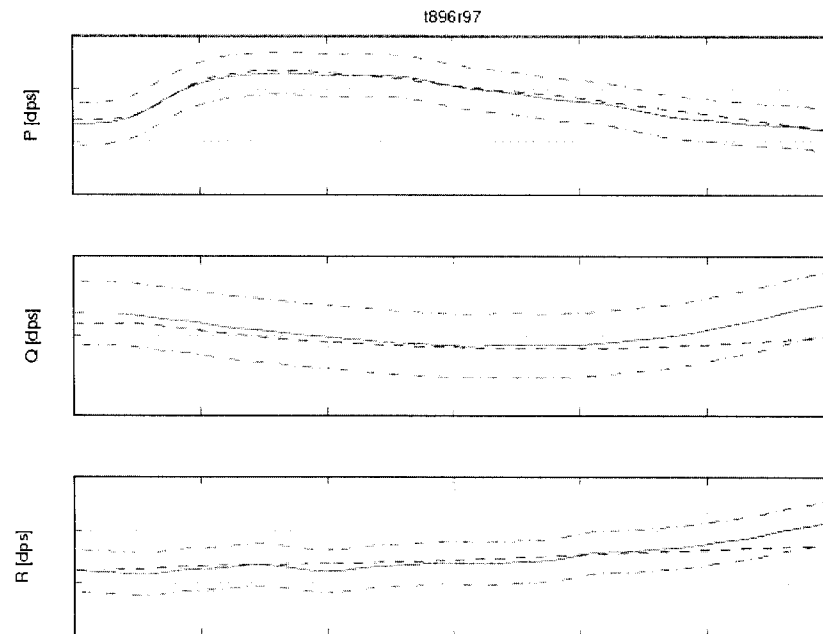Figure 123 Flight test t896r100 controls time history
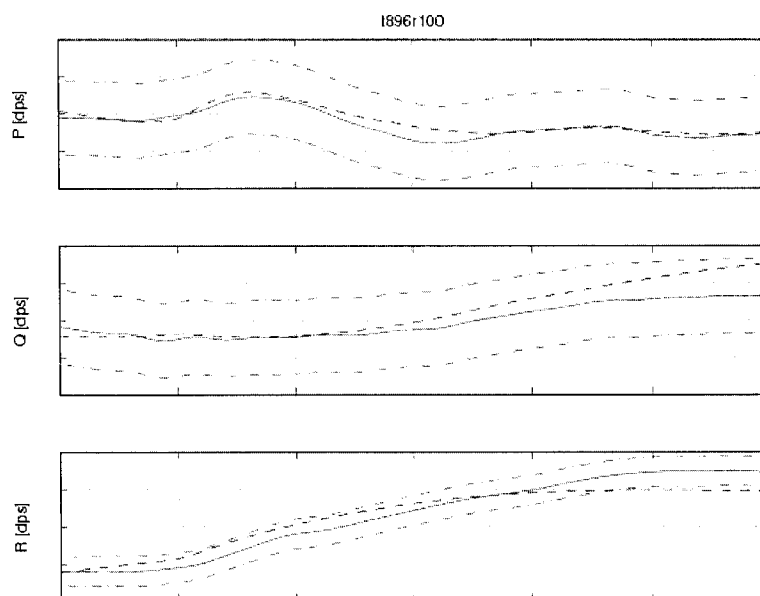
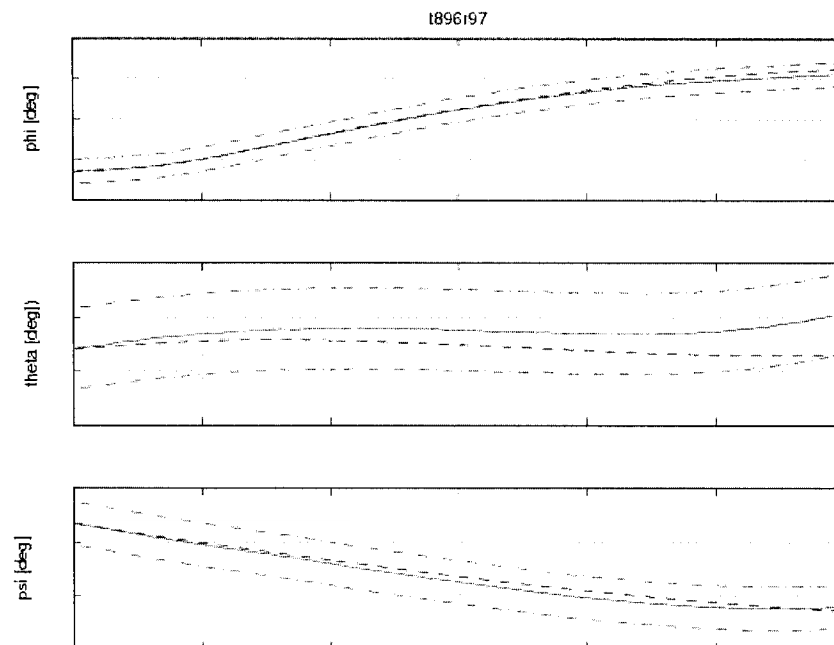Figure 124 Flight test t896r100 attitude rates time history

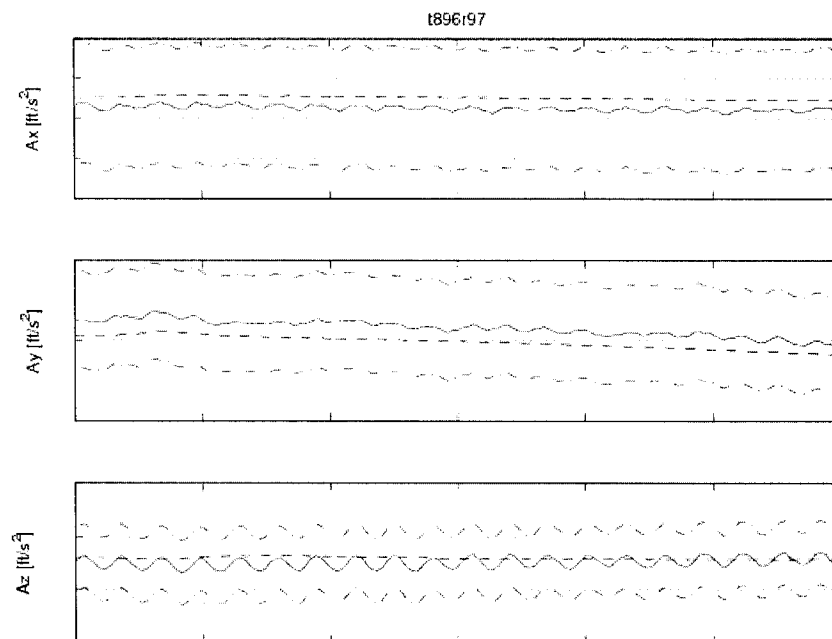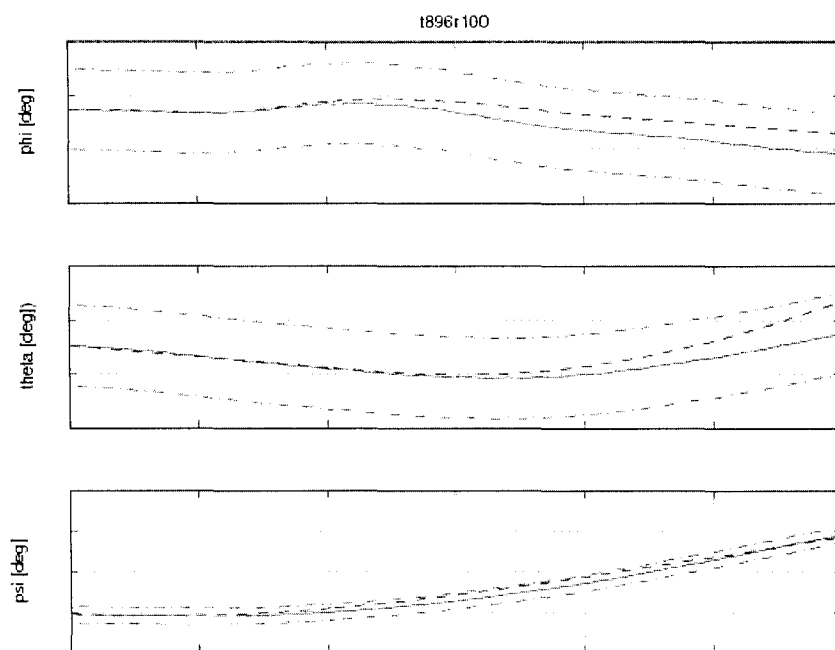Figure 125 Flight test t896r100 attitude angles time history
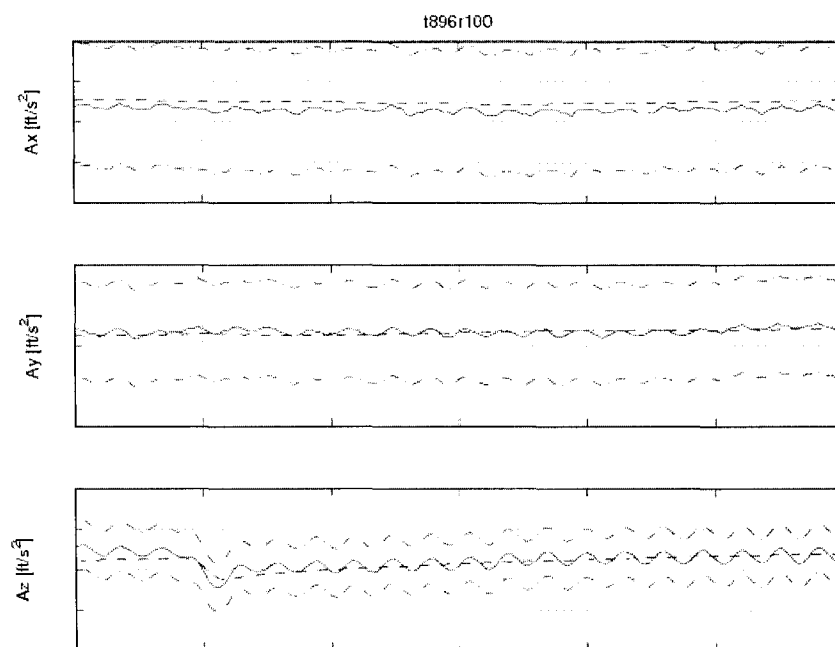
Figure 126 Flight test t896r100 helicopter altitude time history

t896r100

Height [II]
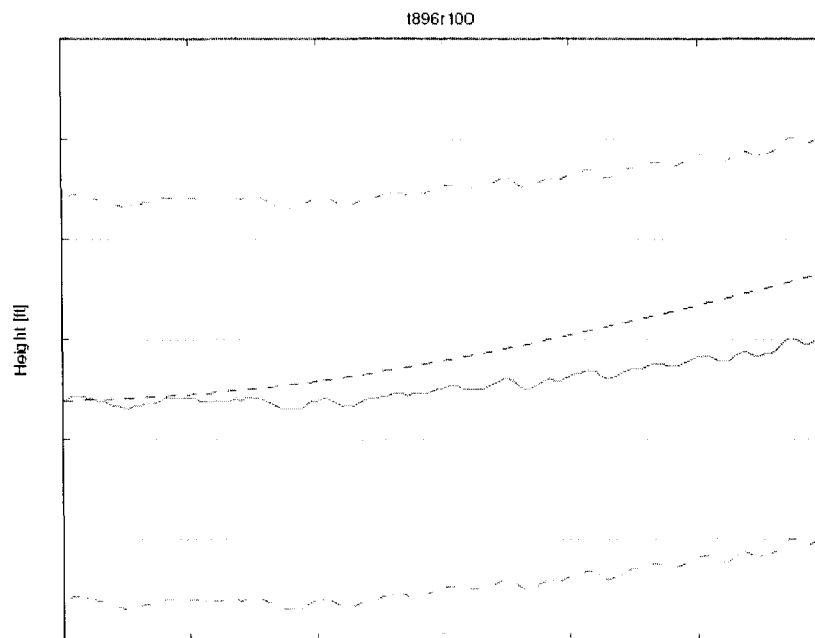
Figure 127 Flight test t896r100 radar altitude time history

In all the four cases shown the model simulation matched perfectly with the flight test, and the certification requirements of the AC for the hover control response chapter (Table V, 2b3) are satisfied.

CHAPTER 7

AUTOROTATION PERFORMANCE VALIDATION

7.1   General considerations

The autorotation is a balanced, steady flight condition which occurs when engine power drops due to a failure and the entire main rotor thrust is provided only by the aerodynamic forces [3], [4], [10]. This flight condition consists of four stages: the transition stage between the engines powered horizontal flight or the "entry phase", the steady descent phase, the "flare" manoeuvre which is done by the pilot to decelerate the helicopter descent and the "touchdown" or the landing phase [5]. These stages are shown in Figure 128:
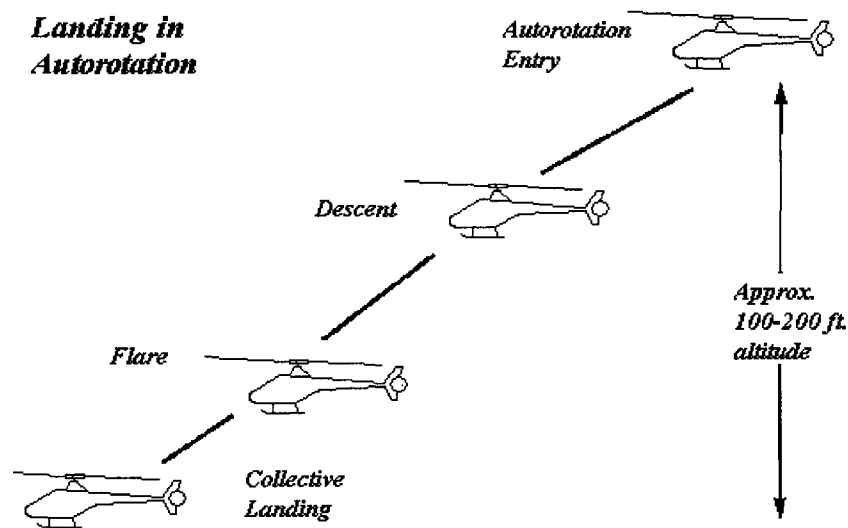
Figure 128 The four stages of the autorotational landing manoeuvre

During the autorotation, the main rotor from propeller becomes a "wind mill". During the descent, the rotor blade is subjected to air coming up at it from below. The blade twist reduces the rearward tilt of the thrust vector as shown in Figure 129. At some rate of descent, the forward tilt of the lift vector is equal to the drag component. This is the condition of "autorotation", since no torque needs to be applied to maintain rotor speed. In an actual rotor, some blade regions will have more drag than the forward component of lift (this is the driven region); but on other regions of the blade the situation will be reversed (driving or propeller region). Autorotation occurs when the integration of torque along the blade is zero or, for an actual helicopter, is sufficiently negative to compensate for losses in the tail rotor, transmissions, and accessories. For a given helicopter at a given gross weight, there is a unique combination of rate of descent, rotor speed, and blade pitch that defines this condition [3].
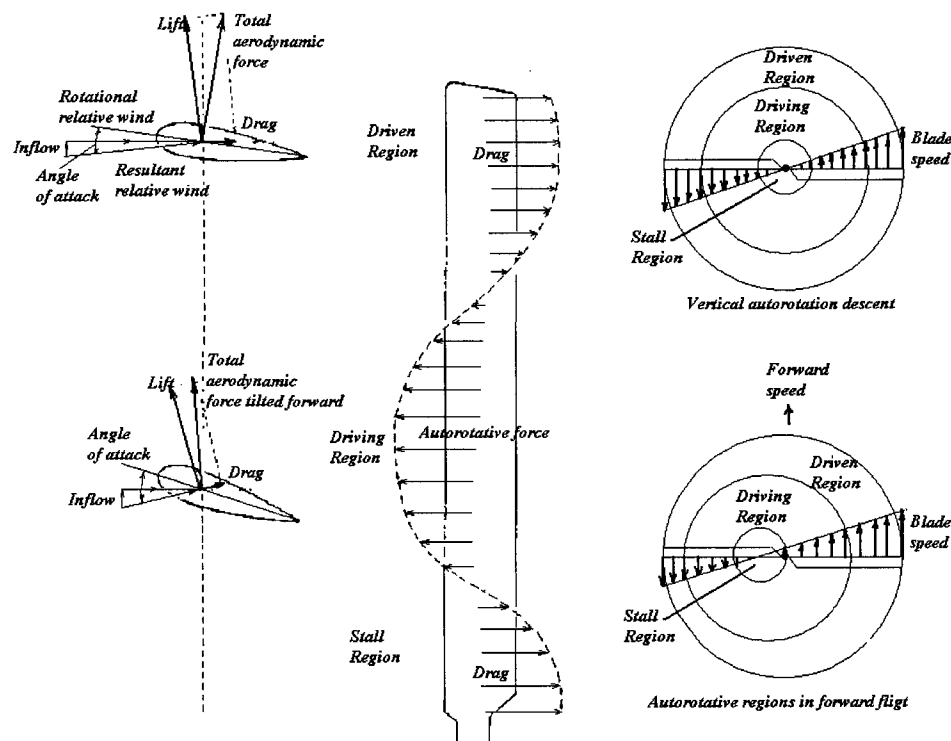
Figure 129 The aerodynamic forces of the blade during autorotation

After engines failure, before autorotation entry, if the pilot doesn't take any action to put the rotor blades in autorotation, the drag forces would slow down the rotor speed leading to the helicopter's crash [5]. In fact to maintain the rotor speed at a constant value after the engine failure is the most critical action. If pilot put the collective to the minimum position, the rotor enters the autorotation condition. During autorotation, the rotor thrust is equal to the gross weight and the rotor speed remains constant.

Autorotation once established is stable. If the rotor speed decreases, then the horizontal velocity of the rotor decreases while the inflow remains constant, this making to increase the incidence angle of the resultant relative wind, as shown in Figure 129. The lift vector will decrease accordingly but will be tilted further forward, thus tending to increase the rotor speed. The opposite effect occurs when the rotor speed increases from its original value. The pilot can control the rotor speed by adjusting the blade pitch. A reduction of pitch initially decreases the rotor lift, as that the descent rate increases, thus tilting the lift vector forward and accelerating the rotor. As the rotor speeds up, the lift reaches a value equal to the weight of the helicopter, and a new set of equilibrium conditions is reached with a higher rotor speed and a slightly different descent rate than the one before the blade pitch was decreased.

For each helicopter, there is an upper and a lower limit of rotor speed which the pilot should notice :

- The upper limit is the speed at which the centrifugal forces in the blades and the hub reach the structural design limit. The upper limit is generally 10-20% above the normal speed for hover flight condition.
- The lower limit is the speed at which, in order to maintain rotor thrust equal to the gross weight, each blade section is operated at or near its stall angle of attack. Once the blade stalls, the drag increases rapidly and becomes greater than any forward tilt of the lift vector can compensate. At this point, the rotor

slows down until it stops, and the flight becomes catastrophic. The lower limit may be as low as 20-30% below the normal speed.

Figure 130 shows the successions of manoeuvres that a pilot must accomplish to successfully make an autorotational landing.
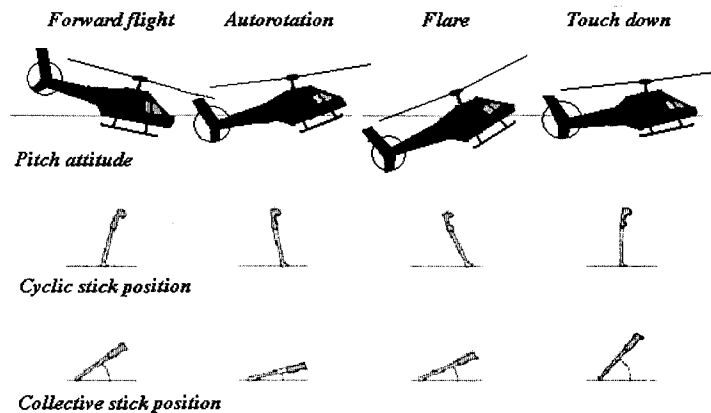
Figure 130 Landing manoeuvres in autorotation

The autorotation model is a separate model from the UAA model due to its specific aerodynamics characteristics. Additionally these aerodynamic characteristics are very different when the helicopter is in the neighbourhood of the ground where in ground effect (IGE) occurs.

7.2 Autorotation entry validation

Autorotation entry is the transition between the forward flight and the steady autorotation as seen in Figure 131. Due to the change of the airflow through the rotor, all aerodynamic forces will change, which means that a different model is required to simulate the autorotation flight condition. This model should link the helicopter forward flight condition with the steady descent condition. For the simulation of this transition, the AC requires to fit the pitch attitude θ within a tolerance of ± 2 degrees,

the roll attitude φ within a tolerance of ± 3 degrees, the yaw attitude ψ within a tolerance of ± 5 degrees, airspeed within a tolerance of ± 5 knots (8.44 ft/sec), vertical velocity within a tolerance of ±200 ft/min (3.33 ft/sec) and all controls (longitudinal cyclic stick, lateral cyclic stick, collective stick position, pedals position) within a tolerance of ± 5% of range motion. Time history should fit the helicopter response to a rapid throttle reduction to idle. The chosen trim function was the "trimAngAccel" because this function allows the editing of the initial condition for angular accelerations *Pdot*, *Qdot* and *Rdot* ($\dot{p}, \dot{q}, \dot{r}$). The sub-trim function with the best results was "subtrimRate" in which the rates attitudes are the only constraints.
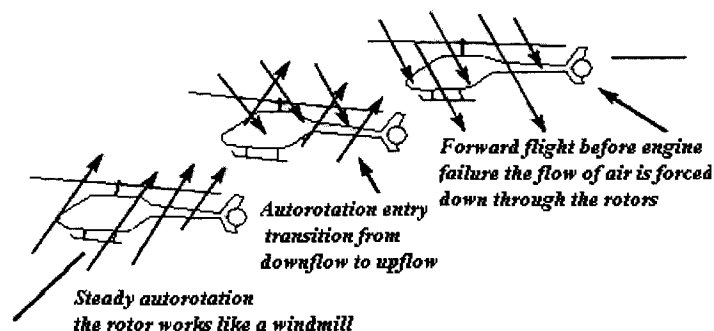
Figure 131 The transition between the forward flight and autorotation

In Figure 132, the case t890r18 of autorotation entry performance at an altitude of 3400 ft for the helicopter in light-aft (LA) gross weight configuration is shown:
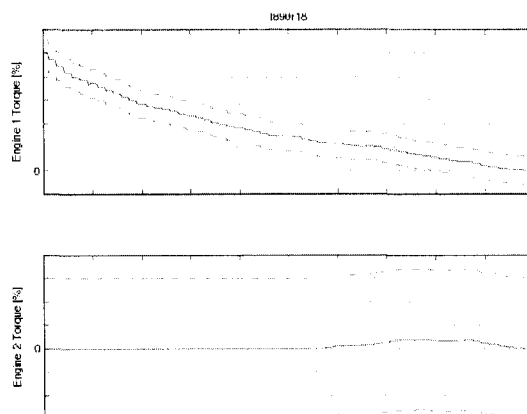
Figure 132 Flight test t890r18 helicopter engines torque time history
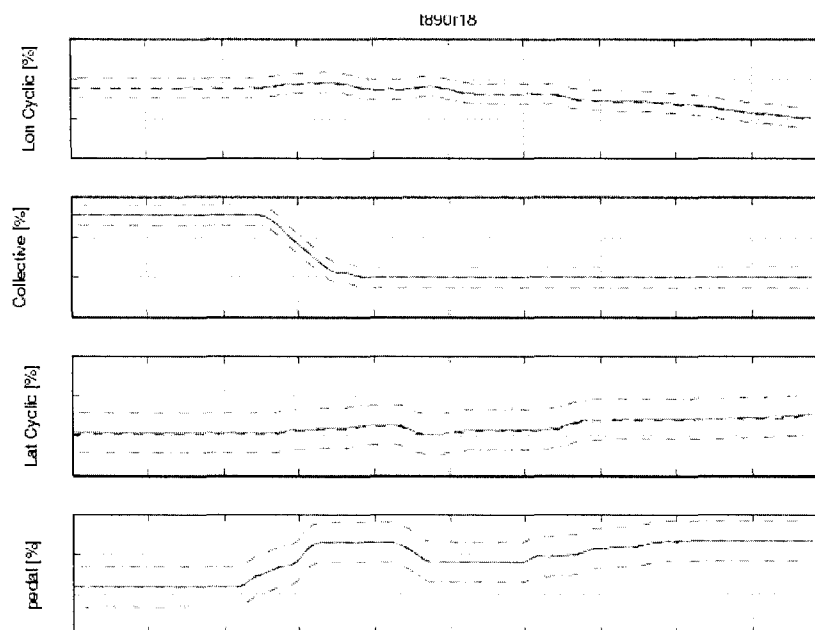
t890r18

Figure 133 Flight test t890r18 controls time history
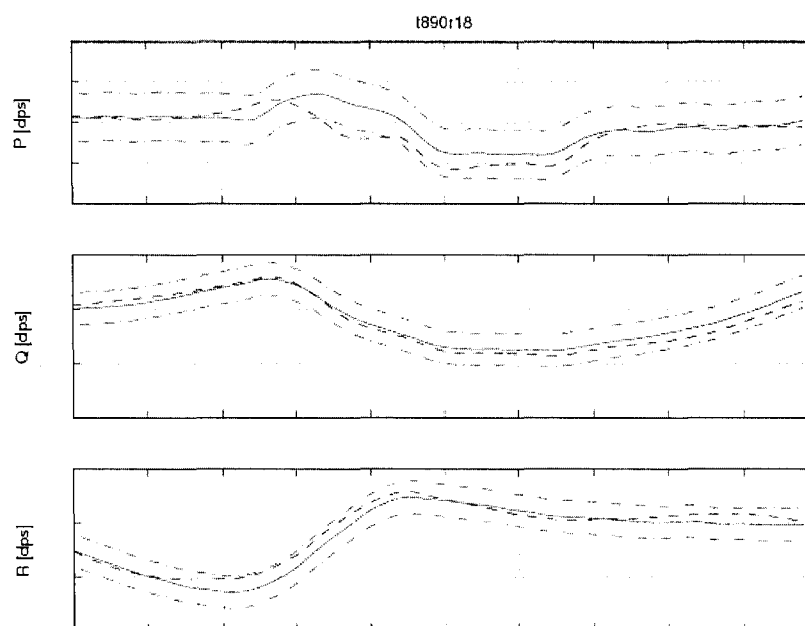
t890r18

Figure 134 Flight test t890r18 attitude rates time history
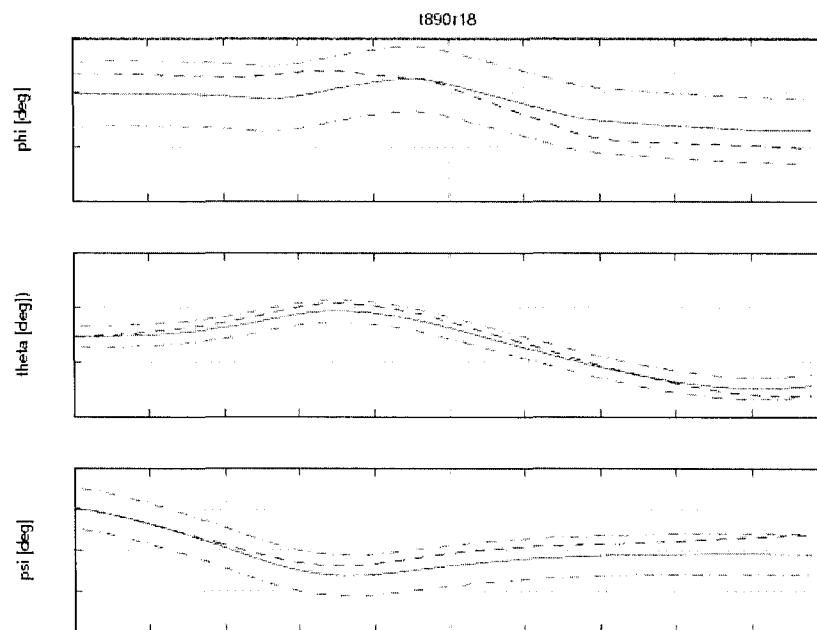
Figure 135 Flight test t890r18 attitude angles time history
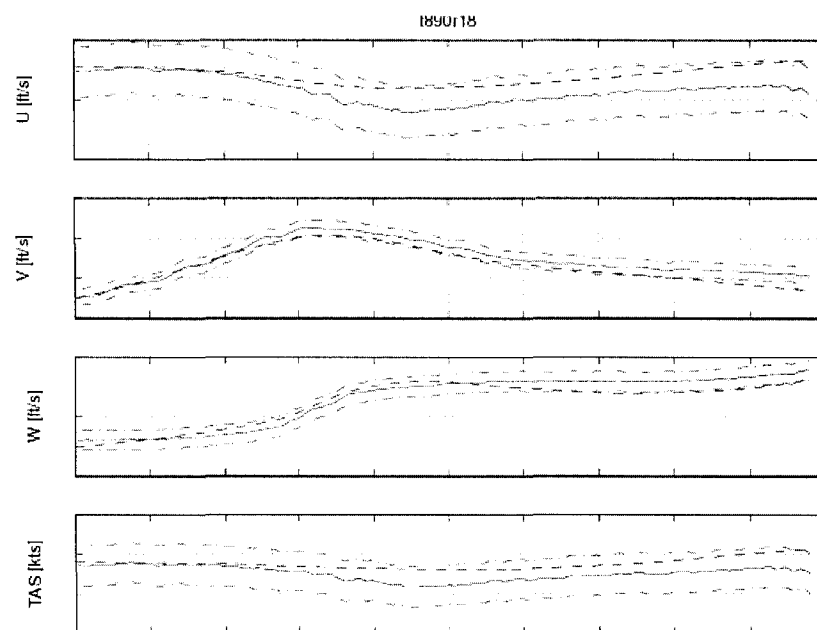
Figure 136 Flight test t890r18 speeds in body reference system time history
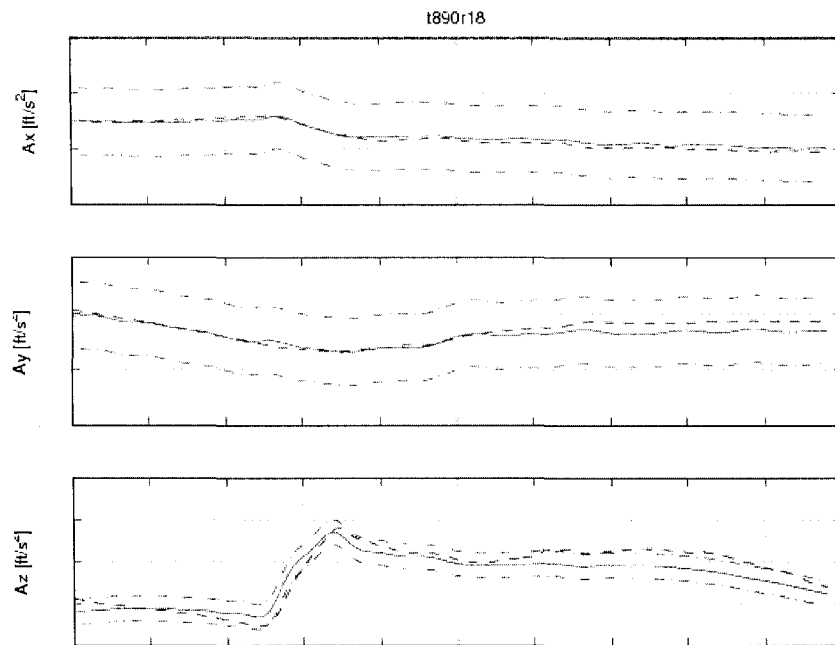
Figure 137 Flight test t890r18 helicopter accelerations time history
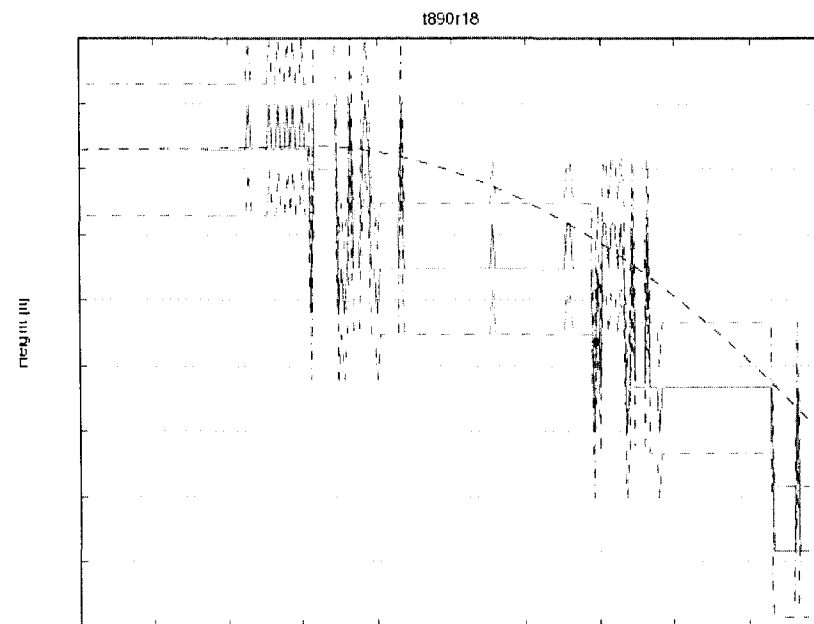
Figure 138 Flight test t890r18 density altitude time history

7.3   Steady descent autorotation validation

For the validation of the autorotation performance and trimmed flight control position are required two gross weights (Light or Heavy) at normal operating rotor speed in a steady descent to match. The matching may be a "snapshot" which means that 2-3 seconds of matching is acceptable. The parameters required by the AC to match are the pitch attitude θ within a tolerance of $\pm$ 1.5 degrees, sideslip angle (yaw attitude ψ) within a tolerance of $\pm$ 2 degrees, vertical velocity within a tolerance of ±100 ft/min (1.67 ft/sec) and all controls (longitudinal cyclic stick, lateral cyclic stick, collective stick position, pedals position) within a tolerance of $\pm$ 5% of range motion. The chosen trim function was "trimSideslipM" because this function trims the initial sideslip angle and airspeed. The sub-trim function giving the best results was "subtrimRate" in which the rates attitudes are the only constraints.

In Figure 139, the same case t890r18 of autorotation descent performance at an altitude of 2500 ft, for the helicopter in light-aft gross weight configuration is shown:
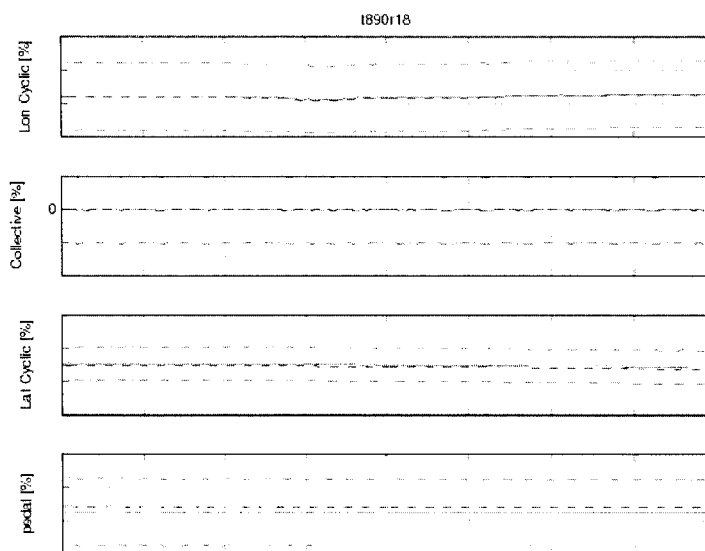

Figure 139 Flight t890r18 autorotation descent controls time history
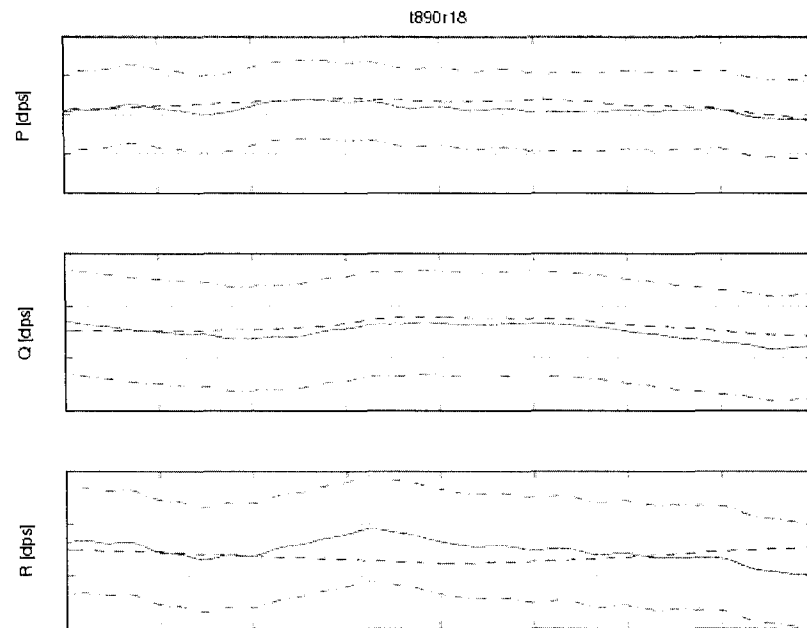
Figure 140 Flight t890r18 autorotation descent attitude rates time history
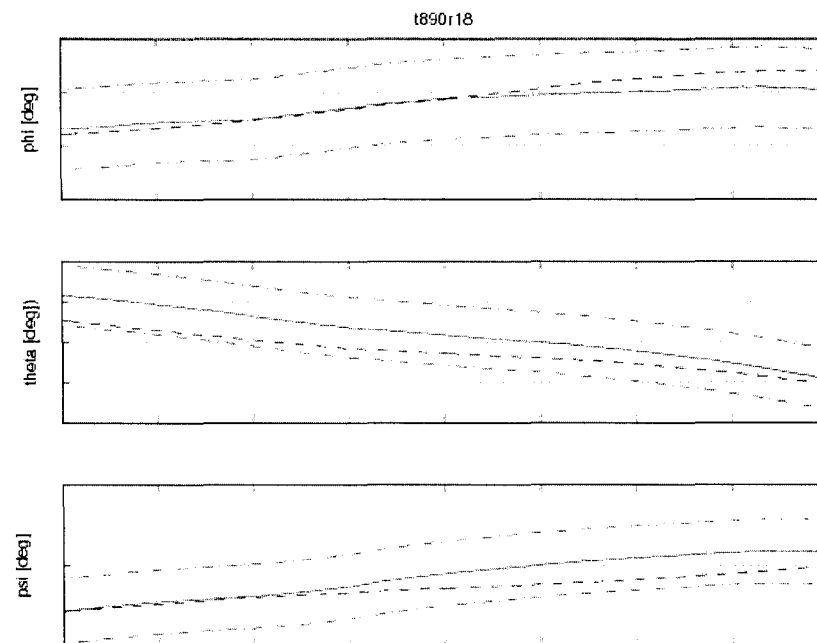
Figure 141 Flight t890r18 autorotation descent Euler angles time history
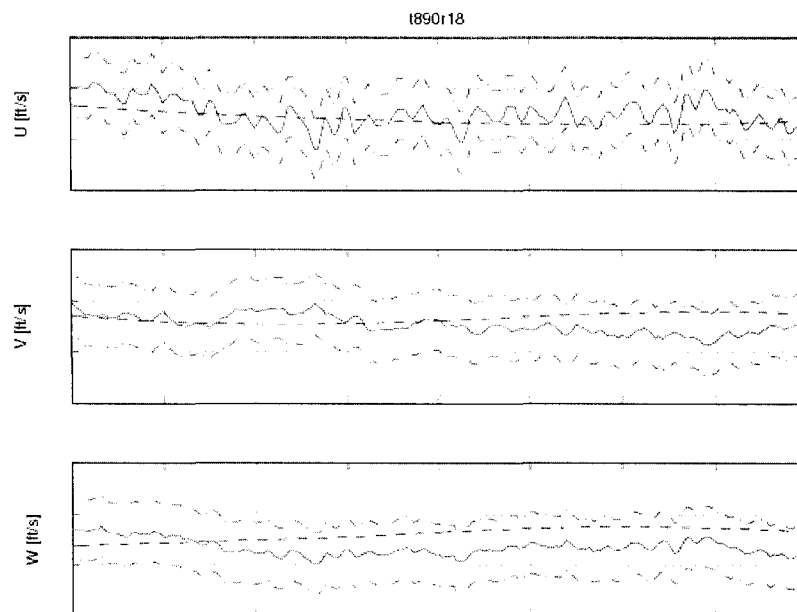
t890r18

Figure 142 Flight t890r18 autorotation descent speeds in body reference system time history
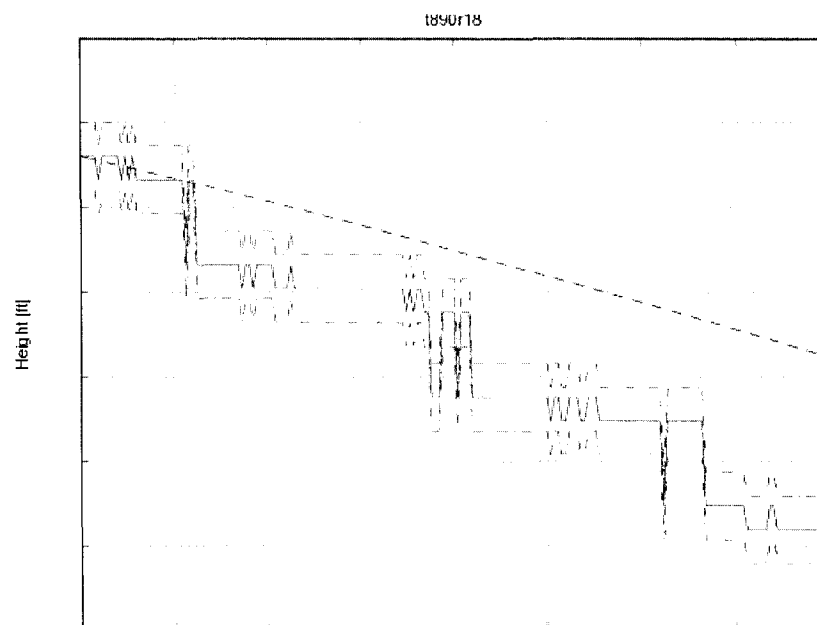
t890r18

Figure 143 Flight t890r18 autorotation descent density altitude time history

7.4 Autorotation landing

This chapter will treat the dynamic transition between the steady autorotational descent and the touch down point when the helicopter interacts with the ground. This flight phase is named "the flare" which is a manoeuvre done by the pilot to decelerate the helicopter descent [5]. This manoeuvre is done by pulling the control stick to the maximum to increase the rotor blades pitch and using the inertial momentum of the main rotor to gain extra thrust. This manoeuvre is done simultaneously with an increase of the helicopter pitch attitude θ, as shown in Figure 144. In Figure 144 two autorotational landings cases t900r70 and t910r55 are shown. The time history shows the last 10 seconds before the touchdown.
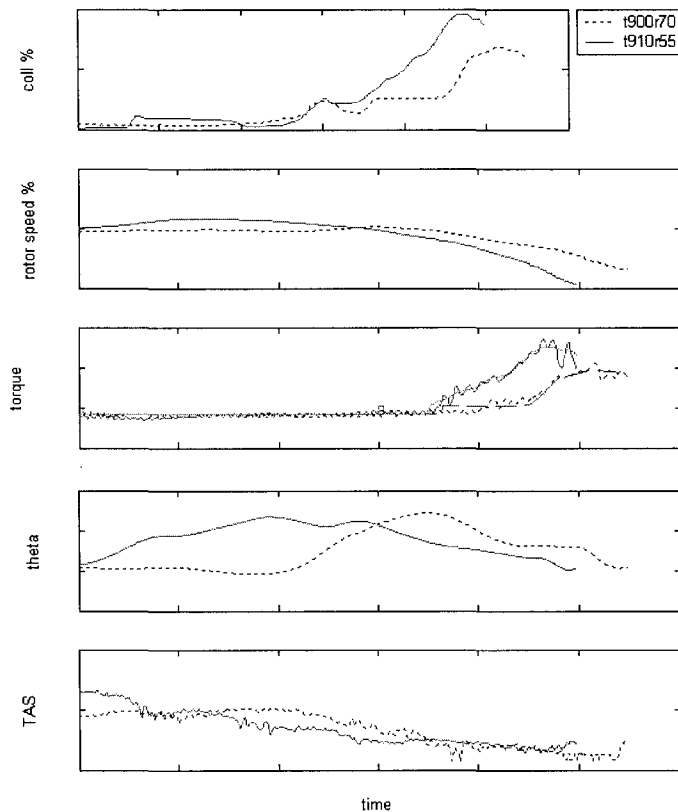
Figure 144 Flight tests t900r70 and t910r55 autorotational landing parameters

The flare manoeuvre for the flight t910r55 begins at the second 1, while the flare manoeuvre for the flight t900r70 begins 5 seconds later. At the end of the flare manoeuvre, the helicopter should be close to the ground with its vertical velocity equal to zero or at least below the design sink rate of the undercarriage.

During the steady autorotation the recorded rotor torque is a small negative value which correspond to the friction of the gears and auxiliary equipments mechanically linked to the main rotor shaft. Theoretically the rotor torque which represents the integrated autorotational forces and aerodynamical drag forces is equal to zero assuming that the engine failed completely and provides zero torque. The rotor speed is 100 % at the nominal value due to the equilibrium of aerodynamical forces. As the ground approaches more thrust is needed to decelerate the helicopter descent which is accomplished by increasing the pitch blades, which in turn will increase the aerodynamical drag forces making the rotor speed to decay [5]. The rotor speed decay rate can be estimated by applying simple rotational mechanics to the problem:

$$Q = -J\dot{\omega}$$
$$\dot{\omega} = \frac{d\Omega}{dt} = -\frac{Q}{J} \tag{7.1}$$

where $\dot{\omega}$ is rotor speed decay rate, Ω is rotor speed, Q is rotor torque and J moment of inertia of rotor system.

To estimate the rotor torque during the flare manoeuvre we need a relation between collective stick position and Q when no engine power is supplied to the rotor. From the data shown in Figure 144 we can see a linear relation between the collective position and torque value.

The torque predicted by this linear equation it is shown in Figure 144 in the same plot with the recorded value of the torque.
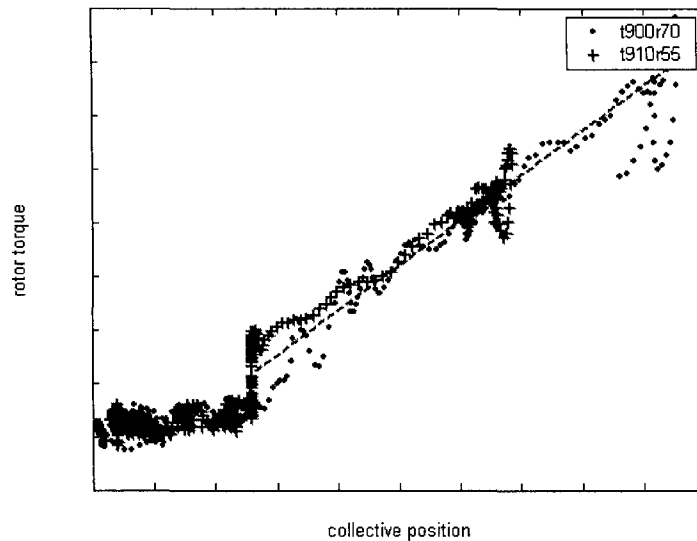
Figure 145   Linear variation between the collective stick position and rotor torque during the autorotational landing

The equation (7.1) was simulated in Simulink in the following manner as shown in Figure 146:
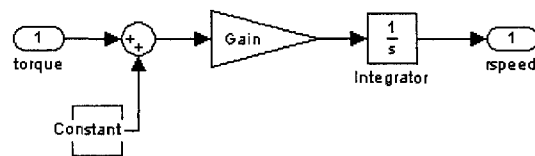
Figure 146 Simulink schema of the rotor speed decay equation

The gain is the momentum inertia of the rotor opposed to the movement of rotation and the constant is the residual torque recorded during the steady descent.

This simple model with only one input (collective control, i.e. torque) gives a good rotor speed decay estimation during flare but does not take into account the "flare" effect which is given by the helicopter pitch attitude angle increase just before the touchdown. A second input is needed to introduce in the model, as the pitch attitude

angle. The airspeed of the helicopter is not necessary to introduce as input parameter since all autorotational landings are performed at the same vertical and horizontal airspeed.

To build a model with two inputs and one output we used the Matlab® System Identification Toolbox. The method of estimation was ARX method which will be shortly presented in the following paragraphs [11].

The most used model structure is the simple linear difference equation which relates the current output $y(t)$ to a finite number of past outputs $y(t-k)$ and inputs $u(t-k)$.

$$y(t)+a_1 y(t-1)+\ldots+a_{n_a} y(t-n_a)=b_1 u(t-n_k)+b_2 u(t-n_k-1)+\ldots+b_{n_b} u(t-n_k-n_b+1)+e(t) \quad (7.2)$$

The structure is thus entirely defined by the three integers n_a, n_b, and n_k. n_a is equal to the number of poles and n_b-1 is the number of zeros, while n_k is the pure time-delay (the dead-time) in the system. For a system under sampled-data control, typically n_k is equal to 1 if there is no dead-time. For multi-input systems n_b and n_k are row vectors, where the i-th element gives the order/delay associated with the i-th input.

$$A(q)y(t)=B(q)u(t-n_k)+e(t)$$
$$A(q)=1+a_1 q^{-1}+\ldots+a_{n_a} q^{-n_a} \quad (7.3)$$
$$B(q)=b_1+b_2 q^{-1}+\ldots+b_{n_b} q^{-n_b}$$

where n_a, n_b are the orders of polynomials $A(q)$ and $B(q)$, and n_k is the delay and $e(t)$ is the white noise. B and A are polynomials in the delay operator q^{-1}, and $A(q)y(t)$ is short for:

$$A(q)y(t)=\sum_{k=1}^{n_a} a_k y(t-k)$$

The coefficients b and a in the ARX model structure are estimated by use of the least-squares method which minimizes the sum of squares of the right-hand side minus the left-hand side of the expression 7.2, with respect to b and a.

The model obtained with ARX method has the inputs variables the pitch attitude θ and collective position and the output variable is the rotor speed. This model does not need to introduce as input parameter the torque variable, since there is a direct link between the torque and the control stick position.

In Figures 147 and 148 are shown the simulations of the rotor speed estimated by the ARX model (the red plot) compared with the flight test data (the black plot). The model was obtained using the flight test t910r55 data. The flight test t900r70 data is used for the model validation.

Measured and simulated model output

Time
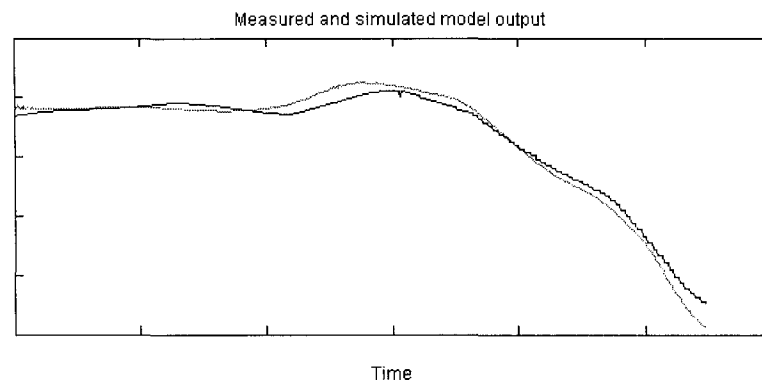
Figure 147   The simulation of the rotor speed decay using the ARX method for the test flight t900r70

Measured and simulated model output

Time
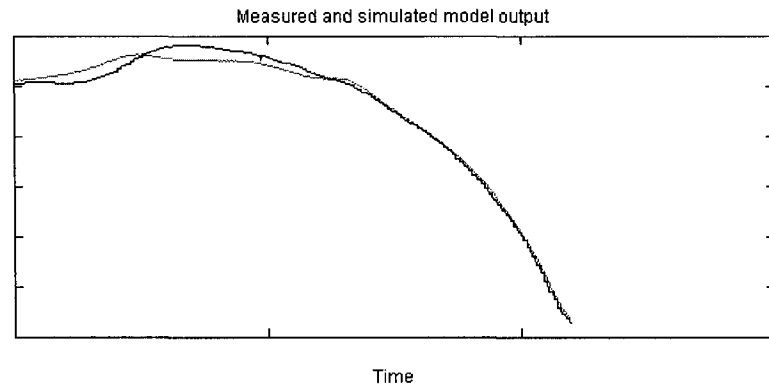
Figure 148   The simulation of the rotor speed decay using the ARX method for the test flight t910r55

As shown in both figures the model obtained using the system identification box ARX method gives very good results compared with the flight test data.

This method is proposed to be used in the future work in order to complete the transitional model from a steady autorotational descent until the ground dynamics appear in the landing manoeuvre. This model is not implemented yet into the POM software, remaining to be developed into the future versions.

CONCLUSION

The global model of the helicopter has passed through all the points of the QTG list and has been compared with the flight tests. The number of cases passed through this analysis was shown in Table I in the Introduction chapter. For each point of the QTG list, one of the best simulations was picked to demonstrate the matching of the simulation with the flight tests as required by the FAA AC 120-63. Following the validation process completion, the model revealed its strong and weakness points. As shown in the previous chapters, the model is divided in several loading-airspeed-flight condition combinations modules. For each module there are better and worse simulations which will be discussed in the following paragraphs.

From the analysis of multiple cases run with the new version of POM, it can be concluded that the Up-And-Away (UAA) helicopter model in configuration heavy-aft (HA) and heavy-forward (HF) simulates much better than the helicopter light-aft (LA) module. In the same manner, the light-aft module at higher airspeeds (120 knots) gives better results than the light-aft module at lower airspeeds (60 knots). For the heavy-aft module, it can be concluded that the lower speeds module simulates better than the higher speeds module. The cases with a longer simulation time as 10-20 seconds showed that the Dutch roll was excited for the real helicopter, but is not captured by the simulation. These observations will be used in the following adjustments of the global module for the next step in the certification procedure. The "2d - lateral/directional stability" AC requirements are satisfied.

From the analysis of multiple cases ran with the POM software, it can be concluded that the hover module has a good fit with the real helicopter for both configurations heavy-mid (HM) and light-mid (LM) in both conditions Out of Ground Effect (OGE) and In Ground Effect (IGE). Anyway for the helicopter in configuration heavy-mid

(HM) the model simulates better than the light-mid (LM) module. The "1d – hover performance" and "2b3 – control response in hover" AC requirements are satisfied.

The Autorotation module has a very good fit in all loading configurations (HA, HF, LA). Since the autorotation steady descent is similar to an engine powered descent but at a constant airspeed of approximately 80 knots it can be concluded that there are similarities in the Autorotation module and UAA module. The "2c2 – static stability in autorotation" AC requirement is satisfied.

The entry in autorotation is well simulated in the Light-Aft configuration and the "1i – autorotation entry" AC requirements is satisfied partially only for the Light-Aft configuration. The Heavy-Aft (HA) and Heavy-Forward (HF) remains to be developed at a later time to complete the "1i" requirements validation.

Since the models were built upon the recorded flight tests using the Maximum Likelihood Estimation method we conclude that the errors in data recording as well as the atmospheric perturbations has a great influence in the final model. The heavy helicopter responded much accurately and with less interference from wind gusts which conducted to a more accurately model than the light loaded helicopter. For the model in the light loading configuration more adjustments are needed to fulfill all the requirements of a certified simulator.

The model at this stage of development is capable of passing the certification requirements for a standard level D simulator. In the actual stage the model has a good fitting in all the flight conditions and helicopter loadings and configuration. For a full level D simulator certification, further work is required to complete QTG list.

RECOMENDATIONS

The process of building the helicopter model does not stop at this stage; the level D certification must be completed. The AC requirements for level D certification imply a global model capable of simulating a flight in all the phases such as: take-off, climb, level flight-cruise, descent, landing as well as the emergency cases such as: OEI flight, autorotation entry, autorotation descent, autorotation landing. The simulations by use of the actual POM version were performed for short intervals of time, for a stable flight condition of the helicopter.

In order to satisfy the full level D certification requirements, a transition flight model is needed to simulate the dynamic evolution of the helicopter inside the flight envelope between the various states of the flight conditions. Full level D certification requires an engine model blended with the aerodynamical model to simulate the engines failures and a ground dynamics model which simulates the mechanical interactions between ground and helicopter at the moment of touch down and after touch down.

These two separate models will be integrated in the global helicopter model. In chapter 7.4, a method is proposed to build a model for the rotor speed during the autorotation flight condition. This model is used in the transition between the flight model and ground dynamics model developed at ÉTS.

In chapter 5.6, it was shown that only Light-Aft module satisfied the certification requirements. For the Heavy-Forward and Heavy-Aft modules, the requirements were not satisfied because of the differences in the damping and period of oscillations between the simulations and flight tests. The model in these two configurations needs further analysis in the A* matrices eigenvalues and adjustments.

The need for accurate prediction model and for a more extensive and comprehensive validation became mandatory. Because of the enormous quantity of data which needs to be analysed to obtain the best possible match, automated software procedures become necessary. For this purpose, is recommended to develop an interface to the main POM software.

REFERENCES

[1]   Etkin, B., & Reid, L. D. (1996). *Dynamics of flight: stability and control* (3rd ed.). New York, N.Y.: J. Wiley and Sons.

[2]   Nelson, R. C. (1998). *Flight stability and automatic control* (2nd ed.), Boston, Mass.: McGraw Hill.

[3]   Prouty, R. W. (2002). *Helicopter performance, stability, and control.* Malabar, Flor.: R. E. Krieger.

[4]   Bramwell, A. R. S., Done, G., & Balmford, D. (2001). *Bramwell's helicopter dynamics* (2nd ed.). Reston, Va. Oxford, Angleterre: American Institute of Aeronautics and Astronautics.

[5]   Cooke, A. K., & Fitzpatrick, E. W. H. (2002). *Helicopter test and evaluation.* Reston, Va.: American Institute of Aeronautics and Astronautics ;.

[6]   Padfield, G. D. (1996). *Helicopter flight dynamics the theory and application of flying qualities and simulation modeling.* Washington, D.C.: American Institute of Aeronautics and Astronautics.

[7]   Crisan, E. G. (2005). *Validation of a mathematical model for bell 427 helicopter using parameter estimation techniques and flight test data,* M.Eng thesis, Montreal, ETS.

[8]   Wolowicz, C. H. (1966). *Considerations in the determinations of stability and control derivatives and dynamic characteristics from flight data,* AGARD Rep.549-Part 1.

[9]   Federal Aviation Administration, Advisory Circular AC 120-63 (1994). *Helicopter simulator qualification,* U.S Department of Transportation.

[10] Seddon, J. (1990). *Basic helicopter aerodynamics an account of first principles in the fluid mechanics and flight dynamics of the single rotor helicopter.* Washington, D.C.: American Institute of Aeronautics and Astronautics.

[11] The MathWorks, Inc., *System Identification Toolbox,* Mathlab User's Guide.

[12] Gebhard, A. (1992). *Flight path calculations for a helicopter in autorotative landing.* AAAF, European Rotorcraft Forum, 18th, Avignon, France, Sept.15-18, 1992, Paper

[13] Karapetian, G. R. (1992). *MI-26 autorotational landings*. AHS, Annual Forum, 48th, Washington, June 3-5, 1992, Proceedings. Vol. 1 (A93-35901 14-01). Alexandria, VA, American Helicopter Society, 1992, p. 671-688.

[14] Okuno, Y., & Kawachi, K. (1994). Optimal control of helicopters following power failure. *Journal of Guidance, Control, and Dynamics, 17*(1), 181-186.

[15] Houston, S. S. (2002). Analysis of rotorcraft flight dynamics in autorotation. *Journal of Guidance, Control, and Dynamics, 25*(1), 33-39.

[16] Houston, S. S. (2003). Modeling and analysis of helicopter flight mechanics in autorotation. *Journal of Aircraft, 40*(4), 675-682.

[17] Leishman, J. G. (2004). Development of the autogiro: a technical perspective. *Journal of Aircraft, 41*(4), 765-781.

[18] Cavalcanti, S., & Papini, M. (2004). Preliminary model matching of the EMBRAER 170 Jet. *Journal of Aircraft, 41*(4), 703-710.

[19] Jategaonkar, R., Fischenberg, D., & von Gruenhagen, W., (2004). Aerodynamic modeling and system identification from flight data – recent application at DLR. *Journal of Aircraft, 41*(4), 681-691.

[20] Mehra, R. K., & Prasanth, R. K., (2004). Time-domain system identification methods for aeromechanical and aircraft structural modeling. *Journal of Aircraft, 41*(4), 721-729.

[21] Devesa, B., Jourdan, C., & Marc, C., (2004). Ground-effect identification and autoland system validation from flight data. *Journal of Aircraft, 41*(4), 730-734.

[22] Theodore, C. R., Tischler, M. B., & Colbourne, J. D., (2004). Rapid frequency-domain modeling methods for unmanned aerial vehicle flight control applications. *Journal of Aircraft, 41*(4), 735-743.

[23] Drobik, J. S., & Brian, G. J., (2004). Application of system identification techniques to the F-111C and PC 9/A aircraft. *Journal of Aircraft, 41*(4), 744-751.

[24] Wang, K. C., & Iliff, K. W., (2004). Retrospective and recent examples of aircraft parameter identification at NASA Dryden Flight Research Center. . *Journal of Aircraft, 41*(4), 752-763.